HYDRAULIC FRACTURING WITH PARTICULAR REFERENCE TO SOIL CYLINDERS

A THESIS

submitted in fulfilment of the
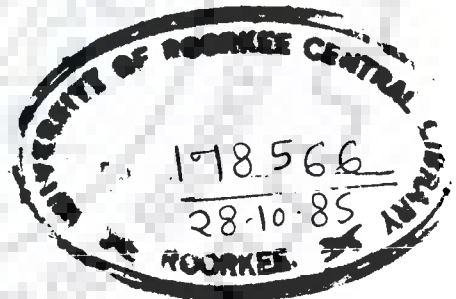requirements for the award of the degree
of
DOCTOR OF PHILOSOPHY
in
WATER RESOURCES DEVELOPMENT

By

ABDUL WAHED HASSANI

WATER RESOURCES DEVELOPMENT TRAINING CENTRE
UNIVERSITY OF ROORKEE
ROORKEE-247 667 (INDIA)

December, 1984

To
The memory of my
Parents

ACKNOWLEDGEMENTS

SYNOPSIS

Hydraulic fracturing is a live problem these days in the field of geotechnical engineering. The application of the concept of hydraulic fracturing to geotechnical problems, and in particular, to the development of cracks in the core of earth dams due to excessive hydraulic pressure is a matter of concern to researchers and design engineers. Cracks which develop in the impervious core of earth dams and cause leakage, have been observed in Hyttejuvet dam (Norway), Balderhead dam (England) and Teton dam (USA). Hydraulic fracturing is also known to be one of the major causes of loss of drilling fluid through bore-holes in impervious cores of embankment dams.

Hydraulic fracturing is also important in other fields such as in oil exploration, determination of in-situ stresses, evaluation of allowable grout pressures and the pressure in piezometers for determination of in-situ permeability.

The induced cracking in soil mass due to excessive hydraulic pressure is called 'Hydraulic Fracturing'. Hydraulic fracturing would cause water to penetrate through very fine cracks and then would force them to open wider.

The changes in the total stresses which occur in the core of embankment dams during construction, reservoir filling and subsequent drawdowns, test boreholes and grouting are extremely complex and affect the safety against hydraulic fracturing. The contradictory opinions about the parameters involved indicate that a comprehensive investigation is necessary to have

a clear insight into the mechanism of hydraulic fracturing.

A detailed experimental investigation has been carried out here, in order to study the effect of some of the parameters involved in the mechanism of hydraulic fracturing under laboratory controlled conditions. The main factors investigated are; moisture content, confining pressures, degree of saturation, type and rate of hydraulic pressure application, tensile strength of the soil, types of the soil, pattern of cracks and anisotropy of pressure application.

Initially saturated as well as partially saturated solid cylindrical soil specimens having 3.81 cm diameter and 8.2 cm length have been tested in triaxial apparatus under various cell pressures. As a refinement, an improved experimental technique has been developed which consists of testing hollow cylindrical soil specimens of 10.16 cm (4 in) outer diameter, 1.27 cm (0.5 in) inner diameter and 11.3 cm in height representing a confined borehole. Experiments were conducted on saturated as well as partially saturated specimens in triaxial apparatus.

In order to corroborate the results of experimental investigation, theoretical analysis has also been carried out. Stresses have been obtained in the hollow cylindrical specimen subjected to uniform pressures on the inner and outer surfaces considering elastic behaviour of the soil mass. Hydraulic fracturing pressure has been evaluated with the assumption that hydraulic fracturing will take place when the effective stress in the soil mass is tensile and equals the tensile strength of

v

the soil. Since the stresses in the soil mass are limited by the strength of the soil, theoretical analysis based on the well-known Mohr-Coulomb failure criterion has been carried out.

In order to evaluate the effective stresses, a technique based on the finite element method for evaluating pore pressure development under steady state as well as transient conditions in an axisymmetric flow domain has been used. Various parameters affecting the transient flow are studied. These results can be used for prediction of pore pressure throughout the soil mass at different time instants.

The results indicate that hydraulic fracturing in soil mass occurs at hydraulic pressure greater than the confining pressures, with linear relationship between hydraulic fracturing pressure, u_f and the confining pressure, P_o. The increase in compactive water content results in a decrease in u_f value. The increase of moisture content above OMC results in lower value of u_f which increases the potential of occurrence of hydraulic fracturing. Partially saturated specimens indicate higher values of u_f compared to those obtained for saturated specimens. The pattern of cracks observed is more or less vertical for all the specimens tested. Generally with high rate of pressure application, higher value of u_f has been observed.

Theoretical analysis shows a good comparison with experimental results. Both experimental and theoretical investigations show that u_f decreases with increase in the ratio of vertical pressure to lateral pressure. Knowing the pore pressure development and existing state of stresses around boreholes, the

technique developed for prediction of u_f under transient as
well as steady state pressure can be used for field conditions.

Assessment of the safety of an actual high earth and
rockfill dam against hydraulic fracturing has been carried out
based on the available stress analysis of the dam at full re-
servoir condition. The results show that an earth and rock-
fill dam with inclined core shows lower potential against
hydraulic fracturing in comparison of the dam with central
vertical core.

CONTENTS

NOTATIONS

Symbol		Description
A	=	Skempton's pore pressure parameter
a,b	=	Inner and outer radii of hollow cylindrical specimen respectively
[B]	=	Matrix of derivative of shape functions
c,c'	=	Total and effective stress cohesion intercept
C_b	=	Material bulk compressibility
C L	=	Inorganic silty clays with low plasticity
C_r	=	Material matrix compressibility
C_s	=	Compressibility of soil skeleton
C_u	=	Ultimate undrained strength
C_w	=	Compressibility of water
D	=	Diameter of sample for split cylinder test
d	=	Slope of line $\varepsilon_2/\varepsilon_1$ Vs ε_2
E	=	Modulus of elasticity
F	=	Slope of the line of initial tangent Poisson's ratio Vs log (σ_3/P_a)
$\{F_o\}$	=	Matrix of nodal forcing function under steady state condition
$\{F_{(t)}\}$	=	Matrix of nodal forcing function at any time, t
[G]	=	Matrix associated with specific storage of material
H	=	Henry's constant
[H]	=	Matrix associated with permeability of material
K	=	Coefficient of permeability
K_o	=	Coefficient of earth pressure at rest
K_r, K_z	=	Coefficients of permeability in the radial and vertical directions

L	=	Length of sample for split cylinder test
LL	=	Liquid limit of soil
m	=	number of nodal points on which the pressure is to be computed
ML	=	Inorganic clayey fine sands with low plasticity
m_o	=	Slope of line describing variation of u_f with P_o
$[N]$	=	Matrix of shape functions
N_c	=	Bearing capacity factor
n	=	Porosity of the soil
OMC	=	Optimum moisture content
P	=	Applied pressure
P_a	=	Atmospheric pressure
p_i, p_o	=	Internal and external applied pressures respectively
PI	=	Plasticity index
PL	=	Plastic limit of the soil
q	=	The number of boundary nodal points on which the pressure is known
$[R]$	=	Matrix of coefficients of permeability
R_o	=	Centroidal radial distance
r	=	Radial distance at which the stresses are evaluated
r_c	=	Critical radius
S	=	Degree of saturation
S_o	=	Initial degree of saturation
S_1	=	Boundary at which ϕ_i is defined
S_2	=	Boundary at which ϕ_o is defined
S_3	=	Impervious boundary where flow normal to it is zero
S_s	=	Specific storage
t	=	Time parameter
u	=	Pore pressure in soil mass

CANDIDATE'S DECLARATION

I hereby certify that the work which is being present-
ed in the thesis entitled 'HYDRAULIC FRACTURING WITH PARTI-
CULAR REFERENCE TO SOIL CYLINDERS' in fulfilment of the
requirement for the award of the Degree of Doctor of
Philosophy, submitted in the Department of Water Resources
Development Training Centre of the University is an authentic
record of my own work carried out during a period from
June 1981 to December 1984 under the supervision of
Dr. Bharat Singh, Dr. S.S. Saini and Dr. M.C. Goel.
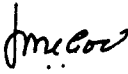
The matter embodied in this thesis has not been sub-
mitted by me for the award of any other degree.

(A.W. Hassani)
Candidate's Signature

This is to certify that the above statement made by
the candidate is correct to the best of our knowledge.

(Dr. S.S. Saini)
Professor
Department of Civil Engineering
University of Roorkee
Roorkee (U.P.), India

(Dr. Bharat Singh)
Vice Chancellor
University of Roorkee
Roorkee (U.P.), India

(Dr. M.C. Goel)
Professor
W.R.D.T.C.
University of Roorkee
Roorkee (U.P.), India

Dated : Dec. 17 ,1984.

u_o = Pore pressure due to P_o under steady state condition

u_b = Water pressure in borehole

u_{ex} = Pressure required to cause cavity expansion

u_f = Water pressure required to cause hydraulic fracturing

u_i = Initial pore pressure

$u_{p\ell}$ = Hydraulic pressure required for initiation of plasticity

y_o = Vertical intercept of line describing variation of u_f with P_o

α = A factor depends on radial distance and dimensions of soil cylinder and determines stresses due to P_i

α_o = Porous elastic parameter

β = The fraction of pore pressure developed in the soil as a function of P_i under transient condition

θ, θ' = Total and effective stress friction angle respectively

γ_w = Unit weight of water

λ = Ratio of vertical stress to horizontal stress

η = Ratio of coefficient of permeability to the specific storage of the soil

υ = Poisson's ratio

$\sigma_1, \sigma_2, \sigma_3$ = Major, intermediate and minor principal total stresses respectively

$\sigma'_1, \sigma'_2, \sigma'_3$ = Major, intermediate and minor principal effective stresses respectively

σ_c = Compressive strength of soil

σ_H, σ_V = Horizontal and vertical total stresses respectively

σ'_H, σ'_V = Horizontal and vertical effective stresses respectively

$\sigma_r, \sigma_\theta, \sigma_z$ = Radial, tangential and vertical total stresses respectively

$\sigma_r', \sigma_\theta', \sigma_z'$ = Radial, tangential and vertical effective stresses respectively

σ_t = Tensile strength of the soil

σ_{θ_o} = Tangential stress due to P_o

$\varepsilon_1, \varepsilon_2$ = Principal strains

$\emptyset$ = Total potential head

$\{\dot{\emptyset}\}$ = Vector of rate of change of potential with respect to time

$\emptyset_o$ = Total potential head at external boundary of the hollow cylinder

$\emptyset_i$ = Total potential head at inner surface of the hollow cylinder

$\emptyset_n$ = Nodal potential head

τ = Normalized factor defined as t/t

Δu = Change in pore pressure

$\Delta \sigma_\theta'$ = Change in effective tangential stress

LIST OF FIGURES

LIST OF PHOTOGRAPHS

LIST OF TABLES

CHAPTER - I

INTRODUCTION

1.1 GENERAL

High fluid pressure may develop cracks in the impervious cores of high earth and rockfill dams. Water may flow through these fine cracks instead of flowing as seepage through soil pores. It is practically impossible to observe these cracks. Failures or damages of earthen structures have been reported to have occurred due to flow of water through such unforeseen cracks. Development of cracks in the impervious core of earth dams and causing leakage, was observed in Hyttejuvet dam[32] and Balderhead dam[70]. Hydraulic fracturing is recognized to be the main cause for the development of cracks in these dams. Hydraulic fracturing is also suspected to have occurred in case of failure of Teton dam.[58,75-77] It is also known to be one of the major causes of loss of drilling fluid through boreholes in impervious cores. Such losses have been reported for many cases, viz., Shek Pik dam, Graminha dam, Djatiluhur dam, Akosombo dam, LaVillita dam, Garrison dam[60,62] and many other dams.

1.2 HYDRAULIC FRACTURING

Hydraulic fracturing is defined as the opening up of tension cracks within the soil mass, due to high fluid pressure when the in-situ effective compressive stresses are reduced to

negative (tensile) value greater than the tensile strength of the soil. Panel on causes of failure of Teton dam[75] defined hydraulic fracturing as the condition leading to the creation and propagation of thin physical séparation in the soil or rock mass due to high fluid pressure. Hydraulic fracturing may cause water to penetrate through very fine cracks and then force them to open wider.

Lofquist[44] mentioned the critical condition for hydraulic fracturing as that in which the total vertical pressure is lower than the reservoir water pressure. Sherard[60], quoted examples of loss of water in boreholes drilled from the crest into clay cores of dams and suggested that the depth at which water loss occurs is that at which the pressure of wash borehole first exceeds the minor principal stress in the soil and the phenomenon could be explained by the mechanism of hydraulic fracturing.

Thus hydraulic fracturing is important in the study of cracking of the cores of dams and also in other fields, such as, to increase the permeability of rock around boreholes in oil wells in order to increase the yield of wells. Haimson[23] proposed the use of this phenomenon for determination of in-situ stresses in rocks. Morgenstern and Vaughan[49] recommended the hydraulic fracturing pressure as an upper limit to allowable grouting pressure. Kennard[33] considered hydraulic fracturing for limiting the pressure which may be applied in performing seepage tests on a borehole or hydraulic piezometer to determine in-situ permeability. Bhandari[4] explained that

hydraulic fracturing is due to local state of zero effective stress generated by fluid pressure. Under such state, clean fine sands liquify, clays develop mud flow volcanoes as the pore water pressure tends to exceed the geostatic stress, and peat generates 'bog bursts'. Thus hydraulic fracturing mainly occurs in fine grained relatively impermeable soils.

The successful correlation of the hydraulic fracturing pressure to the existing state of stress in soil mass around the fracture regions will be a useful technique for prediction of potential for hydraulic fracturing.

1.3 CONFLICTING VIEWS AND GAPS

Significant changes in the total stress and pore pressures occur in an earthen embankment during construction, reservoir filling and any subsequent drawdown. The process of test boreholes for evaluating the quality of core and grouting which are generally performed under high fluid pressures, are very complex as far as the assessment to the risk of hydraulic fracturing is concerned. There are many contradictory opinions about the effect of various parameters involved in the mechanism of hydraulic fracturing. Some of the factors affecting hydraulic fracturing are, the initial state of stress, compactive moisture content, degree of saturation, degree of homogeneity of soil, types of soils and their relative properties, pattern of cracks, duration of hydraulic fracturing test, pore pressure development under steady state as well as transient conditions, type

and rate of hydraulic pressure application etc. Though this problem has been dealt with in detail in Chapter 2, nevertheless to quote one example, Leonards and Narain[42] recommend a wet core to produce flexibility against cracking whereas Kulhawy and Gurtowski[38] are of the opinion that load transfer in case of wet core will be causing more chances of hydraulic fracturing. This shows that many aspects of the phenomenon of hydraulic fracturing are still not well understood.

1.4 SCOPE OF RESEARCH WORK

The present research work was taken up to investigate the phenomenon of hydraulic fracturing in soil mass, with a view to clarify the influence of some of the parameters such as, moisture content, confining pressures, degree of saturation, type and rate of hydraulic pressure application, tensile strength of the soils, type of the soils and anisotropy of pressure application, on the hydraulic pressure at which hydraulic fracturing will occur under laboratory controlled conditions. The study consists of detailed experimental investigation as well as analytical study for determination of hydraulic pressure at which cracks initiate in soil mass and the location of the potential regions of hydraulic fracturing taking into account the effect of pore pressure development under steady state as well as transient conditions and the stress redistribution in the soil mass.

The investigation has been presented under the following subheads.

(i)   Review of literature.

(ii)   Experimental investigation of various parameters on the improved experimental technique developed for study of hydraulic fracturing on hollow cylindrical soil specimens.

(iii) Pore pressure determination under steady state as well as transient conditions of model soil specimen using finite element technique.

(iv)   Analytical investigation of hydraulic fracturing of model soil cylinder and its stress analysis utilizing Mohr-Coulomb failure criterion.

(v)   Comparison of theoretical results with laboratory results and the effect of various parameters on hydraulic fracturing.

(vi)   Assessment of the potential of hydraulic fracturing in a high earth and rockfill dam has also been made.

A review of the literature on hydraulic fracturing in soils has been presented in Chapter 2. Results of tests on solid cylindrical specimens in triaxial apparatus under saturated as well as partially saturated conditions are discussed in Chapter 3.

An improved experimental technique has been developed using hollow cylindrical soil specimens confined at both ends, simulating confined borehole condition in the laboratory. The details of the experimental set-up and the observations during experimentation are presented in Chapter 4. The effect of the various parameters have been studied in detail using this experimental technique. The results of these studies and

corresponding discussions are presented in Chapter 5.

Pore pressure development in the model soil specimen under steady state as well as transient condition has been obtained using finite element technique and presented in Chapter 6. Attempt has been made to investigate the factors affecting pore pressure development under transient conditions.

Chapter 7 presents the theoretical analysis of hydraulic fracturing. Total as well as effective stresses developed in model soil specimen under the action of confining pressures and internally applied pressure which induces cracking in soil mass, have been evaluated. Mohr-Coulomb failure criterion applicable to geotechnical problems has been utilized as a failure criterion. Utilizing pore pressures determined in Chapter 6, expressions for evaluation of hydraulic fracturing pressures under steady state as well as transient conditions are obtained. The technique has been applied to the actual experimental cases and hydraulic fracturing pressure is evaluated. The experimental studies and the conclusions of the study have been presented in Chapter 8.

As an illustration, assessment of the safety of an actual high earth and rockfill dam against hydraulic fracturing has been carried out and presented in Appendix-A. This investigation is based on the available stress analysis of the dam at construction stage and full reservoir condition. Two positions of the core, that is a central vertical core and an inclined core have been considered. The results indicate that

the dam with an inclined core has lower potential against
hydraulic fracturing in comparison to dam with a central ver-
tical core.

CHAPTER - 2

REVIEW OF LITERATURE

2.1 GENERAL

The concept of hydraulic fracturing has been used in petroleum engineering and grouting of rocks, but its importance in geotechnical engineering has been realised recently. In the last few years, some attention has been paid to the mechanism of hydraulic fracturing in the field of geotechnical engineering. Some important theories and their relevant field as well as laboratory measurement studies are discussed in this chapter. Since the field measurement of hydraulic fracturing is generally done in connection with studies of field permeability testing and evaluation of in-situ stresses, a brief summary of existing literature on this aspect is also presented.

2.2 HYDRAULIC FRACTURING IN FIELD PERMEABILITY TESTS AND BOREHOLES

It is well established that water loss from boreholes may occur even in well-constructed dams where no open cracks were observed before the boring was made. Sherard[60] indicated that loss of water from borings flowed through cracks opened by fluid pressure. This may be either due to opening of existing but closed cracks or due to formation of new cracks by fluid pressure. The cases of loss of drilling fluid, for Garrison dam (USA) Lovewell Dam (USA), Djatiluhur dam (Indonesia), Akosombo dam (Ghana), LaVillita dam(Mexico) and El-Isiro dam (Venezuela) have been reported by him.

While drilling borehole at Livingston dam (USA) to install piezometers in foundation, heavy loss of drilling fluid occurred in clay core just above the foundation. It was inferred that the fluid pressure in a borehole during drilling can be very much higher than the weight of a static column of water, and higher pressure can be caused by partial obstruction of the return flow of the drilling fluid and can then cause hydraulic fracturing. The rate of drilling is another important factor. Dry cracks on transverse slopes between two sections of Ilha-Solteira dam (Brazil), constructed at different times, were extended upto a depth of 2m, and resulted in deep erosion gullies from rain runoff. Water was also lost at a boring drilled for piezometer installation at a depth where boring passed through transverse junction. It was concluded that water lost might be due to localized zone of low stress in the embankment.

The outflow in-situ permeability test (where a positive excess head is applied), is often preferred to the inflow test, because it may be carried very quickly. In situations of low permeability the tendency is to use high pressure in order to give adequate flow readings within a reasonable time. This may lead to incorrect results due to occurrence of hydraulic fracturing around piezometers and may record high permeability as compared to the actual field value.

Bjerrum et al[9] carried out permeability tests in impervious core of a dyke in Israel. The core consisted of natural clay dumped into slurry trench. To evaluate the quality of the core, permeability tests were performed by pushing a

porous bronze piezometer into the core and then measuring the
rate of water loss from it by applying an excess head less
than the effective weight of the column of soil above the piezo-
meter indicating the core permeability of the order of 10^{-4} cm/sec.
Further tests were performed at very low head and the permeabi-
lity of unfractured clay at these low heads was of the order
of $2x10^{-7}$ cm/sec., but this increased rapidly when the testing
pressure exceeded by about 50% of the effective overburden pre-
ssure, at piezometer tip.   A number of inflow tests (where
head was reduced below the static ground water level) confirmed
that the true permeability was much smaller than 10^{-4} cm/sec.
It was concluded that the increase in permeability was the
result of hydraulic fracturing around the piezometer, which
occurred at excess head as low as 20% of effective overburden
pressure. The reason for occurrence of hydraulic fracturing
at such low pressure was that the effective vertical stress
in the core was probably smaller than the weight of overburden
due to arching of the core. Additional tests at Fornebu (Oslo)
indicated that hydraulic fracturing occurred at an excess head
of 67% to 86% of effective overburden pressure.

Vaughan[69] reported the observations of water losses
from holes drilled into the core of Balderhead dam after crack-
ing of the core of the dam. Results of water loss tests and
the settlement observations indicated that cracking had taken
place at a number of areas in the dam, but water loss was also
observed in boreholes in areas where evidence suggested that
cracking had not taken place.   It was indicated that these
water losses probably occurred as a result of hydraulic

fracturing of the soil around boreholes. Consequently tests were conducted to determine pressure to cause fracture as well as the close-up pressure. The scatter for fracturing pressure was high whereas close-up pressures were more consistent and were nearer to minor principal stress (σ_3) determined for the dam. Studies of close-up pressures indicated that once fractures were created, they could be re-opened at lower pressures than the required pressures to open them initially.

Tests on small embedded piezometers were performed at Cow-Green dam, when dam was completed to its two-third height. The results showed that the fracture test did not increase the permeability of the clay around the piezometers and fracture pressures were generally equal to nominal overburden pressures.

As there was no damage to the core of Cow-Green dam, by fracture tests, the same were also done at Balderhead dam. Pressure equal to nominal overburden was applied and delayed fracture was observed after five minutes. It was found that the fracture pressure was approximately equal to the overburden pressure. It was also mentioned that the fracture pressure showed great variation but in short term tests, they were much higher than those observed in the water flush tests.

Based on the principle of hydraulic fracturing, i.e. when a crack first appears, the water pressure at which it closes again, may be more reliable as an evaluation of lateral stresses in the ground, Bjerrum and Andersen[8] performed in-situ permeability tests in which water was first forced into the soil to form crack and then water pressure was decreased while observing the flow of water into the clay as well as

the decrease of pressure. An abrupt reduction in the flow of water into the clay was observed when the crack closed. The reason for this was attributed to the fact that contact area between water and clay was drastically reduced. The pressure at which the crack closes is measured, and if the total stresses across the crack are unchanged, this closure pressure is believed to be a close approximation of the total stress across the crack.

It is indicated that due to higher permeability of coarse grained soils, the method is limited to clays. It is also expressed that for K_o (ratio of minor principal stress to major principal stress) values greater than one, a horizontal crack will open and the method will just measure the weight of overburden and therefore, the method can not be used in over-consolidated clays where K_o is greater than one. The results indicate that K_o is approximately constant with depth, and it may increase with time.

Penman and Charles[55] have reported detailed field investigations of the clay core of 80 years old and 20m high Cwmwerndcri dam (England). Vertical boreholes were made by hand augering from dam crest and Cassagrande type stand pipe piezometers were installed at various depths on the centre line of the core near the major section of the dam. Tests were carried out by raising the water level in the stand-pipes to cause hydraulic fracturing in the surrounding clay and then decreasing the pressure. The critical pressure was defined as the pressure at which the excess flow rate decreases to a value compatible with the permeability of clay. The study has

shown that critical pressure can be regarded as a conservative estimate of the pressure required to cause hydraulic fracturing across the core of the dam.

Lefebvre et al[41] carried out hydraulic fracturing tests in the field in two geologically different sensitive clay deposits in order to study the fracture pattern formed around inserted piezometers. The result of these tests indicated that fracture mode is not unique i.e. the hypothesis that only vertical fractures develop in normally consolidated clay, (Bjerrum and Andersen[8]) was not verified. But vertical fractures radiated out from piezometer tips as well as cracks inclined from 20° to 35° from the horizontal, formed an inverted cone-shaped fractures with its apex at the top of piezometer were observed. It is also mentioned that, as hydraulic fracturing test would be sensitive to fluid pressure, it would lead to an overestimate of K_o.

Various researchers have performed in-situ hydraulic fracturing tests by increasing the water pressure in either open boreholes or piezometers. A review of all these tests shows clearly that hydraulic fracturing can easily be induced in boreholes. The pressure required to cause hydraulic fracturing is highly variable, and depends on many parameters such as the in-situ stresses, rate at which the water pressure is increased, the deformation and strength characteristics of the soil, the shape of the borehole or piezometer and the method used to create the borehole or place for the piezometer in the ground. Unfortunately, the separate effects of each

of these factors can not be effectively evaluated from the results of in-situ tests.

2.3 LABORATORY STUDIES OF HYDRAULIC FRACTURING

The literature review of in-situ hydraulic fracturing investigations presented in the preceeding section, has clearly indicated the importance of hydraulic fracturing in geotechnical engineering. The effect of various parameters involved in the mechanism of hydraulic fracturing indicates the necessity of laboratory controlled investigations. In this section some of the case studies of hydraulic fracturing tests performed in the laboratory, are reviewed.

Haimson[23] performed hydraulic fracturing tests on rock samples of 12.7 cm cubical as well as 12.7 cm diameter and 15.2 cm high cylindrical specimens. A vertical borehole was made in the centre of the specimen. The tests were conducted by pressurizing the fluid in the borehole while the external loads were kept constant. The test results indicated that hydraulic fractures were tensile failure and no shear failures were observed.

Bjerrum et al[9] conducted laboratory tests in soil deposit by inserting 6 mm diameter piezometers in soil filled in a tank (Fig. 2.1). The tank had porous stones at both sides which were connected to reservoirs. By varying the reservoir level from one side of the tank relative to the other and waiting until the inflow equalled the outflow, a measure of the overall permeability was obtained. When the monitoring

piezometer showed the ground water level to have returned to the ground surface, an excess head was applied to the second piezometer and maintained for a time interval during which readings of inflow against time were taken. The applied head was increased in increments of 10 cm of water and maintained for a similar period of time while readings of flow rate were taken, until the measured flow rate showed a fundamental change. This was indicated by a sudden rapid rise in the rate of flow of water into the soil. It was concluded that hydraulic fracturing may occur in the flow permeability tests at smaller pressure than overburden pressures.

In the experimental set-up, the specimen is open to atmospheric pressure at the top and there is no arrangement for side pressures as well, the set-up can not be classified as a true representative of actual site conditions.

Bjerrum and Andersen[8] simulated the field test in a triaxial apparatus, where a piezometer 2.7 mm in diameter and 40 mm long was pushed in from the bottom in soil specimen 7.98 cm in diameter and 13 cm long. The specimen was enclosed in a rubber membrane and consolidated under $\sigma_1 = 2\sigma_3$ as shown in Fig. 2.2. The pressure in piezometer was increased to a certain critical value, remained constant for a short time and then started to decrease. In a short time rubber membrane bulged out and the pore pressure increased in the top of specimen, indicating that a crack had been formed. The pressure in piezometer was then decreased and the flow rate was recorded.

The results indicated that the closure pressure was equal to cell pressure, and vertical crack formed extending
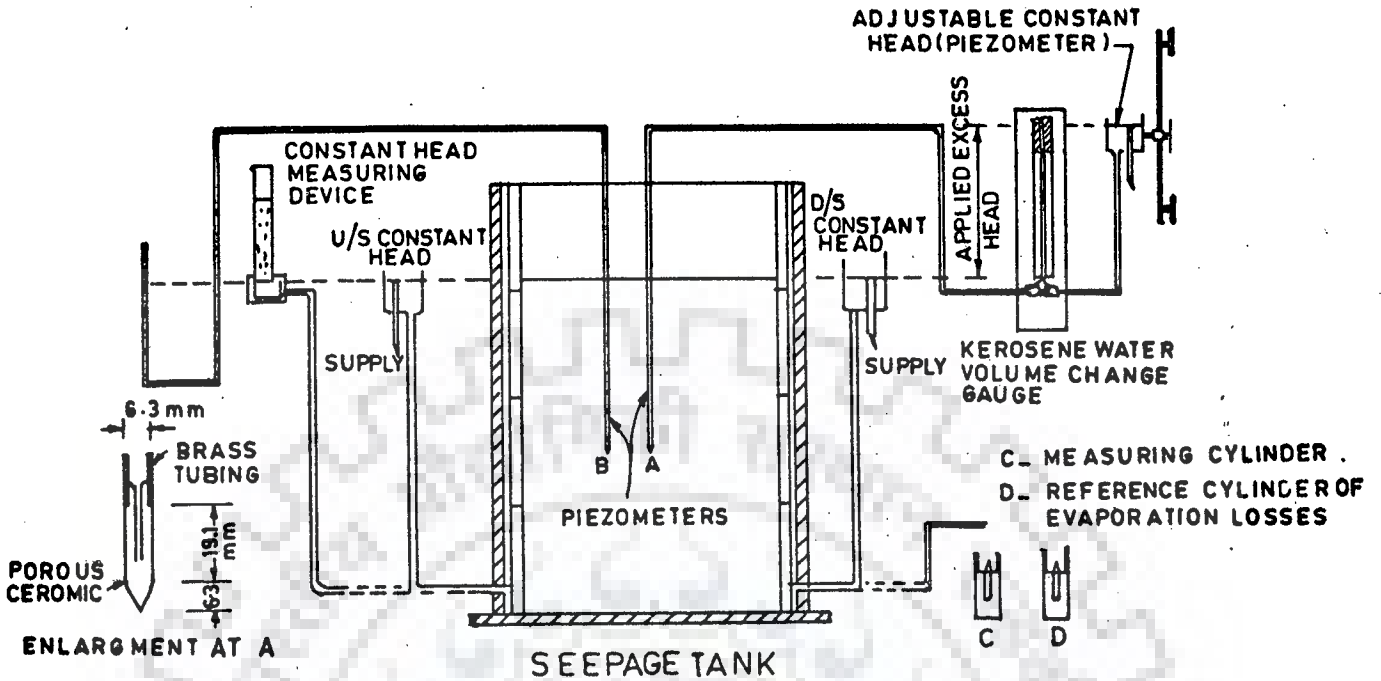
FIG. 2.1 _ TANK FOR MODEL TESTS
(AFTER BJERRUM ET AL, 1972)
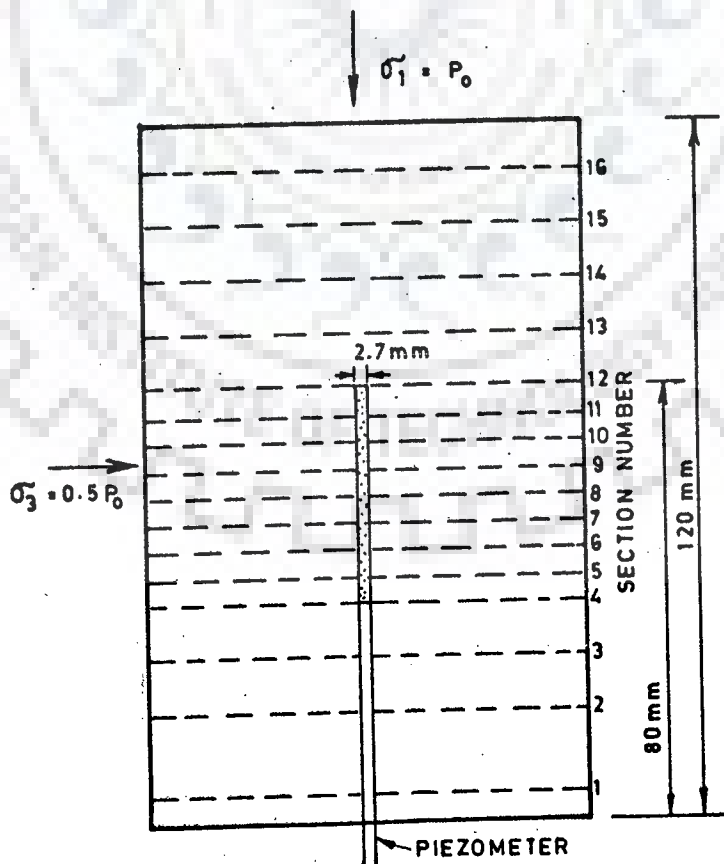
FIG. 2.2 _ SIMULATION OF FIELD TEST IN THE LABORATORY;
SKETCH OF THE SPECIMEN WITH THE PIEZOMETER
(AFTER BJERRUM AND ANDERSON, 1972)

from the tip of the piezometer.

Pushing of 2.7 mm diameter piezometer up to the centre of the specimen, is a difficult task unless otherwise the specimen belongs to soft clay category. In the case of soft clay, any insertion would increase the density around the piezometer tip resulting in increased value of the hydraulic fracturing pressures over the actual value. In case of hard clays, perhaps a drill hole would be required to insert the piezometer and the water may come out along the periphery of the piezometer rather than finding its way into the specimen for causing hydraulic fracturing. Moreover drilling of hole in a small soil specimen will result in stress redistribution around the hole.

Nobari et al[50] carried out, triaxial tests on sandy clay samples of 3.6 cm diameter and 8.9 cm height to investigate hydraulic fracturing. A hole of 0.65 cm diameter was drilled along the axis and filled with sand to which internal pressure was applied to cause hydraulic fracturing. A thin sand layer enclosed in a membrane surrounding the soil was used to apply an external water pressure independent of internal pressure. Cell pressure and deviator stress was also controlled independent of these water pressures (Fig. 2.3). Hydraulic fracturing was caused by the following combination of applied fluid pressure.

(1)   Reducing axial stress, but in the first set internal
        water pressure was kept greater than external, whereas
        in the second set external water pressure was more
        than internal pressure. In both sets hydraulic frac-
        turing was observed to occur gradually along a hori-
        zontal plane. In third set both external and internal
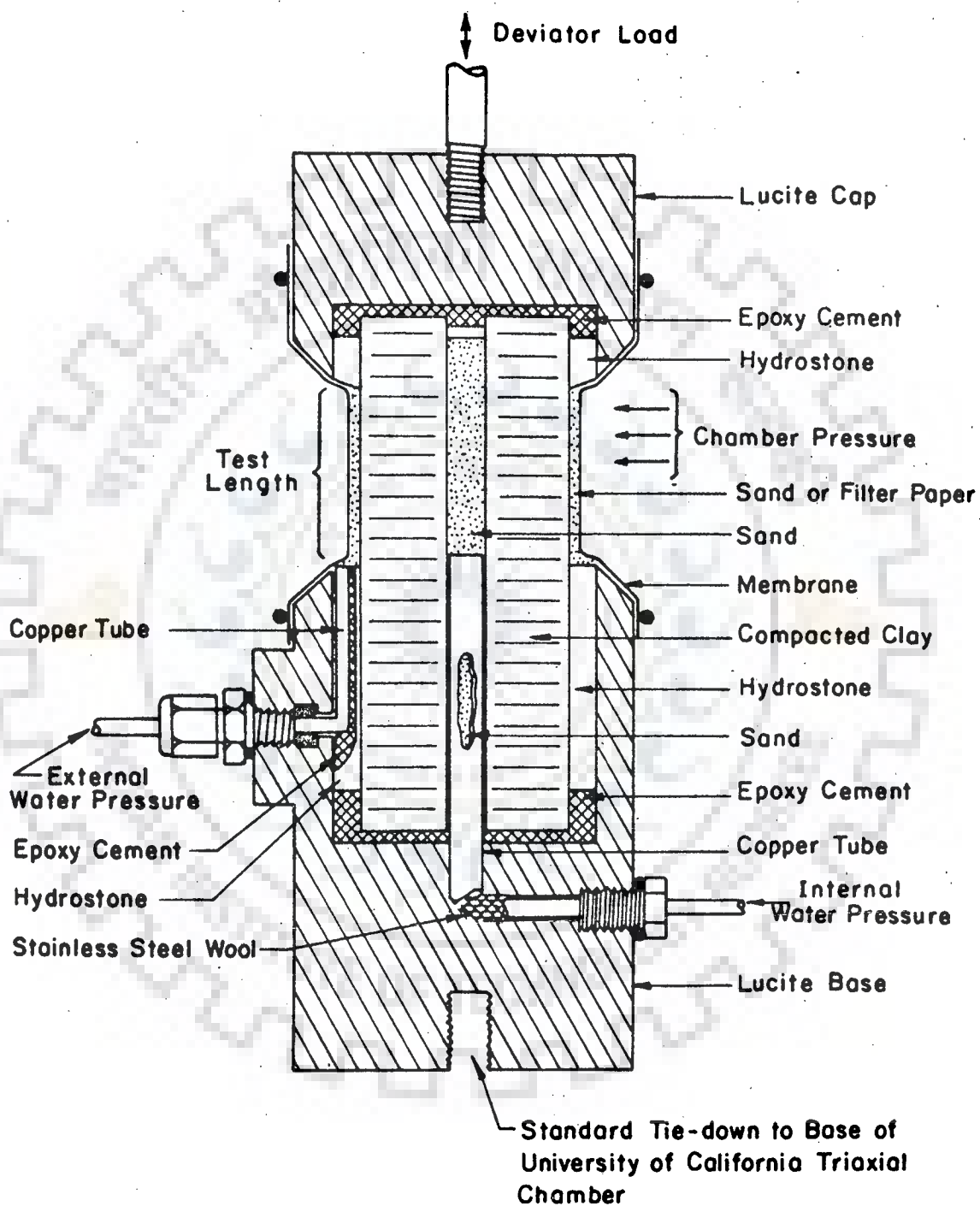
FIG. 2·3 APPARATUS FOR HYDRAULIC FRACTURING
EXPERIMENT

(AFTER NOBARI ET AL., 1973)

pressures were kept constant and a sudden failure along horizontal plane was observed.

(2)   Increasing internal water pressure but keeping external pressure, chamber pressure and deviator stress as constant. The axial stress was greater than chamber pressure, and the failure was along vertical plane.

It was concluded that the mechanism of hydraulic fracturing is a tension fracture developing on the plane of maximum tensile stress. Shear failure or plastic flow was not observed. This is in agreement with the findings of Haimson[23].

Nobari's work gives a good indication of the mechanism of fracture initiation as well as its orientation in the soil mass. However, it is worth mentioning that test length of the soil sample subjected to pressure, is a small fraction of the sample length, thus nonuniformity of stress distribution exists in the soil specimen, specially at the junction of length surrounded by sand and the portion covered by solid lucite material. Further, drilling of 0.65 cm hole in a sample of 3.6 cm diameter may itself create very weak region and stress redistribution and uneven borehole surface which may affect the hydraulic fracturing pressure. The test arrangement indicates that in case if external pressure through sand pocket is higher than the chamber pressure, the bulging of rubber membrane may take place thus reducing the effective external pressure. Moreover, there will not be any significant effect of chamber pressure. In case the chamber pressure is greater than the external pressure as in that case, the external pressure on the specimen would be controlled by chamber pressure and there is no significant use of

external pressure. Thus a need is indicated for further improvement on the testing procedure and experimental set-up.

Jaworski, Duncan and Seed[31] studied borehole fracture tests in the laboratory. In this study cubical soil samples were placed in a 20.3 cm cubical stress apparatus where three independent stresses were applied to the faces as shown in Fig. 2.4. A 0.48 cm diameter uncased borehole, 6.1 cm long was drilled in the centre of the sample and was sealed at the top with an epoxy plug. Water pressure was then applied to the walls of the borehole through a steel tube cemented with epoxy. The material used in the experimental study was obtained from the remainder of core of Teton dam after its failure. This material consisted primarily of ML aeolian silt with small particles of caliche. The samples were trimmed or compacted to form 19 cm cubes and placed in the 20.3 cm cubical apparatus, and the remaining gap around the sample was filled with compacted soil of the same origin. The applied σ_1 was equal to $2\sigma_3$ and the intermediate stress σ_2, was equal to σ_3. Remoulded samples were compacted at 2% dry of optimum, and at 3% wet of optimum, to about the same dry density as the undisturbed block samples.

The test results indicated that hydraulic fracturing pressure was highly variable, because of differences in composition, the densities, the water content, or any combination of these for undisturbed samples. However, for all the tests, hydraulic fracturing pressures u_f, were higher than the total horizontal confining stresses σ_H. Following were the conclusions for these test results.

(1) Variation in soil composition had more pronounced effect on hydraulic fracturing pressure than the variation in density or water content.

(2) For the same composition and density, measured values of u_f were usually higher for samples having lower water content.

(3) The measured value of tensile strength of soil, σ_t, using Brazilian tests as compared to the difference of u_f and σ_H indicated that $u_f - \sigma_H$ were considerably greater than σ_t. Thus the difference between u_f and σ_H can not be explained by σ_t.

(4) u_f was higher for long duration tests. The effect was explained to be due to difference in the extent of the zone of seepage which developed over a longer period of time.

(5) The measured value of u_f increased as σ_H increased.

(6) Higher the compactive effort (and higher dry density), higher is u_f, though the scatter is large. Inconsistent effect of u_f was observed for small variation in densities with same compactive efforts.

It is apprehended that hydraulic fracturing pressure recorded by Jaworski et al[31], might not be true representative because of the following reasons.

(i) Compacting soil in the gap of soil sample and cubical apparatus with steel bar may not result in uniform compaction. At corners it is practically impossible to attain uniform compaction.

(ii) Drilling of the hole in soil specimen would create unevenness at borehole surface as well as stress redistribution in soil mass.

(iii) Hydraulic fracturing pressure is applied only in 5.1 cm test length of specimen against its total length of 19 cm.

(iv)   Water used for hydraulic fracturing tests is not free
of air bubbles as the apparatus consists of air-water
interface chamber. The air bubbles may penetrate in
soil pores and may create negative pressure condition,
thus increasing the effective stress of soil which
would naturally require higher u_f value.

(v)   There is no mention about the degree of saturation of
the specimens tested. The value of strength parameters
indicate that the specimens are not tested under full
saturation condition. Thus the existence of negative
capillary pressure may have contributed to increase the
effective stresses which obviously affect the fractur-
ing pressure.

Decker and Clemence[12] have also reported laboratory
tests to study hydraulic fracture   initiation in soils. The
experimental set-up is shown in Fig. 2.5. The needle was
placed in the soil sample (classified as CL and compacted
at standard Proctor's compaction) such that the holes were
located on the central axis of the cylindrical sample. Sample
was fractured by injecting excess water pressure through the
needle after consolidation as well as back pressure saturation
of the specimen in triaxial cell. The fluid pressure for frac-
turing was increased at uniform rate which was monitored by pore
pressure transducer. Abrupt increase of flow of water through the
flow meter resulted in sudden drop of pressure in the trans-
ducer indicating the occurrence of fracture in sample. The
following were their findings -

(i)   A linear relationship was found to exist between the
pore pressure required to fracture the sample and the
confining pressure.
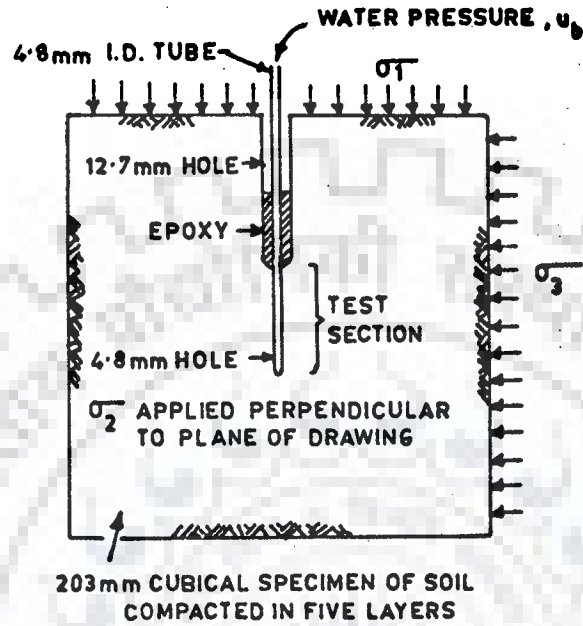
FIG.2·4-LABORATORY TEST OF HYDRAULIC
FRACTURING AROUND MODEL BOREHOLE

(AFTER JAWORSKI ET AL.,1981)
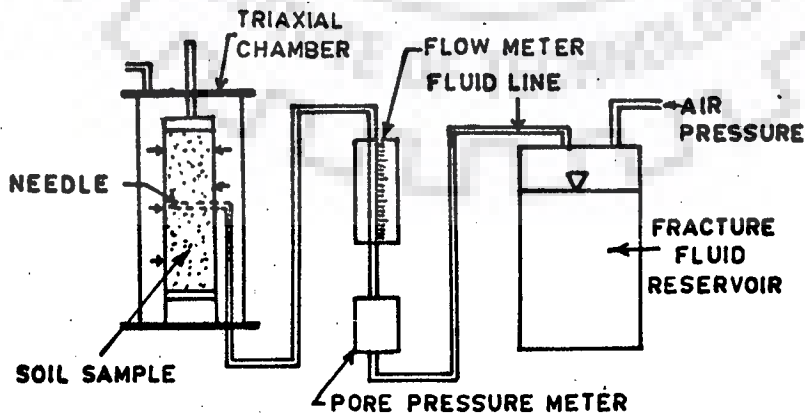
FIG.2·5- DIAGRAM OF HYDRAULIC FRACTURE EQUIPMENT

(AFTER DECKER AND CLEMENCE,1981)

(ii)   The pore pressure to cause fracture at zero confining pressure is a measure of the tensile strength of soil.

(iii) The measured tensile strength was found to be in close agreement with the value that may be predicted from a Mohr-Coulomb analysis.

It is felt that insertion of needle horizontally into the specimen, may create a weak zone by itself, thus increasing the potential of hydraulic fracturing even at low pressures. Further, silicon grease used for sealing between needle and soil specimen might not withstand the high pressures applied through the needle. Also the air-water interface in fluid reservoir, may cause negative pressures in soil sample due to injection of air bubbles as was apprehended in the experimental set-up of Jaworski et al[31].

The review presented in the preceeding paragraphs, highlights the various approaches of different experimental set-up used for evaluation of hydraulic fracturing in the laboratory. With a view to minimize the uncertainities about some of the parameters involved in the mechanism of hydraulic fracturing, an experimental technique has been developed independently. The details of experimental set-up and the results of parameters investigated, are presented elsewhere in this thesis.

2.4 THEORETICAL BACKGROUND OF HYDRAULIC FRACTURING

The review of the research work done by various researchers has shown that the water pressure required to cause hydraulic fracturing is highly variable and depends upon many complex parameters. If the mechanism of hydraulic fracturing can be

related successfully to stresses in soils around the fracture regions, it may be a useful method for prediction of crack occurrence. With this end in view, the conditions and criteria for the occurrence of hydraulic fracturing proposed by various authors are presented in the subsequent paragraphs.

Gibson and Anderson[21] analysed the case of radial stresses under plane strain condition for an ideal elastoplastic material using modulus of elasticity E, Poisson's ratio ν, and ultimate undrained strength C_u. For initiation of plasticity the hydraulic fracturing pressure required would be given by,

$$u_{p\ell} = K_o \; \sigma'_z + u_i + C_u \qquad \qquad ..(2.1)$$

whereas, indefinite expansion of the cylindrical cavity would occur at a pressure given by;

$$u_{ex} = K_o \; \sigma'_z + u_i + C_u \left(1 + \ell n \frac{E}{2C_u(1+\nu)}\right) \qquad ..(2.2)$$

where,

σ'_z = initial vertical effective stress

K_o = ratio of initial horizontal effective stress to the initial vertical effective stress

u_i = initial pore pressure

Ladanyi[39] has shown that the pressure required to expand a spherical cavity at depth is comparable to the ultimate bearing capacity of a pile point and can be given as

$$u_{ex} = K_o \; \sigma'_z + N_c \; C_u \qquad \qquad ..(2.3)$$

where, N_c is the bearing capacity factor, N_c may be of the order of 9.0 for a spherical cavity and of the order of 7.0

for a cylindrical cavity.

To minimize the time required for grouting operation in a borehole by increasing grout pressure but without causing hydraulic fracture, Morgenstern and Vaughan[49], presented a theoretical analysis for isotropic media. They used the Mohr-Coulomb failure criteria with the assumptions, that (i) the presence of borehole does not disturb the stresses in the formation, (ii) the change in total stress around the borehole resulting from increasing the water pressure in the borehole was insignificant compared to the changes in the effective stress which results from an increase in pore pressure, (iii) the distance over which the crack propagates, is small and thus changes in stress in the formation due to cracks are neglected. Based on these assumptions, they gave the following equation for hydraulic fracturing pressure, u_f.

$$u_f = \frac{\sigma_1 + \sigma_3}{2} - \frac{\sigma_1 - \sigma_3}{2 \sin\theta'} + c' \cos\theta' \qquad ..(2.4)$$

where,

σ_1 and σ_3 are the major and minor principal total stresses, c' is the effective stress cohesion and θ' is the effective angle of internal friction.

The sensitivity of equation 2.4 for changes in c', θ' and σ_1/σ_3 was studied by drawing u_f vs σ_3, by varying one of these parameters and keeping others constant. The results showed that the occurrence of tensile failure increases with increasing strength and increasing principal stress ratio.

Haimson[23] carried out theoretical analysis of formation of hydraulic fracturing around a borehole in rock assuming

that the rock behaves as a brittle, elastic, homogeneous, iso-
tropic, porous material and flow follows Darcy's law. He uti-
lized an analogy between thermoelasticity and porous elasti-
city to determine the stress changes resulting from the flow
of fluid through the pores. He also assumed that tectonic
stresses in the ground redistribute themselves around a cylin-
drical borehole according to the Kirsch[34] solution for a
circular inclusion in an elastic stress field. According to
him the application of fluid pressure in a borehole possibly
results in two additional stress changes. One is due to the
fluid pressure at the borehole wall u_b, and can be viewed as
an internal pressure acting on an infinitely thick hollow
cylinder. The other stress change occurs if the fluid is able
to penetrate the rock and flow through the pores.

With increase of pore fluid pressure, the tangential
stresses σ_θ in the material around the borehole would decrease
and eventually become tensile. At the time of hydraulic frac-
turing u_f, is equal to the borehole fluid pressure (u_b) and the
effective tangential stress (σ_θ') become tensile equal in magni-
tude to σ_t. For the case of an equal all-round horizontal effec-
tive stress $(\sigma_H' = \sigma_2' = \sigma_3')$, the following equation for evalua-
tion of u_f is given :

$$u_f = \frac{\sigma_t + 2\sigma_H'}{2 - \alpha_o(\frac{1-2\nu}{1-\nu})} + u_i \qquad \text{..(2.5)}$$

where α_o is the porous elastic parameter, given by

$$\alpha_o = 1 - (C_r/C_b) \qquad \text{..(2.6)}$$

where C_r = material matrix compressibility

C_b = material bulk compressibility.

For soil the value of α_o would usually be between 0.9 and 1.0.

This theory indicates that the hydraulic fracturing pressure is dependent on the initial effective horizontal stress, tensile strength of material, the compressibility of material, Poison's ratio and initial pore pressure. The u_f value will always be greater than the initial horizontal stresses.

Kennard[33] was concerned with predicting a lower bound pressure below which a constant head permeability test could be performed safely, and gave the following expressions using Gibson's[21] approach.

(i) Drained Condition : Full build-up of seepage pressure around borehole

$$\frac{\Delta u}{\sigma'_z} = \frac{2K_o}{1+\nu} \text{ or } 1 \qquad \text{(whichever is least)} \qquad ..(2.7)$$

where Δu is increase in fluid pressure in borehole above initial pore pressure.

(ii) Undrained Condition : Non penetrating fluid

$$\frac{\Delta u_c}{\sigma'_z} = K_o + \frac{K_o}{2A} \text{ or } 1 \quad \text{(whichever is least)} \qquad ..(2.8)$$

where A is the Skempton's[64] pore pressure coefficient.

Vaughan[69] proposed a mechanism for hydraulic fracturing in an embankment due to reservoir filling in terms of total and effective stresses on Mohr-Coulomb diagram (Fig. 2.6). From this figure it could be seen that cracking would occur when $\sigma'_3 = 0$, $u_f = \sigma_3$, and σ_t is ignored. If σ_t is to be
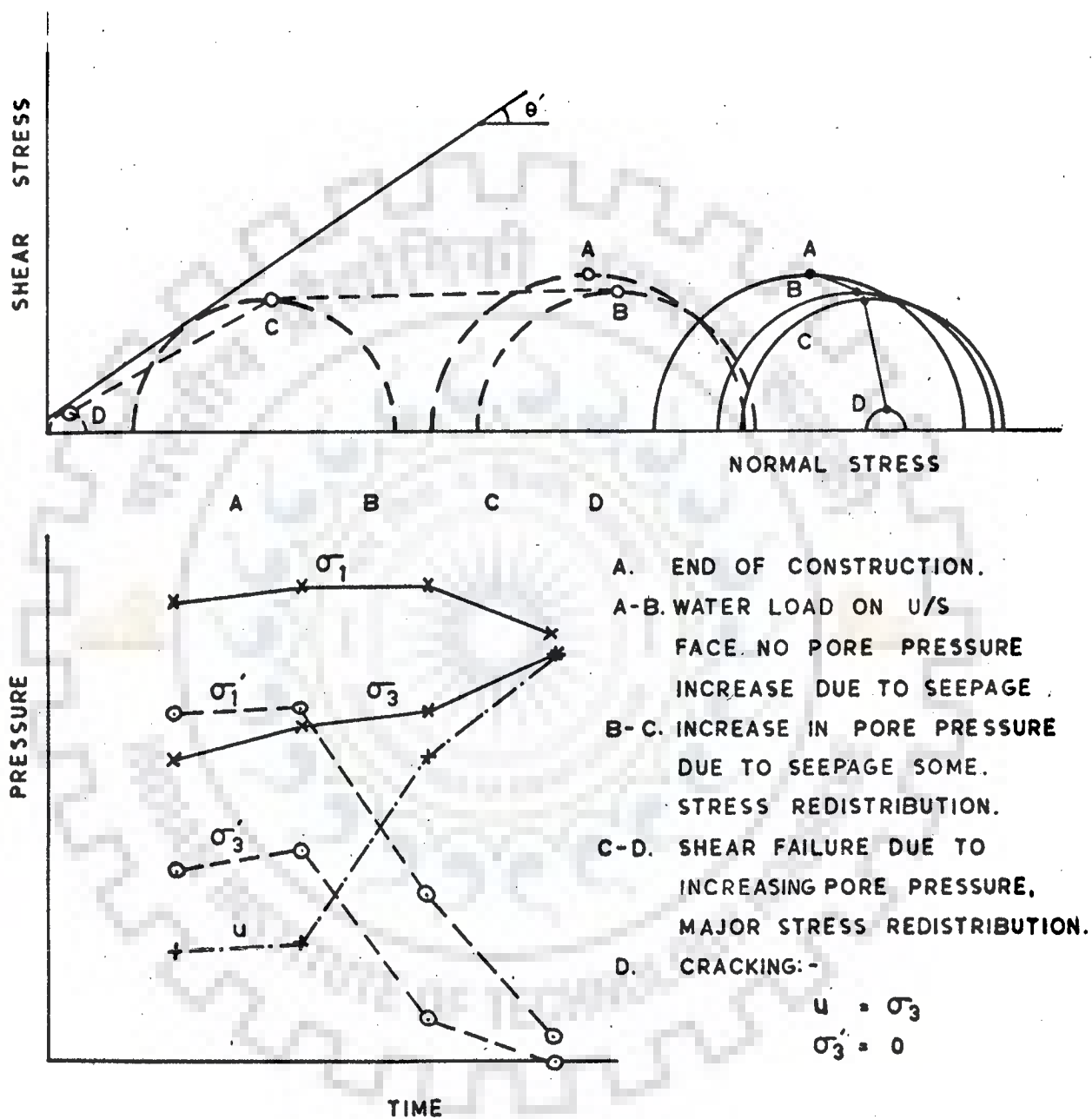
FIG. 2·6 POSSIBLE CRACKING MECHANISM
IN TERMS OF EFFECTIVE STRESS
(AFTER VAUGHAN , 1971)

taken into account, the crack will be formed when the effective stress across a plane becomes tensile by an amount greater than σ_t. The reservoir filling would result in an increase in the stresses in the core due to the water load on the upstream face of the dam, and the changes in effective stress would result in some stress redistribution. If the pore pressure is sufficient enough to induce shear failure, major stress redistribution will take place. It has been shown in Fig. 2.6, that if pore pressure is increased further during steady seepage condition, the stress redistribution would result in an increase in σ_3 and a decrease in σ_1. Thus fracture could be expected to occur when σ_3' becomes less than the tensile strength of the soil.

It was mentioned that a lower bound fracture pressure would be obtained if the soil was assumed to behave elastically, and hydraulic fracturing is assumed to occur, when the effective stress becomes tensile by an amount greater than the tensile strength of the soil. If plasticity is allowed for, an upper bound solution may be obtained by analyzing the pressure required to expand a cavity. The pressure required for cavity expansion would be much greater than the fracture pressure predicted by elastic theory. This suggests that plastic deformation may inhibit hydraulic fracturing. Sherard's[60,61] views are similar to those of Vaughan[69].

Bjerrum et al[9] developed a theory for avoiding hydraulic fracturing in permeability tests. They assumed that the soil is isotropic, homogeneous, fully saturated, elastic and semi-infinite in mass. The piezometer through which excess hydraulic pressure was injected, cylindrical in shape, having diameter much less than its length and of high permeability as

compared to soil, was assumed to be rigid. Plastic strains developed in soil around piezometer during its driving into the soil, were accounted for. The theory takes into account the initial state of stresses, water pressure in the ground, changes in these stresses due to piezometer installation and any other disturbance, magnitude of pressure head and its variation with time as well as deformation characteristics. They have mentioned that as hydraulic excess head is gradually applied, the soil skeleton will experience an outward drag force in radial direction leading to radial movement. At a certain value of excess head, the effective radial stress (σ'_r) in soil next to piezometer will have reduced to zero. Any further increase of head will cause movement of the soil skeleton away from the tip and create a water filled cavity around the tip. The critical head at which such 'blow off' occurs is equal to σ'_r next to piezometer.

It was concluded that for conditions analyzed, the ratio of $\frac{\Delta u}{\sigma'_z}$ (where Δu is the excess pore pressure to cause hydraulic fracturing and σ'_z, the effective vertical stress) varied between 0.5 and 1.0 and the values of excess head at which it is safe to carry out the field permeability tests are therefore very low. It is also mentioned that in situations where arching takes place and σ'_z may be less than the nominal overburden pressure, fracturing occurs merely by filling the borehole casing with water during drillings. The cases of sudden loss of borehole fluid may be due to this cause.

The theory developed by Massarsch[46] for hydraulic fracturing in borehole is based on the assumptions, that

(i) the length of the cylindrical cavity is infinite, (ii) the soil behaves as an ideal elasto-plastic, isotropic material, (iii) expansion of cavity is unaffected by the magnitude of the critical water pressure in the clay, (iv) the soil is saturated and undrained, (v) the effect of arching around the borehole or pre-existing fissures or cracks in the soil is neglected.

The pressure required to cause cavity expansion is given by the following equation,

$$u_{ex} = C_u \ln \left[\frac{1.36\ E}{C_u(1+\nu)} \right] \qquad ..(2.9)$$

where E and ν are elastic parameters and C_u is the undrained shear strength.

Changes in total stress within plastic zone are found to be a function of the radial distance from the borehole, and the changes in pore pressure Δu, within the soil mass due to the applied pressure in the borehole can be determined using Skempton's[64] pore pressure parameter, A. The resultant effective tangential stress (σ_θ') would be given as

$$\frac{\Delta \sigma_\theta'}{C_u} = -0.428 - 1.733A \qquad ..(2.10)$$

For a fracture to occur as a result of cavity expansion, the changes in tangential stress must equal or exceed the horizontal effective stress (σ_H'), neglecting σ_t of the soil, i.e. $\sigma_H' + \Delta \sigma_\theta' \leq 0$, the condition required for hydraulic fracturing to occur in a plastic zone around the borehole is expressed as,

$$\sigma_H' = C_u\ (1.73A + 0.43) \qquad ..(2.11)$$

For the values of σ'_H greater than that given by equation (2.11), hydraulic fracturing is possible and the fracturing pressure is given that by equation (2.9), for smaller values, hydraulic fracturing is not possible.

Jaworski, Duncan and Seed[30] also used Kirsch[34] solution for investigating hydraulic fracturing theoretically around a circular hole in soil mass. They assumed that the soil mass is impermeable, linearly elastic and, stress deformation is taking place under plane strain condition. Using superposition, the tangential stress distribution was found by adding the changes in stress resulting from an increase in borehole water pressure u_b, (Timoshenko and Goodier[68]), and the initial stress distribution because of all-round pressure (Kirsch[34]).

For hydraulic fracturing to occur around a borehole, the maximum tangential effective stress must be tensile by an amount equal to σ_t, and u_b will be equal to u_f. Thus,

$$u_f = \sigma_H + \frac{\sigma_t}{2} \qquad ..(2.12)$$

This equation indicates that hydraulic fracturing is affected by state of existing stress and tensile strength of material.

To study the importance of actual stress-strain behaviour of soils, Jaworski et al[30] performed an axisymmetric finite element analysis considering non-linear, stress-strain behaviour of the soil. Material properties were those reported by Independent Panel[75] for the Teton dam core material. The results indicated that hydraulic fracturing pressure is always greater than σ_H and the difference increases with increase of

σ_H. The range of hydraulic fracturing pressure calculated using different values of ν, E, c and Θ was quite small. The effect of varying each of them showed that none of these has a significant effect on the value of u_f.

It was also indicated that the non-linear behaviour of soil has only a small effect on u_f. The elastic analysis indicated that u_f value was independent of soil properties, with the exception of σ_t. The finite element analysis leads to the same conclusions, indicating that the value of u_f was quite insensitive to the properties of the soil.

Using core material properties of Teton dam, a comparative study of the theories presented by Morgenstern and Vaughan[49], Haimson[23], Vaughan[69], Massarsch[46] and Jaworski et al[30] for evaluation of hydraulic fracturing is reproduced in Fig. 2.7 (Jaworski et al[30]). It is seen that an upper bound solution is obtained using Massarsch's[46] criterion, while Morgenstern and Vaughan's[49] criterion predict that u_f occurs at a borehole water pressure even lower than horizontal stress. Morgenstern's theory was later amended by Vaughan[69] stating that the u_f values must at least be equal to σ_H.

In this comparison, the effect of σ_t and the initial pore pressures were neglected, while each of the criterion indicates that hydraulic fracturing will take place when the effective stress in the soil becomes tensile. The higher value of Massarsch's criteria is due to the assumption that pressure required to expand a cavity plastically is the highest pressure which a borehole can support, while the lower bound solution

(k/ft^2)

Massarch (1978)
(Upper bound solution)

Vaughan (1971)

Haimson (1968)

Morgenstern and
Vaughan (1963)

(k/ft^2)

Elastic Analysis

Finite Element Method

u_f – Hydraulic Fracturing Pressure (kg/cm^2)

σ_H – Horizontal Stress (kg/cm^2)
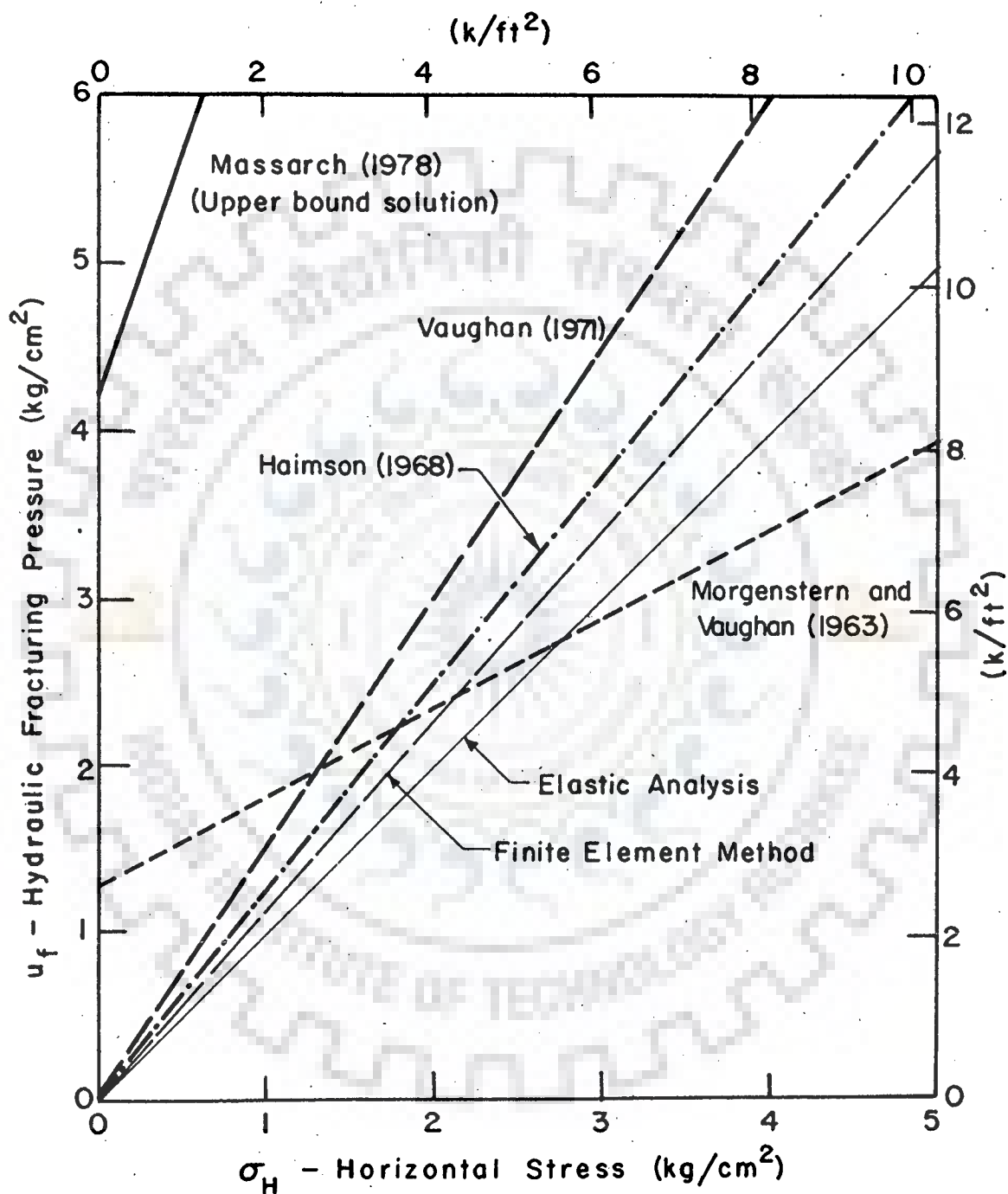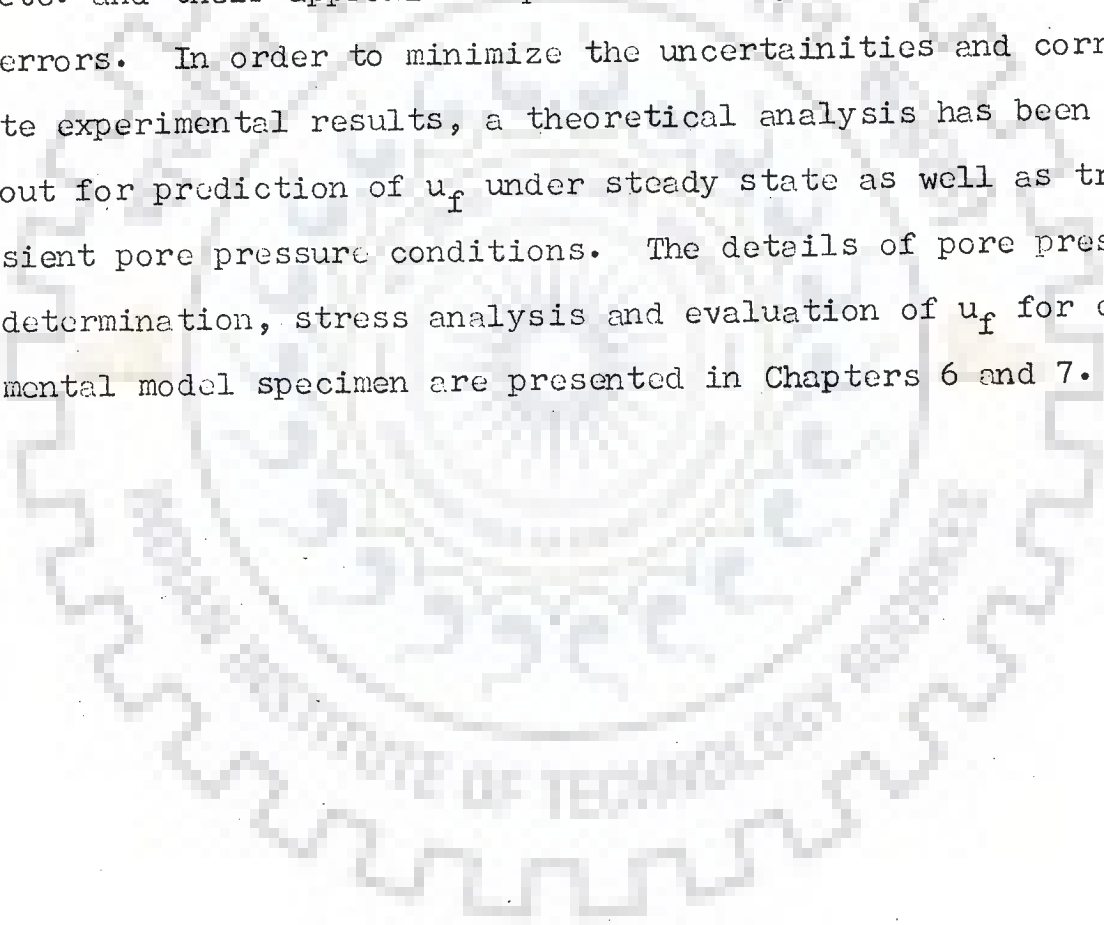
FIG. 2·7   COMPARISON OF PORPOSED CRITERIA
FOR HYDRAULIC FRACTURING

(AFTER JAWORSKI ET AL. 1979)

assumes linear behaviour and stress distributions are not accounted for.

It is seen that different approaches have been used for stress analysis and evaluation of u_f by different researchers. The difference involved in the exact evaluation of some of the parameters, such as compressibility of soil, elastic parameters (E and ν), Skempton's pore pressure coefficient, etc. and their approximate prediction may involve considerable errors. In order to minimize the uncertainities and corroborate experimental results, a theoretical analysis has been carried out for prediction of u_f under steady state as well as transient pore pressure conditions. The details of pore pressure determination, stress analysis and evaluation of u_f for experimental model specimen are presented in Chapters 6 and 7.

CHAPTER - 3

EXPERIMENTAL INVESTIGATION USING SOLID CYLINDRICAL SPECIMENS

3.1 GENERAL

So far, limited experimental work has been done to evaluate the mechanism of hydraulic fracturing in soil mass. It is felt that more detailed investigations are needed to have a clear insight into the mechanism of hydraulic fracturing.

At the initial stage of experimental studies, solid cylindrical soil specimens having 3.81 cm diameter and 8.2 cm height were tested in triaxial apparatus to investigate the induced hydraulic fracturing pressure at various confining pressures under controlled laboratory test conditions. This test set-up is shown in Fig. 3.1, but the experimental technique and test set-up were subsequently changed and an improved set-up has been used for further investigations.

3.2 EXPERIMENTAL SET-UP

Fig. 3.1 shows a diagrammatic layout of experimental set-up, composed of various units. The lateral pressure assembly is used for the application of chamber pressure in triaxial cell through a water-air interface. The air pressure supplied from compressor will push water into the triaxial cell. The gauge mounted on top of the assembly will indicate the confining pressure. The triaxial cell consists of a perspex chamber to
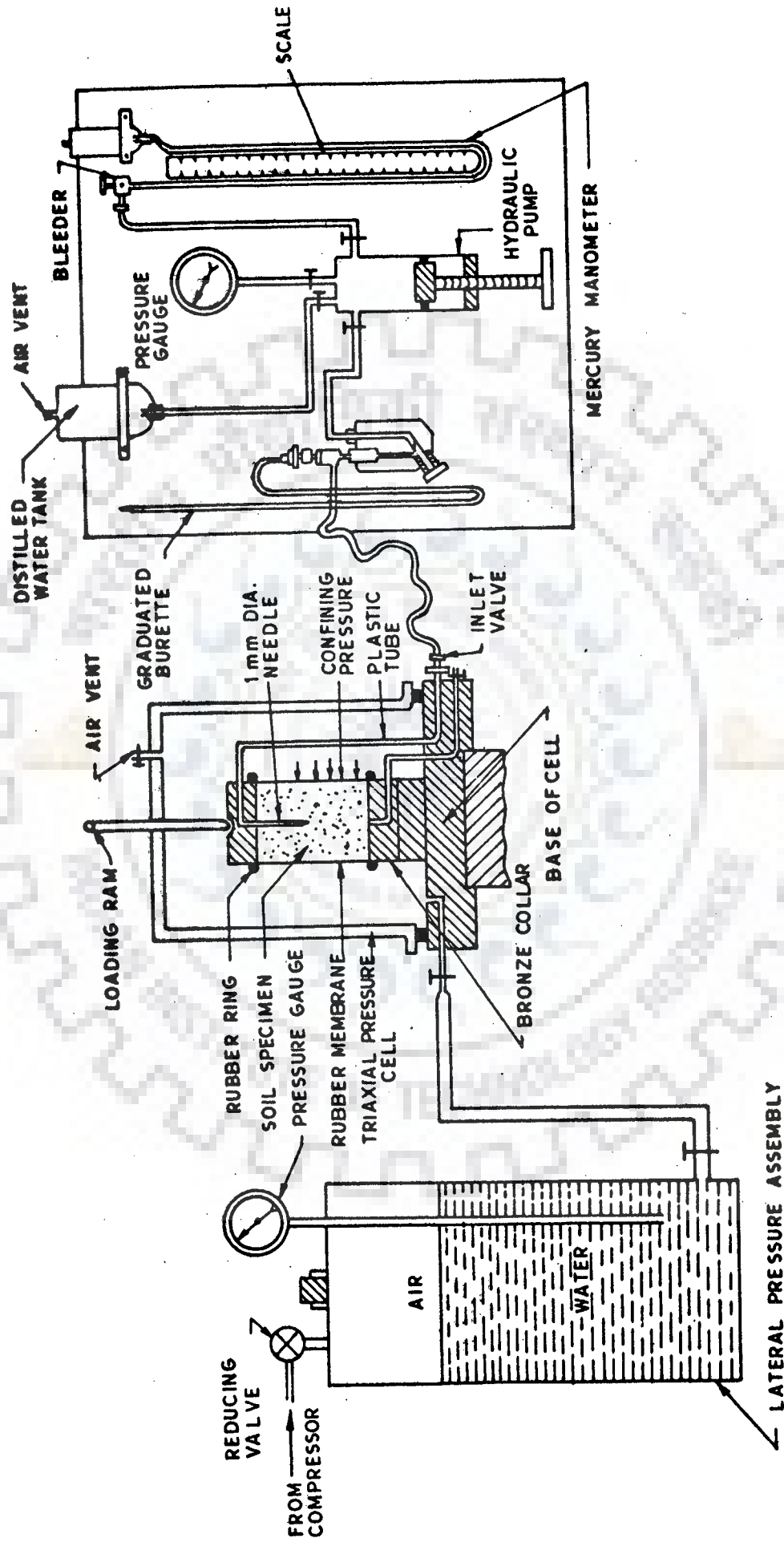
FIG. 3.1 - DIAGRAMMATIC LAYOUT OF EXPERIMENTAL SETUP

38

accommodate the soil specimen and confining fluids. The soil specimen is enclosed in a rubber membrane and placed in the triaxial cell. Hydraulic pressure is applied through the needle inserted axially through the specimen by means of the Bishop's pore pressure apparatus.

3.3   EXPERIMENTAL SOIL AND SPECIMEN PREPARATION

The soil used for testing is classified as CL according to unified soil classification system. This soil is called soil 'A' throughout the present discussion and subsequent chapters. The index properties of the soil are given in Table 3.1

TABLE 3.1   CHARACTERISTICS OF SOIL 'A'

Liquid limit	= 32.5 %
Plastic limit	= 22 %
Plasticity index	= 10.5 %
Optimum moisture content(Proctor's)	= 16.5 %
Dry density at OMC	= 1.77 g/cm^3
Angle of internal friction (drained test)	= 27°
Cohesion	= 0.10 Kg/cm^2
Permeability (Saturated condition and compacted at OMC)	= 3.95x10^{-7} cm/sec
Porosity (compacted at OMC)	= 33.5 %
Void ratio (compacted at OMC)	= 0.521
Specific gravity	= 2.68
Sand	= 40 %
Silt	= 41 %
Clay	= 19 %

For preparing specimen, 2.0 Kg soil was oven dried for a minimum of 24 hours, and then cooled in desicator to avoid the absorption of air moisture. The soil was broken with a

wooden mallet and screened through No. 40 sieve. The calculated amount of water was added to bring it up to OMC. After proper mixing of soil it was collected in plastic bags and kept for seasoning in a humid chamber for 24 hours. The correct moisture content of the soil was ascertained before compaction at standard Proctor compactive effort. Cylinders of 8.2 cm height and 3.81 cm diameter were prepared by driving sampling tubes into the Proctor mould and extracted by the sample extractor. Thereafter, soil cylinders were cut to size very carefully.

3.4 EXPERIMENTAL TECHNIQUE AND TESTING PROCEDURE

Two bronze collars, 3.5 cm in length and 3.81 cm in diameter were fabricated[24]. One of these collars had an injection needle of 1.0 mm diameter at the centre. The needle has circular holes at the periphery and the length is equal to half that of the soil specimen.

A thin layer of adhesive was applied on the upper collar and the soil specimen surface in order to have a watertight interface between the collar and the soil specimen. The specimen was enclosed in a rubber membrane and subjected to saturation through the bottom. The soil specimen achieved near full saturation in a minimum time of 10 days under a head of water of 30 cms from the base of the specimen. Saturation was ensured by observing flow of water through the needle inserted axially in the specimen.

Experiments were conducted by placing the specimen in a triaxial apparatus (Fig. 3.1). Tests were conducted at various cell pressures. Hydraulic fracturing was induced by increasing water pressure linearly through the inserted needle. The failure was detected by sudden drop of mercury level in the manometer as well as pressure gauge depending on the range of pressure. The reduction in pressure indicates the initiation of cracks in the soil mass. The failure pressure was recorded as the hydraulic fracturing pressure under corresponding confining pressure. In order to get consistent values, three to five specimens were tested for each range of confining pressure. The applied confining pressure range is from zero to 2.2 Kg/cm^2.

Partially saturated specimens of the same size and prepared under similar conditions as above, have also been tested. These tests were conducted immediately after compaction at OMC, allowing a nominal time for the adhesive to set, while necessary precautions were taken to prevent the specimen from drying.

The results of both series of tests i.e. saturated and partially saturated specimens are presented in Table 3.2.

3.5 EVALUATION OF TENSILE STRENGTH OF SOIL

Cracking in an earth structure develops in regions of tensile strain resulting from the application of various loads on the structure as well as geometery of the construction site and types and properties of embankment materials. Tensile strength of the soil plays an important role in order to

TABLE 3.2   RESULTS OF SOLID CYLINDRICAL SPECIMENS

Sl. No.	Confining pressure (Kg/cm²)	Hydraulic fracturing pressure (Kg/cm²)	Sl. No.	Confining pressure (Kg/cm²)	Hydraulic fracturing pressure (Kg/cm²)
SATURATED SPECIMENS					
1	0.00	0.132	15	0.80	0.817
2		0.140	16		1.004
3		0.098	17		0.985
4		0.151	18		1.023
5		0.129	19		0.994
6		0.143	20		1.012
7	0.40	0.639	21		0.982
8		0.647	22		0.967
9		0.529	23		1.023
10		0.486	24	1.60	1.933
11	0.60	0.800	25		1.933
12		0.874	26	2.20	2.531
13		0.874	27		2.611
14		0.774	28		2.496
PARTIALLY SATURATED					
1	0.00	0.800	12	0.80	1.825
2		0.963	13		1.820
3		0.942	14	1.44	2.450
4		0.858	15		2.750
5	0.23	1.300	16		2.650
6		1.214	17		2.400
7		0.956	18		2.250
8		0.953	19		2.450
9	0.66	1.675	20		2.350
10		1.750	21	1.98	3.100
11		1.450	22		3.400

decrease the potential of cracking, specially in the mechanism of hydraulic fractures. In this study Brazilian testing technique[1] has been adopted to determine the tensile strength of the soil under investigation.

When cylindrical specimen is compressed diametrically, uniform tensile stress would develop normal to the loaded diameter causing the cylinder to fracture along the diametral plane. It has been mathematically shown by Timoshenko and Goodier[68] that a compressive load applied perpendicularly along the axis of the cylinder, will result in tensile stress, acting normal to the loaded diameter in a diametral plane. The magnitude of tensile strength σ_t, could be obtained as,

$$\sigma_t = \frac{2P}{\pi D L} \qquad \qquad ..(3.1)$$

where P is the applied load, D is the diameter and L is the length of the soil cylinder. The same has also been observed by Frocht[18] in the photo-elastic studies on a circular disc.

Soil samples compacted at OMC according to standard Proctor's compaction have been tested both under partially saturated as well as under fully saturated conditions for evaluation of tensile strength. The test set-up and failure mode of specimens are shown in Photos 3.1 and 3.2, respectively. The details of the results are presented in Table 3.3. From this table it will be seen that under saturated condition, the tensile strength of the soil varies from 0.100 to 0.114 Kg/cm^2 with an average value of 0.105 Kg/cm^2, whereas at OMC the same varies from 0.211 to 0.286 Kg/cm^2 with an average value of 0.249 Kg/cm^2.
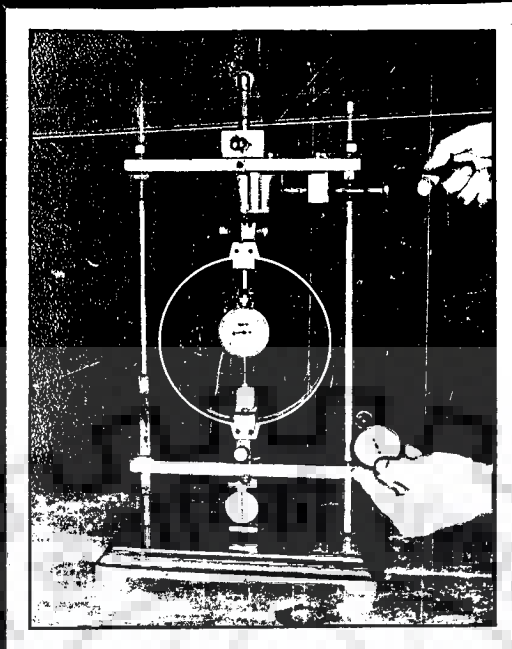
PHOTO: 3·1 - TENSILE STRENGTH TEST SET-UP
(SPLIT CYLINDER TEST)

PHOTO: 3·2 - FAILED SPECIMENS OF SPLIT
CYLINDER TESTS

TABLE 3.3 TENSILE STRENGTH OF SOIL 'A'

Sl. No.	Tensile Strength (Kg/cm^2)	
	Partially saturated (at OMC)	Saturated Condition
1	0.238	0.100
2	0.286	0.114
3	0.211	0.101
4	0.226	-
5	0.286	-
Average	0.249	0.105

The average tensile strength at -1% OMC for partially saturated specimens has been evaluated as 0.460 Kg/cm^2.

3.6 ANALYSIS AND DISCUSSIONS

To evaluate the effect of confining pressures on fracture initiation in soil under various confining pressures, the average experimental tests results are plotted in Fig. 3.2. Curve I shows the plot between observed hydraulic fracturing pressure (u_f) and confining pressure (P_o) for saturated specimens and curve II for partially saturated samples (at OMC).

The plots show that u_f is a linear function of P_o. The linear relationship between u_f and P_o has been also reported by other researchers[12,31]. At full saturation when confining pressure is equal to zero the only resisting strength can be the tensile strength of the soil. In case this is valid, the linear relationship may be written as

$$u_f = m_o P_o + y_o$$

..(3.2)

TABLE 3.3 TENSILE STRENGTH OF SOIL 'A'

Sl. No.	Tensile Strength (Kg/cm^2)	
	Partially saturated (at OMC)	Saturated Condition
1	0.238	0.100
2	0.286	0.114
3	0.211	0.101
4	0.226	-
5	0.286	-
Average	0.249	0.105

The average tensile strength at -1% OMC for partially saturated specimens has been evaluated as 0.460 Kg/cm^2.

3.6 ANALYSIS AND DISCUSSIONS

To evaluate the effect of confining pressures on fracture initiation in soil under various confining pressures, the average experimental tests results are plotted in Fig. 3.2. Curve I shows the plot between observed hydraulic fracturing pressure (u_f) and confining pressure (P_o) for saturated specimens and curve II for partially saturated samples (at OMC).

The plots show that u_f is a linear function of P_o. The linear relationship between u_f and P_o has been also reported by other researchers[12,31]. At full saturation when confining pressure is equal to zero the only resisting strength can be the tensile strength of the soil. In case this is valid, the linear relationship may be written as

$$u_f = m_o \, P_o + y_o \qquad ..(3.2$$

FIG. 3.2 - HYDRAULIC FRACTURING PRESSURES VS
CONFINING PRESSURES

where m_o is the slope of the line and y_o is the vertical inter-cept of the line at zero confining pressure. The prediction of slope and vertical intercept are a complex phenomenon and may depend upon strength of the soil and the way of redistribution of effective stresses take place in the soil which change as a result of increase in pore pressure.

Curve I indicates that when confining pressure is equal to zero, the value of hydraulic fracturing pressure is equal to 0.130 Kg/cm^2 which is in close agreement with the saturated tensile strength of the soil. It is seen from Curve II that when confining pressure is equal to zero, the value of hydraulic fracturing pressure is about 0.85 Kg/cm^2, whereas average value of tensile strength of the partially saturated samples at OMC was of the order of 0.25 Kg/cm^2. It is thus seen that the value of u_f at zero confining pressure is higher than the ten-sile strength of the soil. The higher value of u_f for partially saturated condition might be due to the following reasons,

(i)   In performing hydraulic fracturing tests, hydraulic pre-ssure was applied at a point through the inserted needle inside the specimen. In such a case, the pressure dis-tribution is not uniform throughout the length of the specimen. In contrast, tensile strength tests were conducted under uniform load distribution through the horizontal strips over the full length of the specimen.

(ii)   As injection needle for application of hydraulic frac-turing pressure is inserted up to the mid-height of the specimen, therefore, penetration of water in lower half will be less as compared to the upper half. Thus the effect of time needed for water pressure to act on the

full surface of the specimen may have caused an increased value of u_f.

(iii)   Since water pressure is applied as a point load through the needle, therefore, water may spread in spherical direction causing three dimensional effect instead of two dimensional effect as expected in a cylindrical soil specimen subjected to all-round uniform pressures. Thus three dimensional effect of water penetration could cause higher values of u_f.

CHAPTER - 4
IMPROVED EXPERIMENTAL TECHNIQUE FOR INVESTIGATION OF HYDRAULIC FRACTURING USING HOLLOW CYLINDERS

4.1 GENERAL

The experimental set up and the results obtained from hydraulic fracturing tests performed on solid cylindrical specimens have been discussed in Chapter 3. With a view to better representation of stress conditions in a borehole, an improved technique based on testing of hollow cylindrical soil specimens which is nearer to actual borehole conditions, has been developed. The experimental technique adopted and described is an improvement over the experimental techniques used by previous researchers reviewed in Chapter 2.

The technique developed can be used with the help of a triaxial apparatus. The experimental technique is based on the measurement of induced hydraulic fracturing pressure inside a hollow cylindrical soil mass subjected to all-round confining pressures, representing confined borehole conditions.

The main factors investigated in this study affecting hydraulic fracturing are; compactive moisture content, degree of saturation, confining pressures, type and rate of hydraulic pressure application, tensile strength of the soil, types of soil, pattern of cracks and anisotropy of pressure application.

4.2 EXPERIMENTAL TECHNIQUE

4.2.1 Experimental Set-Up

Fig. 4.1 shows a diagrammatic layout of the experimental set-up consisting of four units. Unit I consists of soil specimen enclosed in a rubber membrane and placed in the triaxial cell. In order to assess the measurement of the volume changes which may take place in the specimen during testing, a single burette volume change apparatus (Unit II) is used. The constant pressure self compensating mercury control system (Unit III) is used for application of confining pressures. This apparatus maintains constant confining pressures in the triaxial cell throughout the test period, regardless of the volume change occurring in the cell due to expansion of the cell chamber under high pressures, minor leakage, entry of loading plunger into the cell, distortion and consolidation of the soil specimen. Bishop's pore pressure apparatus[7] consisting of hand operated screw type hydraulic pump, pressure gauge, manometer but without null indicator as shown in Unit IV, was used for application of hydraulic fracturing pressure.

4.2.2 Soil Specimen Preparation

The soil specimen as shown in Photo 4.1 was used for hydraulic fracture testing. It was prepared in Proctor's compaction mould. A steel rod 1.27 cm (0.5 in) in diameter was placed centrally in the compaction mould with the help of a 0.4 cm thick plate having a hole of 1.28 cm in the centre to accommodate the steel rod. The outer diameter of the plate is

UNIT-I _ TRIAXIAL SETUP

UNIT-II _ VOLUME CHANGE DEVICE

UNIT-III _ CONSTANT PRESSURE SELF COMPENSATING MERCURY CONTROL SYSTEM

UNIT-IV _ BISHOP PORE PRESSURE APPARATUS
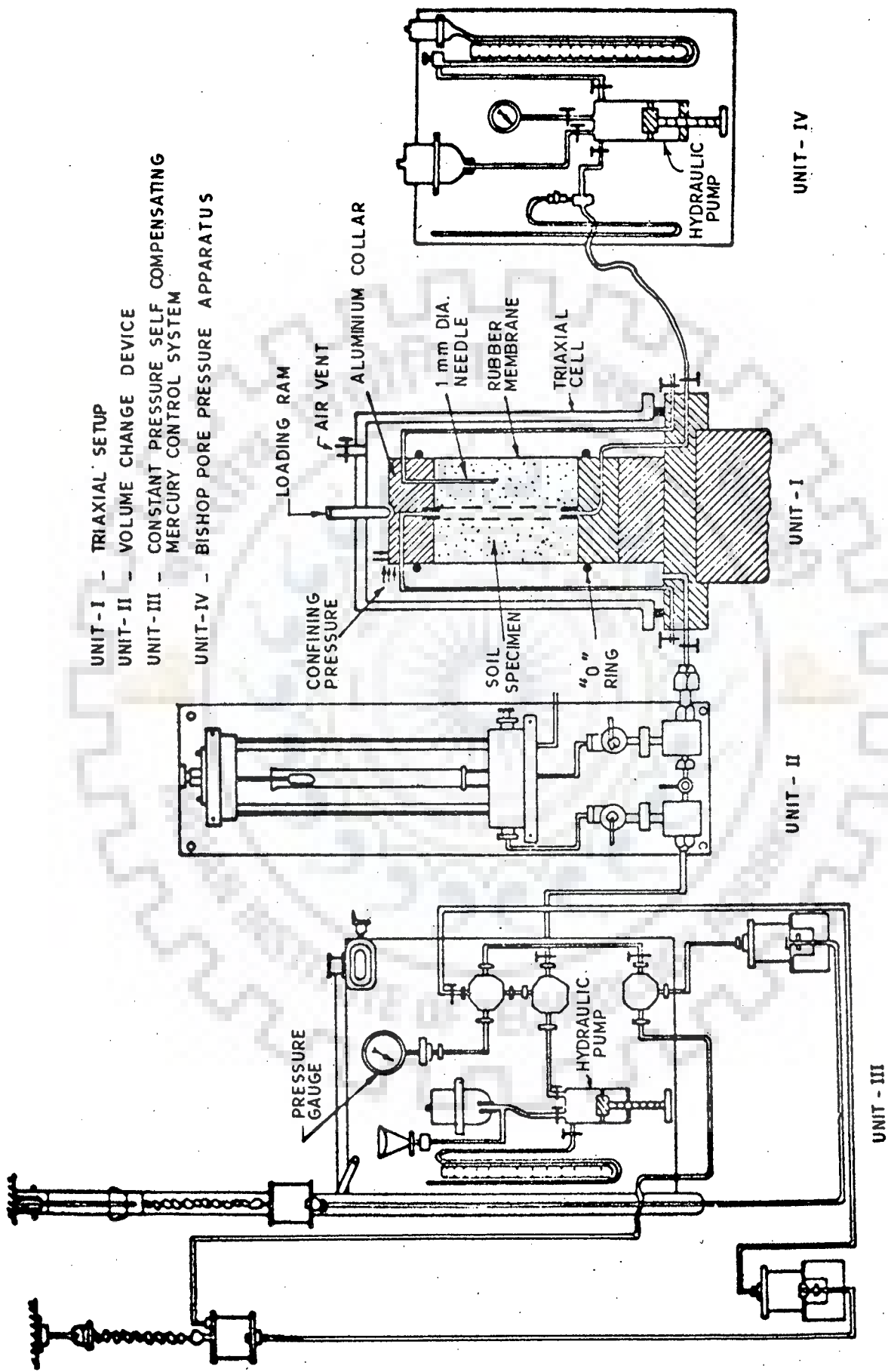
FIG. 4.1._ DIAGRAMMATIC LAYOUT OF EXPERIMENTAL SETUP FOR HOLLOW CYLINDRICAL SOIL SPECIMEN WITHOUT BACK PRESSURE SATURATION AND WITHOUT PORE PRESSURE MEASUREMENT

51

equal to the inner diameter of the compaction mould. Photo 4.2 shows the steel rod and circular plate placed in position on the base plate of Proctor's mould.

Since a rod is placed in between the Proctor's compaction mould, the conventional blows by Proctor's compaction hammer directly over the soil would not be able to compact the soil uniformly to the required density. Therefore, a rigid frame assembly as shown in Fig. 4.2 was fabricated. The rigid frame is 20.3 cm high having three 1.2 cm thick plates at top, bottom and middle supported by four welded steel rods. The diameter of the three plates of this frame is just under size to 10.16 cm (4 in) i.e. internal diameter of Proctor's mould. The middle and bottom plates have 1.3 cm hole at the centre to accommodate the steel rod.

The soil mixed with distilled water, was put in the annular space in three layers in between cylindrical walls of Proctor's mould and the steel rod. After placing the soil the rigid frame was placed over it and soil layer was compacted by giving blows of standard Proctor's hammer over the top plate of the frame. Photo 4.3 shows the set-up of compaction of specimen. The number of blows required were calibrated to obtain the density equivalent to that of standard Proctor's compaction. After compaction excess soil around the steel rod was trimmed off so as to flush the compacted soil with the top of the compaction mould. Base plate was opened and the soil specimen along with the steel rod was taken out from the mould with the help of sample extracting frame. Thereafter, central rod was slowly pulled out of the specimen by hand without disturbing the soil
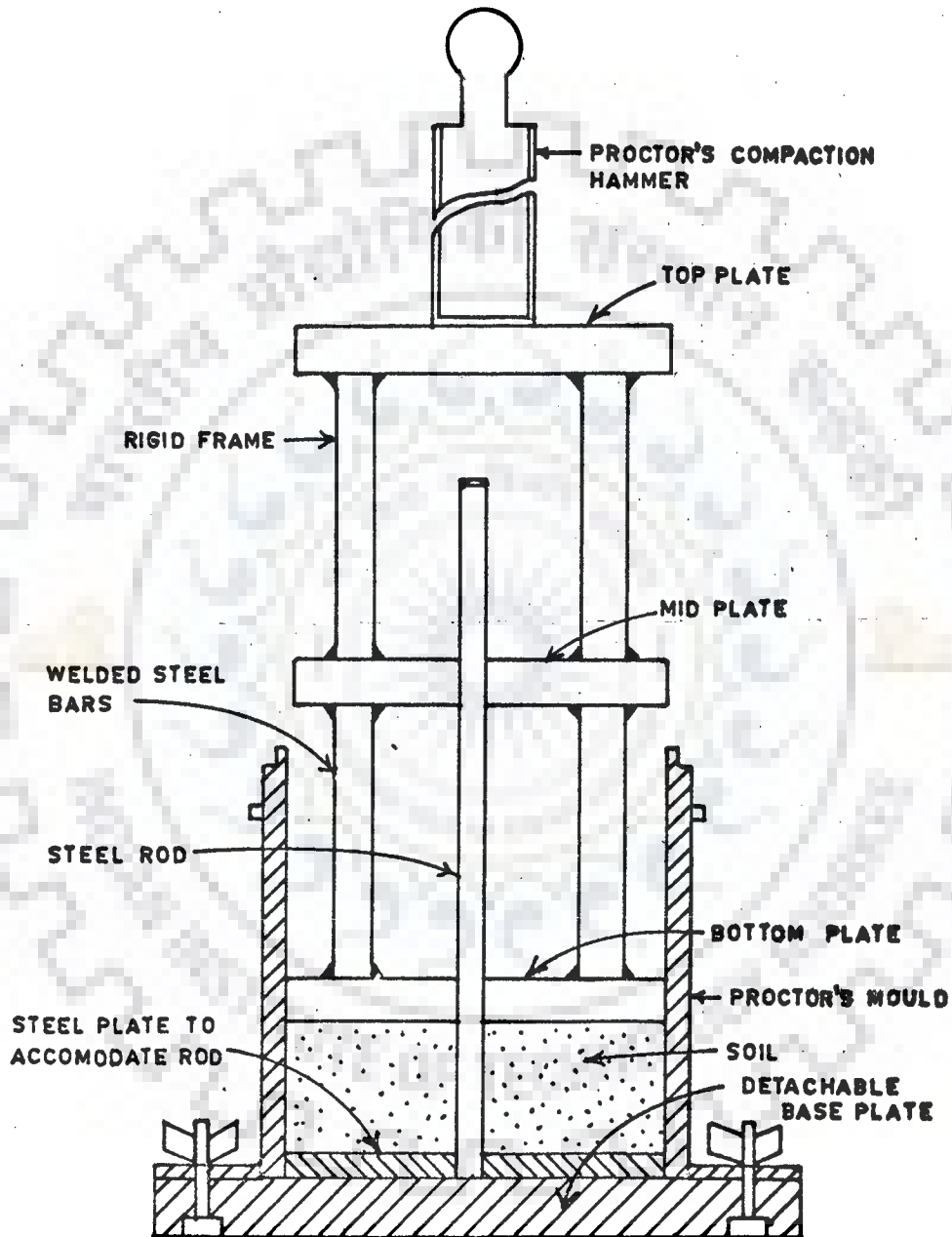
FIG.4.2- SPECIMEN COMPACTION ARRANGEMENT
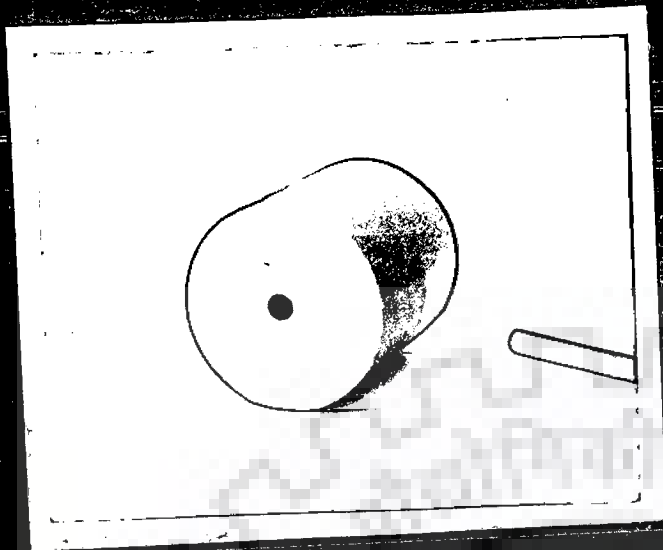
PHOTO:4·1- HOLLOW SOIL CYLINDER

PHOTO:4·2- STEEL ROD ON BASE PLATE OF PROCTOR'S MOULD
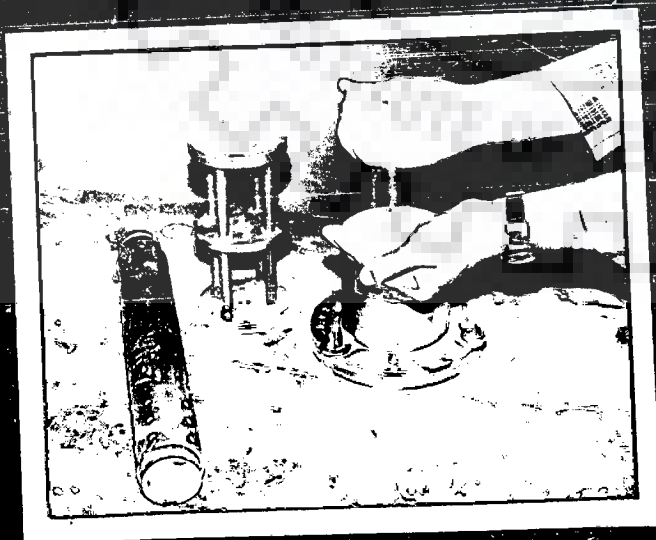
PHOTO:4·3- COMPACTION IN PROGRESS

specimen. Soil specimens were prepared at OMC, and $\pm$ 1% OMC for the soil 'A' described in para 3.3.

4.2.3 Testing Technique

Two aluminium collars to be put on the top and bottom of the specimen 10.16 cm (4 in) in diameter and 3.81 cm (1.5 in) in thickness as shown in Fig. 4.3 were fabricated[25]. To facilitate the placing of the collars centrally on the soil specimen, each collar had a 1.0 cm long protrusion of 1.2 cm diameter so as to fit in the hollow of the cylinder. Holes were made through the upper collar probe for air vent and through bottom collar probe for saturation of specimen. The hole in bottom collar probe was also used for application of hydraulic fracturing pressure to the specimen. An injection needle was attached to the upper collar so as to be inserted in the middle thickness of the soil cylinder up to the mid height. The diameter of the needle was 1.0 mm having circular holes at the periphery. Firstly the needle was used to detect whether the sample was saturated and later to determine the pore pressure at the middle of the specimen as direct flow through the needle was possible.

Filter paper was placed at inner surface of the soil cylinder in order to prevent direct exposure of the soil to water. A thin layer of an adhesive cement, was applied on the surface of collars and on the surfaces of soil specimen in order to have a water tight interface between the collars and the soil specimen. The soil specimen so prepared represents a borehole confined at both ends (Photo 4.4). After setting of

AIR VENT

OUT-LET VALVE

UPPER COLLER

CIRCULAR HOLE

1 mm DIAMETER
CIRCULAR NEEDLE

PROBE

LOWER COLLAR

INLET VALVE
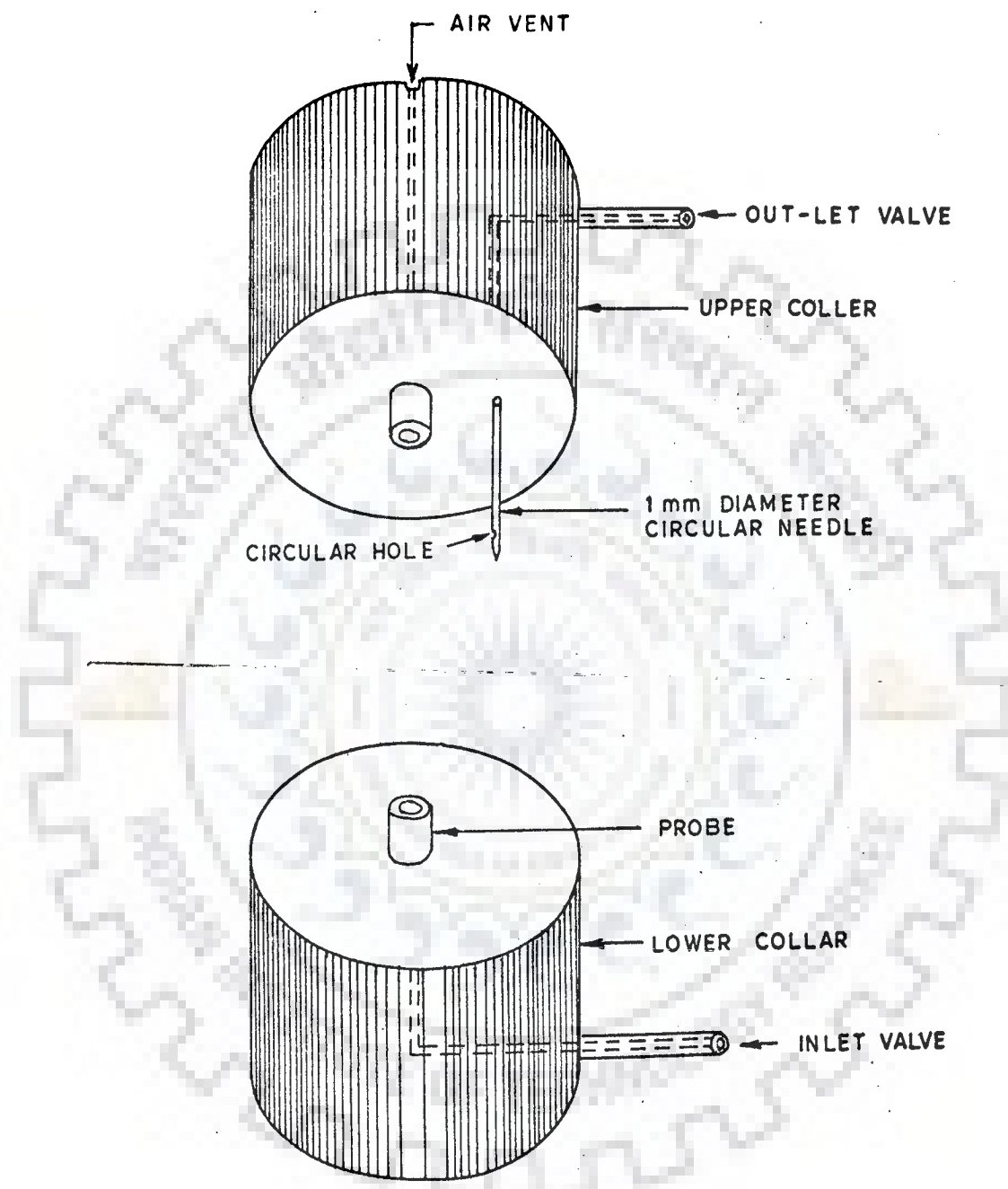
FIG. 4.3 _ ALUMINIUM COLLARS FABRICATED
FOR HYDRAULIC FRACTURING TEST

quickfix, the specimen was then enclosed in a rubber membrane, and 'O' rings together with two to four rubber bands each having two folds were stretched on the collars to make the sample completely water tight.

Saturation of the specimen was achieved by exposing the soil specimen to water from inside the hollow soil cylinder under a nominal water head of 20 cm for a minimum of 15 days. On completion of saturation, the soil specimen was placed in the triaxial cell and subjected to external confining pressure, by means of a constant pressure self compensating mercury control system. The internal pressure was applied using hand pump similar to that used in Bishop's pore pressure apparatus (Unit IV), and increased linearly to induce hydraulic fracturing.

Hydraulic fracturing in the soil sample was detected by sudden drop of pressure read either by manometer or pressure gauge. The drop in pressure indicates the formation of cracks. After the completion of test, both external and internal pressures were slowly decreased to zero and specimen was carefully examined for the orientation of the cracks.(Photo 4.5).

Experiments were conducted at various confining pressures ranging from zero to $2.2 \ Kg/cm^2$. Three to five specimens were tested at each range of confining pressure in order to have representative results. Distilled water was used as experimental fluid in all the tests performed.

4.2.4 Testing Conditions

Broadly speaking, the testing can be divided into two series viz.

(A)   Moisture condition and

(B)   Rate of application of internal pressure.

Under series (A) the soil samples were tested for
(a) saturated condition and (b) partially saturated condition.
In addition, the effect of initial degree of saturation was
also studied by compacting the specimens at OMC, + 1% OMC and
-1% OMC. For testing under partially saturated condition, after
preparing the specimen at the desired degree of initial satura-
tion and allowing nominal time for quickfix to set, the hollow
of the cylinder was subjected to internal pressure causing frac-
ture at the desired rate of pressure application. For testing
under saturated condition, after setting of quickfix, the speci-
men was exposed to water for saturation. After saturation the
sample was tested in the same way as for partially saturated
case.

Under series (B), the internal pressure applied into the
hollow of the cylindrical soil specimen causing hydraulic frac-
turing was applied at three different rates viz.

(i)   Instantaneous

(ii)   Short term

(iii) Long term

Under instantaneous application of pressure the water
pressure was increased through the hand pump in a very short
period of half to one minute till fracture occurred. Under
short term tests, the water pressure causing fracture was
increased linearly in a period of about 12 minutes. In long
term tests, the internal pressure was increased in incremental
steps over a total period varying from 3 hours to 24 hours

depending upon the range of external confining pressures. Strain controlled tests for longer duration could not be performed because of lack of availability of such apparatus.

4.3 EXPERIMENTAL OBSERVATIONS

Hollow cylindrical soil samples compacted at OMC, +1% OMC and -1% OMC as described in para 4.2.2, were tested under saturated condition for all the rates of pressure application. The test results of specimens tested under different testing condition and under various confining pressures are presented in Table 4.1.

In all 50 specimens were tested under saturated condition. The testing for one rate of pressure application under saturated condition alone took about 5 months. Total time spent in these tests under saturated condition was about 23 months.

The test results of partially saturated specimens tested at OMC and ± 1% OMC under various confining pressures are given in Table 4.2. Partially saturated specimens were tested under short term test conditions only.

4.4 IMPROVEMENT UPON EXPERIMENTAL TECHNIQUE

Fine grained soils have lower undrained shear strength when tested under saturated condition compared to that under partial saturation. In the experimental set-up defined in para 4.2.1, the conventional method of saturation i.e. saturating

TABLE 4.1 TEST RESULTS OF HOLLOW CYLINDRICAL SATURATED SPECIMENS

Sl. No.	Confining Pressure P_o (Kg/cm^2)	Hydraulic Fracturing Pressure u_f (Kg/cm^2)	Sl. No.	Confining Pressure P_o (Kg/cm^2)	Hydraulic Fracturing Pressure u_f (Kg/cm^2)
INSTANTANEOUS					
(Initial Compaction at OMC)					
1	0.00	0.248	6	1.60	1.925
2	0.00	0.253	7	1.98	2.260
3	0.40	0.607	8	2.20	2.500
4	0.40	0.658	9	2.20	2.400
5	0.80	1.100	10	2.20	2.510
SHORT TERM					
(Initial Compaction at OMC)					
1	0.00	0.268	5	1.20	1.395
2	0.00	0.277	6	1.60	1.863
3	0.40	0.564	7	2.20	2.350
4	0.70	0.850			
(Initial Compaction at +1% OMC)					
1	0.00	0.071	6	1.00	1.750
2	0.00	0.041	7	2.20	2.140
3	0.40	0.547	8	2.20	2.090
4	0.40	0.495	9	2.20	2.075
5	1.60	1.700			
(Initial Compaction at -1% OMC)					
1	0.00	0.166	6	1.60	1.910
2	0.40	0.547	7	2.20	2.390
3	0.80	1.064	8	2.20	2.375
4	1.60	1.960	9	2.20	2.490
5	1.60	1.864	10	2.20	2.475
LONG TERM					
(Initial Compaction at OMC)					
1	0.00	0.090	7	0.80	0.892
2	0.00	0.087	8	1.20	1.305
3	0.29	0.392	9	1.60	1.615
4	0.40	0.564	10	1.60	1.617
5	0.60	0.651	11	2.20	2.320
6	0.80	0.879	12	2.2	2.390

TABLE 4.2   TEST RESULTS OF HOLLOW CYLINDRICAL
PARTIALLY SATURATED SPECIMENS

Sl. No.	Confining Pressure P_o (Kg/cm^2)	Hydraulic Fracturing Pressure u_f (Kg/cm^2)	Sl. No.	Confining Pressure P_o (Kg/cm^2)	Hydraulic Fracturing u_f (Kg/cm^2)
		SHORT TERM			
		(Initial Compaction at OMC)			
1	0.00	0.276	6	1.43	1.730
2	0.29	0.688	7	1.53	1.790
3	0.29	0.620	8	1.53	1.900
4	0.29	0.715	9	2.14	2.540
5	0.80	1.028	10	2.92	3.190
		(Initial Compaction at +1% OMC)			
1	0.00	0.442	5	0.84	1.180
2	0.29	0.592	6	1.74	1.920
3	0.29	0.579	7	1.74	1.900
4	0.84	1.205			
		(Initial Compaction at -1% OMC)			
1	0.00	0.415	6	2.38	2.540
2	0.00	0.484	7	2.38	2.755
3	0.29	0.688	8	2.38	2.970
4	0.84	1.096	9	2.97	3.295
5	1.74	2.485			

hollow cylindrical specimen under a head of 20 cm of water was used. A doubt arises as to whether the specimen is actually fully saturated under such low heads. In case specimen is not fully saturated, negative capillary pressure may develop contributing to additional resistance. Consequently it was thought that the specimen be saturated by back pressure saturation technique, after making necessary changes in the experimental set-up. In the previous experimental set-up, Bishop's pore pressure apparatus without null indicator was used for application of hydraulic fracturing pressure, and thus, pore pressure could not be measured. Generally triaxial experimental results should be supported by pore pressure measurement. Consequently one more complete Bishop's pore pressure measuring apparatus (including null indicator), was added to the existing experimental set-up to measure pore pressures[28]. This is called Unit V and the improved experimental set-up is shown in Fig. 4.4. A pictorial view is presented in Photograph 4.6. Unit IV was used for application of back pressure for saturation of sample and later on for applying hydraulic fracture pressure.

Under actual conditions of loading, anisotropic loading condition prevails as compared to isotropic loading condition. In the earlier testing, hydraulic fracturing tests were conducted under equal all-round confining pressures. Under improved testing programme, anisotropy of loading in vertical and lateral directions was also taken into account.

UNIT – V
BISHOP PORE PRESSURE APPARATUS

NULL INDICATOR

UNIT – IV
APPRATUS FOR APPLYING HYDRAULIC
FRACTING PRESSURE

MERCURY MANOMETER

PRESSURE GAUGE

HYDRAULIC PUMP

LOADING RAM

AIR VENT

ALUMINUM COLLAR

1 mm DIA. NEEDLE

RUBBER MEMBRANE

TRIAXIAL CELL

CONFINING PRESSURE

SOIL SPECIMEN

"O" RING

UNIT – I
TRIAXIAL SETUP

UNIT – II
VOLUME CHANGE DEVICE

PRESSURE GAUGE

HYDRAULIC PUMP

UNIT – III
CONSTANT PRESSURE SELF COMPENSATING
MERCURY CONTROL SYSTEM

FIG. 4.4 – DIAGRAMMATIC LAYOUT OF EXPERIMENTAL SETUP

PHOTO:4·4-PLACEMENT OF
COLLARS ON SPECIMEN
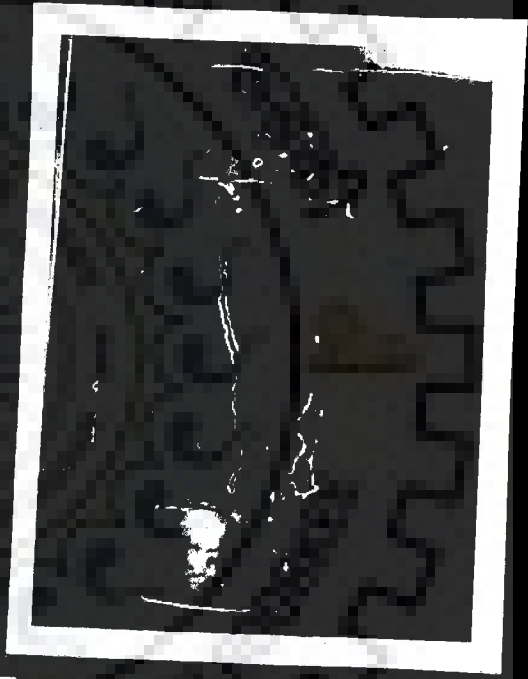
PHOTO:4·5-SAMPLE AFTER
FRACTURING
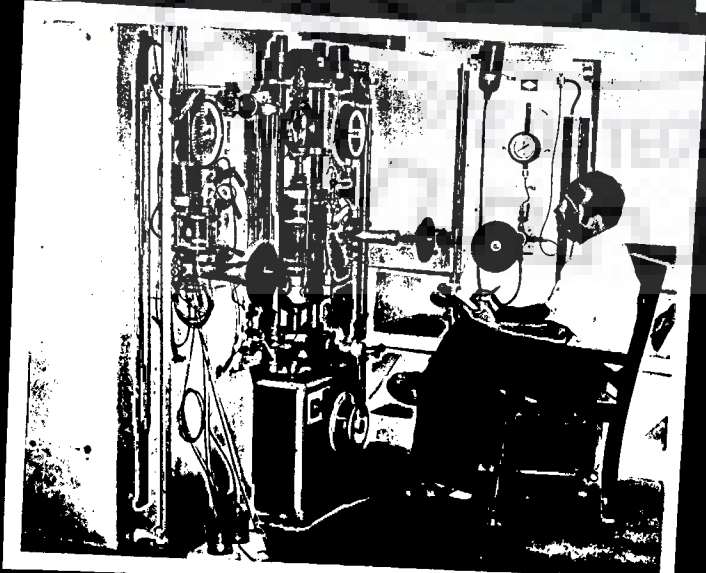
PHOTO:4·6-EXPERIMENT
IN PROGRESS

4.4.1   Testing Procedure After Saturation by Back
        Pressure Technique

The prepared hollow cylindrical soil specimen (para 4.2.3)
was placed in the triaxial pressure cell. The hollow of the
cylindr _was   connected to unit IV for applying back pressure
for saturation. Then simultaneous equal pressures were applied
externally around the specimen through unit III and internally
through unit IV in incremental steps. Saturation under each
incremental pressure was allowed for 24 hours.

Hydraulic fracturing tests were planned to be performed
at confining pressures ranging from zero to 6.90 Kg/cm^2. Speci-
means were saturated at increments of 0.20 Kg/cm^2 up to confin-
ing pressure of 1.40 Kg/cm^2, while from confining pressure of
1.40 Kg/cm^2 to 6.9 Kg/cm^2 the increment of back pressure was
about 0.5 Kg/cm^2. The degree of saturation was determined for
these pressures using theoretical expression given by Lowe and
Johnson[45]. After achievement of desired degree of saturation
at which hydraulic fracturing test was supposed to be performed,
the confining pressure was kept constant and internal pressure
was linearly increased in a short duration (instantaneous tests)
to cause failure of the soil specimen. The duration of hydraulic
fracturing tests varied from 1.0 to 3.0 minutes depending upon
the range of confining pressure. Test results are presented
in Table 4.3

TABLE 4.3 TEST RESULTS OF BACK PRESSURE SATURATED SPECIMEN

Sl. No.	P_o (Kg/cm^2)	u_f (Kg/cm^2)
1	0.410	0.751
2	0.410	0.860
3	1.000	1.284
4	2.425	2.675
5	2.425	2.775
6	3.025	3.220
7	3.025	3.270
8	3.575	3.800
9	3.575	3.840
10	6.900	7.025

During experimental observations data were also recorded for pore pressures as well as water intake by the soil specimen.

4.5 ANISOTROPIC PRESSURE APPLICATION

In this series of tests, back pressure saturated specimens were subjected to axial pressures, 25% and 50% greater than the confining pressures. Axial pressure was applied under undrained conditions at a constant strain rate of 0.005 cm/minute (0.02 in/minute). On completion of specific axial pressure, specimen was subjected to hydraulic fracturing tests by applying excess hydraulic pressure through the hollow of the cylinder by unit IV (para 4.4.1). It was found that in higher range of confining pressures, the soil under investigation could not resist

axial load of 1.5 P_o. The specimen failed by bulging in the process of application of deviator stress, indicating that the saturated specimen could not bear vertical loads of 1.5 P_o. A few tests were conducted at lower range of confining pressures. The results of these tests are presented in Table 4.4.

TABLE 4.4   TEST RESULTS OF ANISOTROPIC
PRESSURE APPLICATION

Sl. No.	P_v/P_o	P_o (Kg/cm^2)	u_f (Kg/cm^2)
1	1.25	0.410	0.574
2		1.000	1.186
3		1.400	1.675
4		1.400	1.530
5		2.425	2.515
6		2.425	2.590
7		3.025	3.220
8		4.975	5.125
9	1.50	0.410	0.578
10		1.000	1.176
11		1.400	1.580

4.6   TYPES OF SOIL

In order to investigate the effect of type of soil on hydraulic fracturing pressure, attempt has been made to study various types of soil under similar testing conditions. The following types of soil were tested.

TYPE 'A' SOIL

The description of soil 'A' is already given in Chapter 3. This soil is classified as CL soil according to unified soil classification. The detail of strength parameters and its index properties are presented in Table 3.1.

TYPE 'M' SOIL

This soil is a mixture of 50% of type 'A' soil and 50% of a highly plastic clayay soil obtained from a nearby village at Dhanauri which has very fine grains (LL = 75, PL = 33, PI = 42). The index properties of soil 'M' were obtained as follows :

LL = 41 %	Clay = 29 %
PL = 22 %	Silt = 39 %
PI = 19 %	Sand = 40 %
γ_d(OMC) = 1.689 g/cm^3	$(\sigma_t)_{sat.}$ = 0.08 Kg/cm^2
OMC = 20.5 %	G = 2.63

Angle of internal friction = 22^0

Hydraulic fracturing tests were performed on back pressure saturated specimens under various uniform confining pressure. The results of these tests are presented in Table 4.5

TABLE 4.5   EXPERIMENTAL OBSERVATION OF BACK PRESSURE SATURATED TYPE 'M' SOIL

Sl. No.	P_o (Kg/cm^2)	u_f (Kg/cm^2)
1	0.40	0.510
2	0.40	0.537
3	0.80	1.013
4	1.00	1.176
5	2.45	2.570
6	2.45	2.590

Efforts were also made to conduct tests on Dhanauri clay, but under saturated condition, the soil could not sustain any measurable load and hence the efforts had to be abandoned.

4.7   FURTHER IMPROVEMENT IN THE EXPERIMENTAL SET-UP

In the experimentation work discussed so far, the internal pressure was applied through a hand operated screw type hydraulic pump (Unit IV) throughout saturation process, and also during sample fracturing. Upon advancement of saturation, water would be seeping into the soil specimen which might result in decreasing of internally applied pressure. Though in the process of back pressure saturation every effort was made to keep the internal pressure constant by having careful watch on manual control of internal pressure and adjusting the pressure periodically through the hand pump, nevertheless, during night and other odd hours, pressure might have reduced because of flow of water into the specimen. It is also true that the chance of any effect on degree of saturation due to anticipated back pressure reduction would not have been appreciable as the water intake was reducing with time, (for example if the saturation was started at 9 A.M. under certain pressure, the water intake at 4 P.M. was about 8 % of the morning intake). However, it was decided to have further improvement in the experimental set-up in order to apply constant internal pressure. For this purpose unit IV comprising hand operated pump, pressure gauge and mercury manometer, was replaced by one additional unit of constant pressure self compensating mercury control system similar to

unit III.   This unit is called unit IVa.   The constant internal pressure was then applied through the hollow of the specimen round the clock.

·In the experiments performed so far, water intake could be measured only in the manometer range.   In order to measure water intake of the soil specimen under higher pressures, a twin burette volume change apparatus was also added.   This is called unit VI.   Pore pressure measurements were taken through unit V as before.   The complete improved experimental set-up is shown in Fig. 4.5.

4.8   ADVANTAGES OF TESTING OF HOLLOW CYLINDERS

Hollow cylindrical soil specimen testing is hoped to result in a clearer insight into the mechanism of hydraulic fracturing.   The adoptation of hollow cylindrical specimen testing technique for the investigation, permits preparation of soil specimen free from all sort of disturbances which are generally encountered in the earlier investigations.   These are tested scientifically with the help of apparatus fabricated and the triaxial machine under constant and controlled stress conditions. This type of test has a number of advantages in comparison to other type of tests performed so far for investigation of hydraulic fracturing.   In this test stress distribution is uniform throughout the length of the specimen, as the internal water pressure is applied uniformly and symmetrically along the inner surface of the hollow cylinder.   Effect of piezometer installation and corresponding change of stresses, geometery of

UNIT-I - TRIAXIAL CELL

UNIT-II - VOLUME CHANGE APPARATUS

UNIT-III - CONSTANT PRESSURE SELF COMPENSATING
& IVa - MERCURY CONTROL SYSTEM

UNIT-V - BISHOP'S PORE PRESSURE APPARATUS

UNIT-VI - TWIN BURETTE VOLUME CHANGE APPARATUS

UNIT-IVa

UNIT-VI

UNIT-V

UNIT-I

UNIT-II

UNIT-III
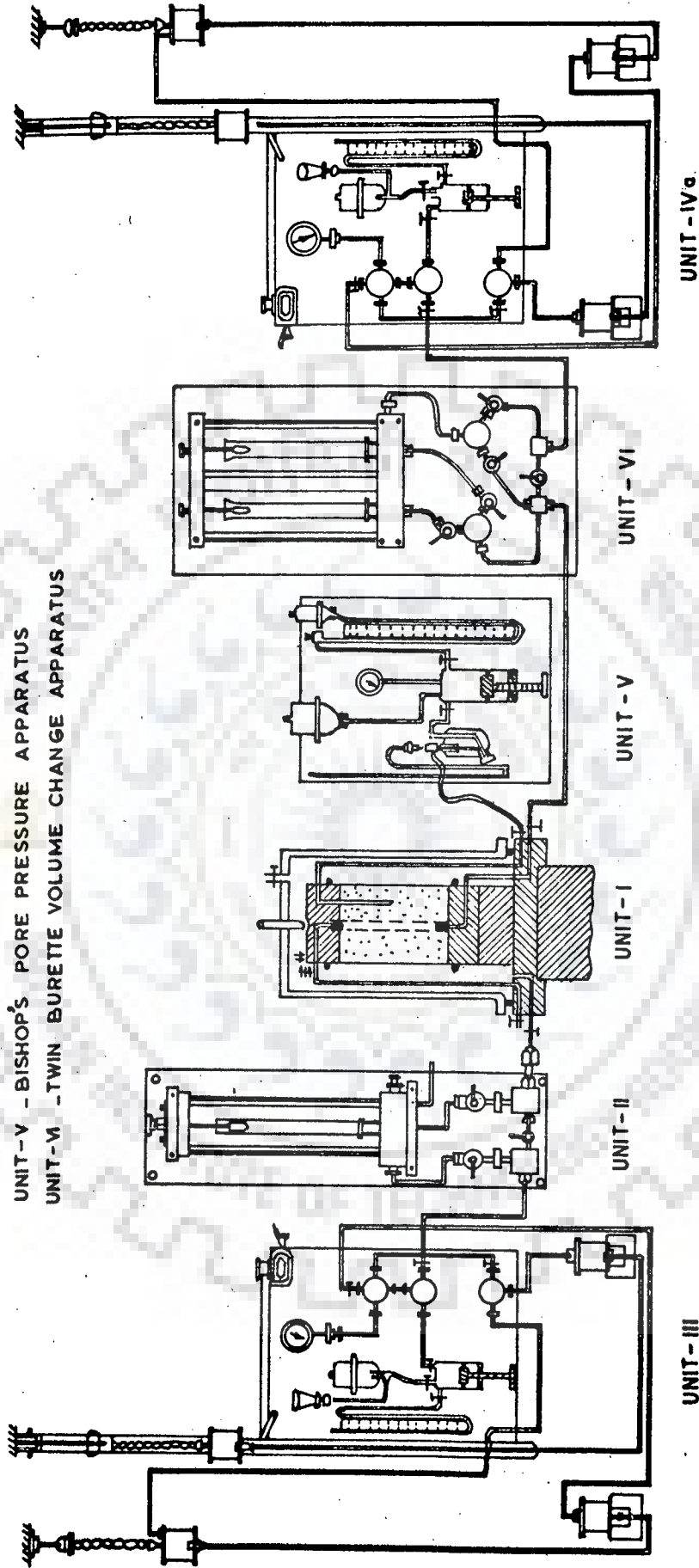
FIG. 4.5 _DIAGRAMMATIC LAYOUT OF EXPERIMENTAL SET-UP WITH CONSTANT INTERNAL AND EXTERNAL PRESSURES

piezometer tip and unevenness of borehole surface which results from drilling of borehole are avoided. Pressure is uniform at the inner surface of hollow cylinder, as compared to the pushing of piezometer or needle in solid body of the soil mass, where pressure concentration is at a smaller area. Pore pressure will develop uniformly throughout the cylindrical soil mass compared to pore pressure development in soil through piezometer tip. The sample variability and the state of applied stresses could be controlled properly. Placement of an annular filter paper will avoid direct exposure of soil mass to the water which may avoid erosion of the soil particles into suspension of water.

On the basis of foregoing reasoning it is felt that hollow cylindrical soil specimen tests with corresponding experimental technique can be considered as a better method of investigation of the mechanism of hydraulic fracturing.

CHAPTER - 5

ANALYSIS OF EXPERIMENTAL DATA AND DISCUSSIONS

5.1 GENERAL

In this chapter the experimental data described in Chapter 4 on hollow cylindrical specimens, is analysed. Firstly hydraulic fracturing pressure has been studied as a function of confining pressures, under the following subheads.

(i) Effect of compactive moisture content on saturated samples.

(ii) Effect of compactive moisture content on partially saturated samples.

(iii) Effect of saturation by back pressure technique.

(iv) Effect of rate of application of pressure causing hydraulic fracturing.

(v) Effect of non-isotropic loading condition.

(vi) Influence of change in soil characteristics.

(vii) Effect of application of constant internal pressure through self compensating mercury control apparatus.

Further, the effect of degree of saturation on hydraulic fracturing pressure, has been studied as function of

(i) Confining pressure, and

(ii) Pore pressure.

5.2 HYDRAULIC FRACTURING PRESSURE AS A FUNCTION OF CONFINING PRESSURE

5.2.1 Approach for Determining Degree of Saturation

Degree of saturation may vary depending upon the technique used for saturating the sample. For example, for back

pressure saturated specimens, the degree of saturation would depend upon the pressure applied whereas under constant head saturation, it will depend upon water intake over a period of time. Theoretically, degree of saturation S, under back pressure P, can be determined by the following formula given by Lowe and Johnson[45].

$$P = P_a \frac{(S-S_o)(1-H)}{1-S(1-H)} \qquad ..(5.1)$$

where

      H = Henry's constant which at normal room temperature is approximately equal to 0.02 CC of air per CC of water

      P_a = the initial absolute pressure (atmospheric pressure)

      S_o = initial degree of saturation at pressure P_a.

Experimentally, in the manometer range of pressure (1.20 Kg/cm^2), the degree of saturation has been worked out by measuring the amount of water intake by soil specimen and the volume changes recorded at each stage of experimentation. In the initial experimental set-up, the degree of saturation could be found out only upto manometer pressure range as beyond this pressure range, the water intake could not be measured. However, theoretical degree of saturation for back pressure saturated specimens could be assessed using equation 5.1. Subsequently, modifications were also made in the experimental set-up to measure water intake which is described in para 4.7.

5.2.2 Saturated Specimens

To evaluate the effect of confining pressure (P_o) on the hydraulic fracturing pressure (u_f) causing crack initiation in

soil mass, a plot between u_f and P_o is shown in Fig. 5.1. In this plot, the results for conventionally saturated specimens compacted at OMC, -1% OMC and +1% OMC and tested for short duration are shown. The plots show that u_f is a linear function of P_o as has been indicated by earlier researchers (Decker and Clemence[12] and Jaworski et al[31]). Further for the conditions investigated, the hydraulic fracturing occurred at pressure greater than the confining pressure. The linear relationship disucssed in Chapter 3, is of the form :

$$u_f = m_o P_o + y_o \qquad \qquad ..(5.2)$$

where,

m_o is the slope of the line, and Y_o is the vertical intercept at zero confining pressure.

Fig. 5.1 indicates that the increase in compactive moisture content resulted in some decrease in hydraulic fracturing pressure. From the figure it is also seen that the slope m_o, for specimens compacted at OMC, is 1.00 and the vertical intercept y_o is 0.18 Kg/cm^2. The tensile strength of the saturated specimen compacted at OMC was found to be 0.10 Kg/cm^2 (para 3.5) by Brazilian testing technique. For samples compacted at -1% OMC and +1% OMC, the corresponding values of m_o and y_o are 1.01, 0.99 and 0.25, 0.10 Kg/cm^2 respectively. It will be seen that m_o value is practically the same in all the three cases. The broad observations, are that hydraulic fracturing pressure is :

(i)   Slightly more than the confining pressure in all the three cases.
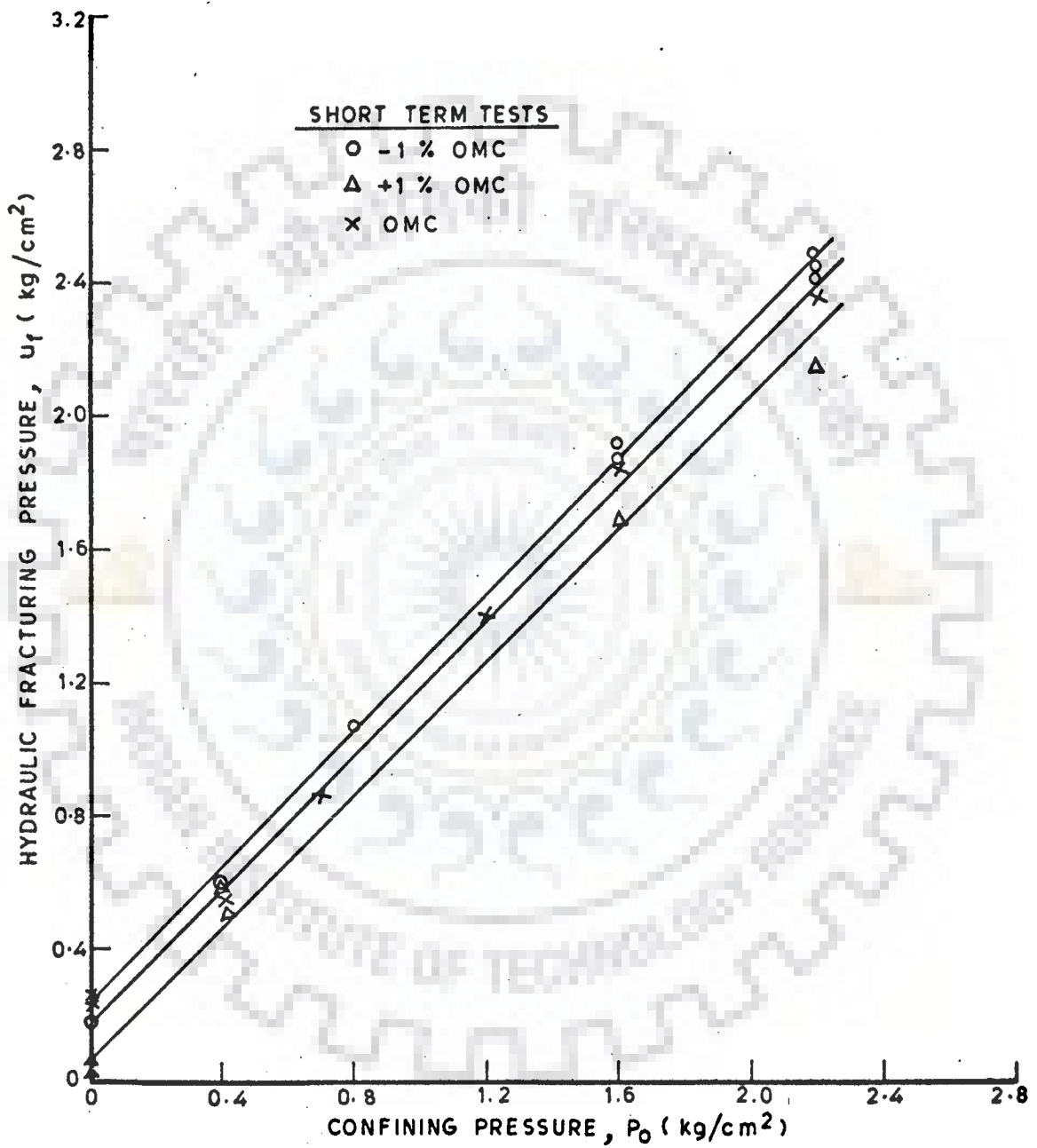
FIG. 5.1 _ EFFECT OF VARIATION OF COMPACTIVE MOISTURE
CONTENT ON HYDRAULIC FRACTURING PRESSURE
FOR SATURATED SPECIMENS

(ii)   Slope of line is independent of initial degree of saturation and is close to unity, and

(iii)   Vertical intercept decreases with increasing initial moisture content and in the worst case, it is equal to tensile strength of the soil, otherwise it is more than that. The reason may be attributed to the effect of initial moisture content on degree of saturation. For example equation 5.1 indicates that for a constant applied pressure degree of saturation increases with increase of initial moisture content. Thus,at higher compactive moisture content, higher degree of saturation would be obtained which obviously needed lower hydraulic pressure to cause fracturing of the specimen compared to that of low degree of saturation.

5.2.3 Partially Saturated Specimens

The results of hydraulic fracturing pressure u_f, against confining pressure P_o, on partially saturated specimens are presented in Fig. 5.2. From this figure it is again inferred that the relationship between u_f and P_o is linear as was for saturated specimens. Further it is seen that as compactive moisture content increases, the hydraulic fracturing pressure required for initiation of cracks, decreases.

The slope m_o, of lines connecting u_f and P_o is 1.01, 0.99 and 0.98 for compaction at -1% OMC, OMC, and +1% OMC respectively which is again close to unity as in the case of saturated samples. The vertical intercepts are 0.41, 0.31 and 0.29 Kg/cm^2 for -1% OMC, OMC and +1% OMC against measured tensile strength of 0.25 Kg/cm^2 for the samples compacted at OMC and 0.46 Kg/cm^2 for samples compacted at -1% OMC. This shows that as the initial compactive moisture increases, the vertical
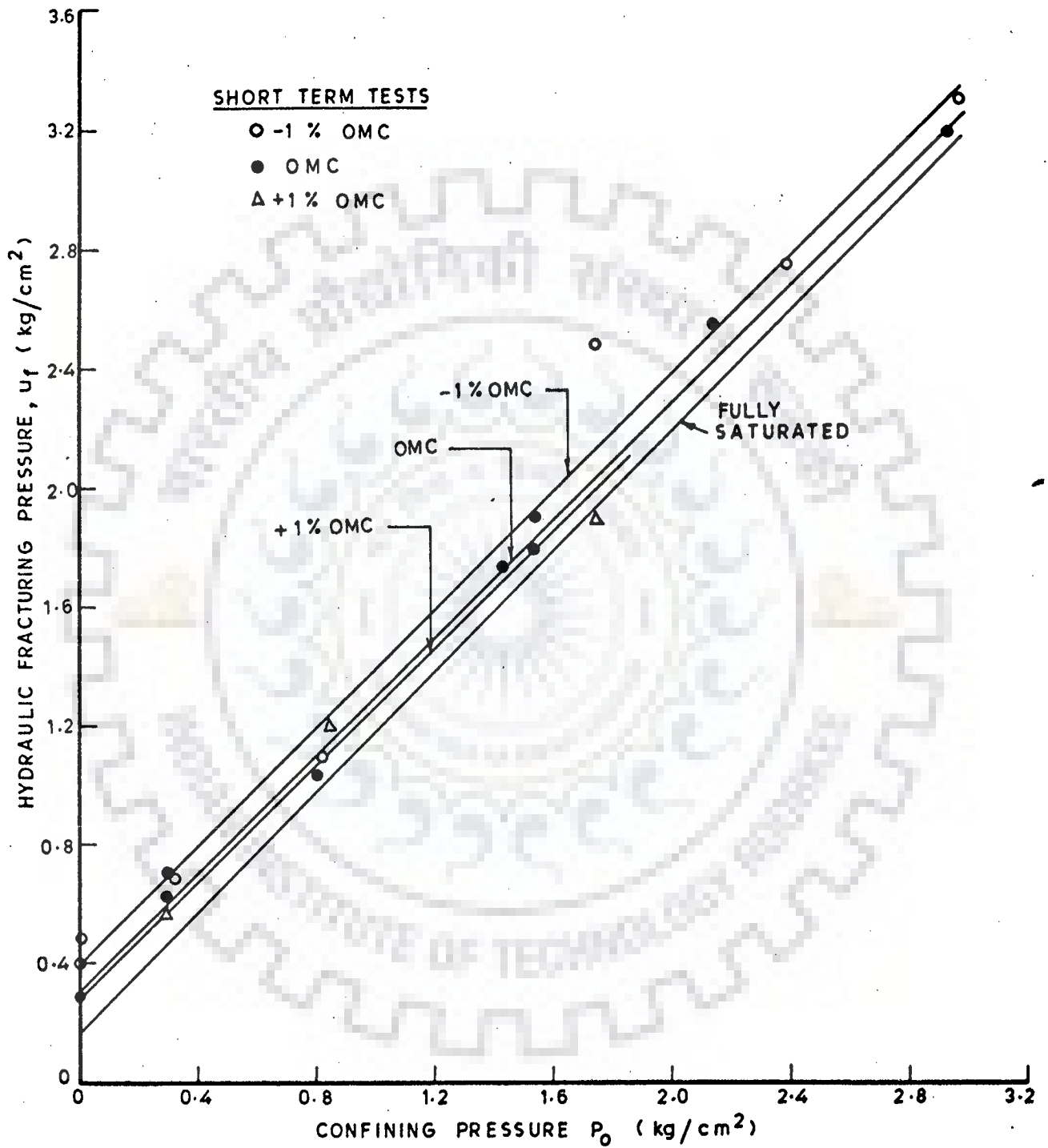
FIG. 5.2 – EFFECT OF VARIATION OF COMPACTIVE MOISTURE CONTENT ON HYDRAULIC FRACTURING PRESSURE FOR PARTIALLY SATURATED SPECIMENS

intercept decreases. For specimen compacted at OMC, the vertical intercept is 0.31 Kg/cm^2 against average tensile strength of 0.25 Kg/cm^2. The tensile strength of soil was found to be varying from 0.211 to 0.286 Kg/cm^2. From this, it could be inferred that the vertical intercept is nearly equal to tensile strength of soil. At -1% OMC, the tensile strength of soil is higher (0.46 Kg/cm^2), compared to σ_t at OMC (0.25 Kg/cm^2), and so higher vertical intercept of 0.41 Kg/cm^2 is justified. At +1% OMC, lower vertical intercept is anticipated, but it is practically the same as that for the specimen tested at OMC (0.29 Kg/cm^2 at +1% OMC, and 0.31 Kg/cm^2 at OMC).

For comparison of hydraulic fracturing pressures of partially saturated soil with saturated soil, the hydraulic fracture test results of saturated specimens compacted at OMC are also plotted on the same figure. From this it could be seen that hydraulic fracturing pressures for partially saturated soil compacted at -1% OMC, at OMC and +1% OMC are always higher than those for the saturated case. The slope of the line in all the cases, is close to unity, but the vertical intercept varies. Higher values of vertical intercept for partially saturated soil can be attributed to the presence of negative capillary pressure, which in turn would result in an increased effective stress of the soil. The increased effective stress would have resulted in higher u_f values.

5.2.4 Rate of Application of Internal Pressure

The results of tests performed at different rates of internal pressure application viz., instantaneous, short term

and long term tests are plotted in Fig. 5.3. From this, it could be seen that the slope of line of instantaneous, short term and long term tests are 1.03, 1.00 and 1.01 respectively, whereas corresponding vertical intercepts are 0.26, 0.18 and 0.10 Kg/cm^2. This shows that the slope of line is practically the same but vertical intercept varies and is higher for instantaneous pressure application in comparison to short and long duration pressure application, indicating that as the rate of pressure application decreases, the hydraulic fracturing pressure required for crack initiation also decreases provided other conditions remain unchanged. This is in agreement with the findings of Vaughan[69], whereas it is in contradiction with the results obtained by Jaworski et al[31]. The reason for higher value of hydraulic fracturing pressure for the tests performed in shorter period of time may be attributed to the rate of pressure application and the presence of air voids left in the specimen. The longer duration tests will result in greater saturation simultaneously with incremental application of pressures. In short duration tests slight development of negative capillary pressure may take place due to existence of the air voids, which obviously increase effective stress and finally result in higher value of u_f.

5.2.5 Back Pressure Saturation

The results of experimental observations of hydraulic fracturing tests performed on back pressure saturated test specimens compacted at OMC, are presented in Fig. 5.4 as a plot of hydraulic fracturing pressure u_f, against total confining
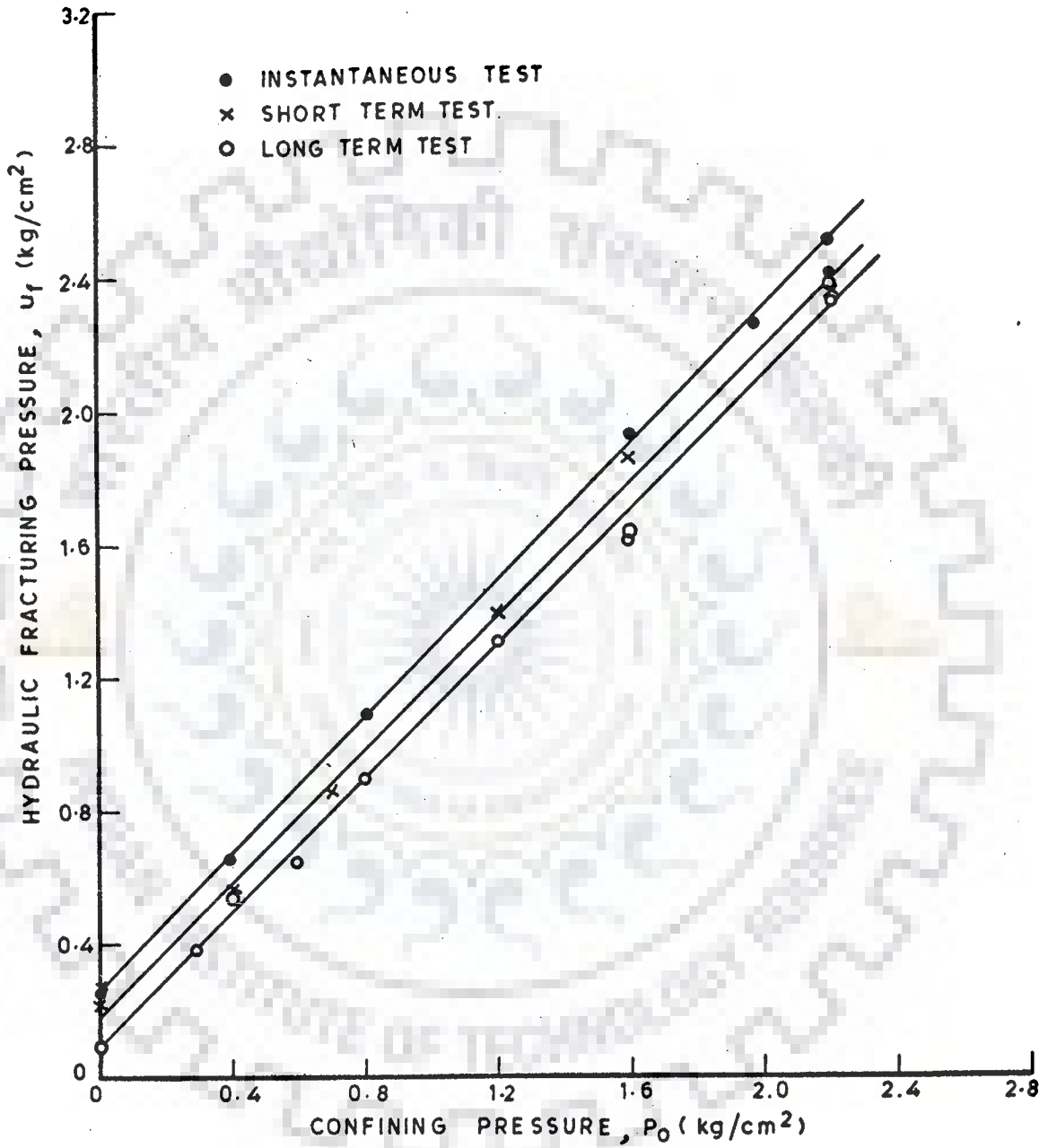
FIG. 5.3 _ EFFECT OF RATE OF PRESSURE APPLICATION
ON HYDRAULIC FRACTURING PRESSURE

pressure, P_o. Tests were conducted by applying internal pressure causing fracture for a period up to three minutes depending upon the testing range of confining pressure, for the individual specimen. In order to cover a large range of P_o and obtain higher degree of saturation, these tests were performed at various confining pressures ranging up to 6.9 Kg/cm^2. From Fig. 5.4, it could be seen that the test results of back pressure saturated specimens are quite consistent throughout the experimental range and following straight line relationship with hydraulic fracturing pressure u_f being greater than confining pressure P_o.

For comparison, the results of back pressure saturated tests and the tests performed on conventionally saturated specimens for instantaneous and short term tests, are plotted in Fig. 5.5 up to confining pressure of 2.2 Kg/cm^2. The slope and vertical intercept for back pressure saturation are 0.97 and 0.30 Kg/cm^2, whereas, the same for instantaneously tested, but conventionally saturated specimen are 1.03 and 0.26 Kg/cm^2 respectively. From, this it could be inferred that for back pressure saturated specimen, the vertical intercept is slightly greater than that of conventionally saturated whereas, slope of line is lower for back pressure saturated specimen. The higher vertical intercept for back pressure saturated specimens may be attributed to the fact that at low confining pressures, the sample was under saturation for lesser period of time, compared to conventionally saturated specimens. For example at confining pressure of 0.4 Kg/cm^2 and 1.4 Kg/cm^2, the total duration for saturation was 2 and 7 days respectively against 15 days
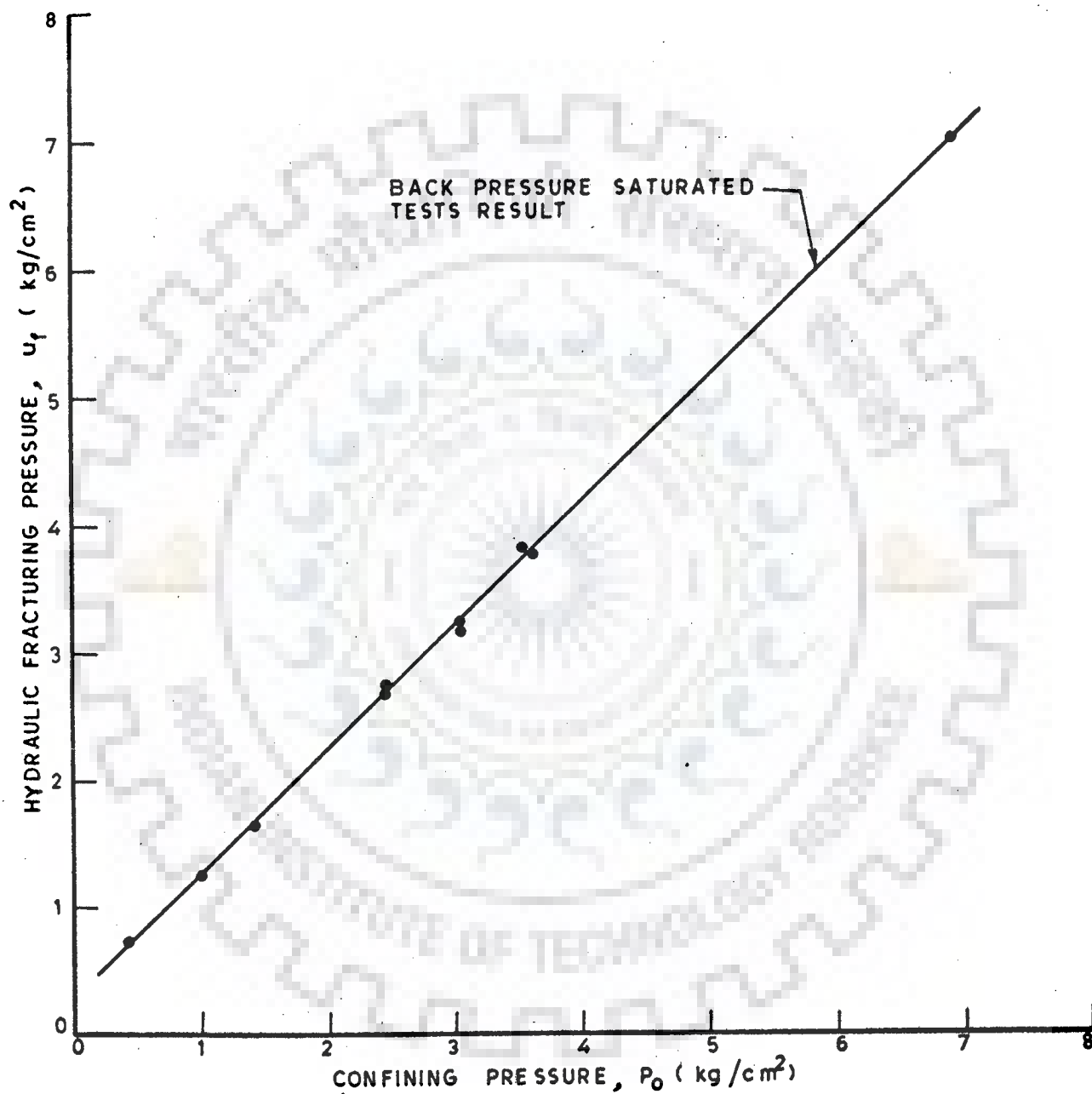
FIG. 5.4 _ HYDRAULIC FRACTURING PRESSURE VS CONFINING
PRESSURE FOR BACK PRESSURE SATURATED SPECIMENS

in all the cases for conventional method of saturation. The fact that the volume of a single bubble of air statically suspended in a large body of water decreases as function of time was shown by Lee and Black[40]. Shuurman[57] suggested that for degree of saturation greater than 85%, the pore air is present as individual bubbles rather than as a continuous phase. Barden and Sides[2,3] found that a very long time was required for air to diffuse through a partially saturated sample of clay. Thus the longer duration of saturation process may have resulted in compression of air bubbles and increased degree of saturation.

Using equation 5.1, degree of saturation for confining pressures of 0.4 Kg/cm^2 and 1.4 Kg/cm^2 was found to be 89% and 94.3% respectively for back pressure saturated specimen compacted at OMC, which is much lower than the accepted limit of about 98% saturation for treating the sample as fully saturated. Thus, the sample which is being said as saturated is in fact partially saturated at low confining pressures. To achieve 98% saturation, the sample is required to be saturated at confining pressure of the order of 3.65 Kg/cm^2.

Moreover, the vertical intercept is measured at zero confining pressure, that means at zero back pressure. Thus, the vertical intercept should be equal to that of partially saturated specimens compacted at OMC. It is seen that vertical intercept is 0.30 Kg/cm^2 and 0.31 Kg/cm^2, for back pressure saturated case and partially saturated specimens at OMC respectively, which are practically the same.

Hydraulic fracturing pressure for back pressure saturated case is slightly higher than that of instantaneously tested
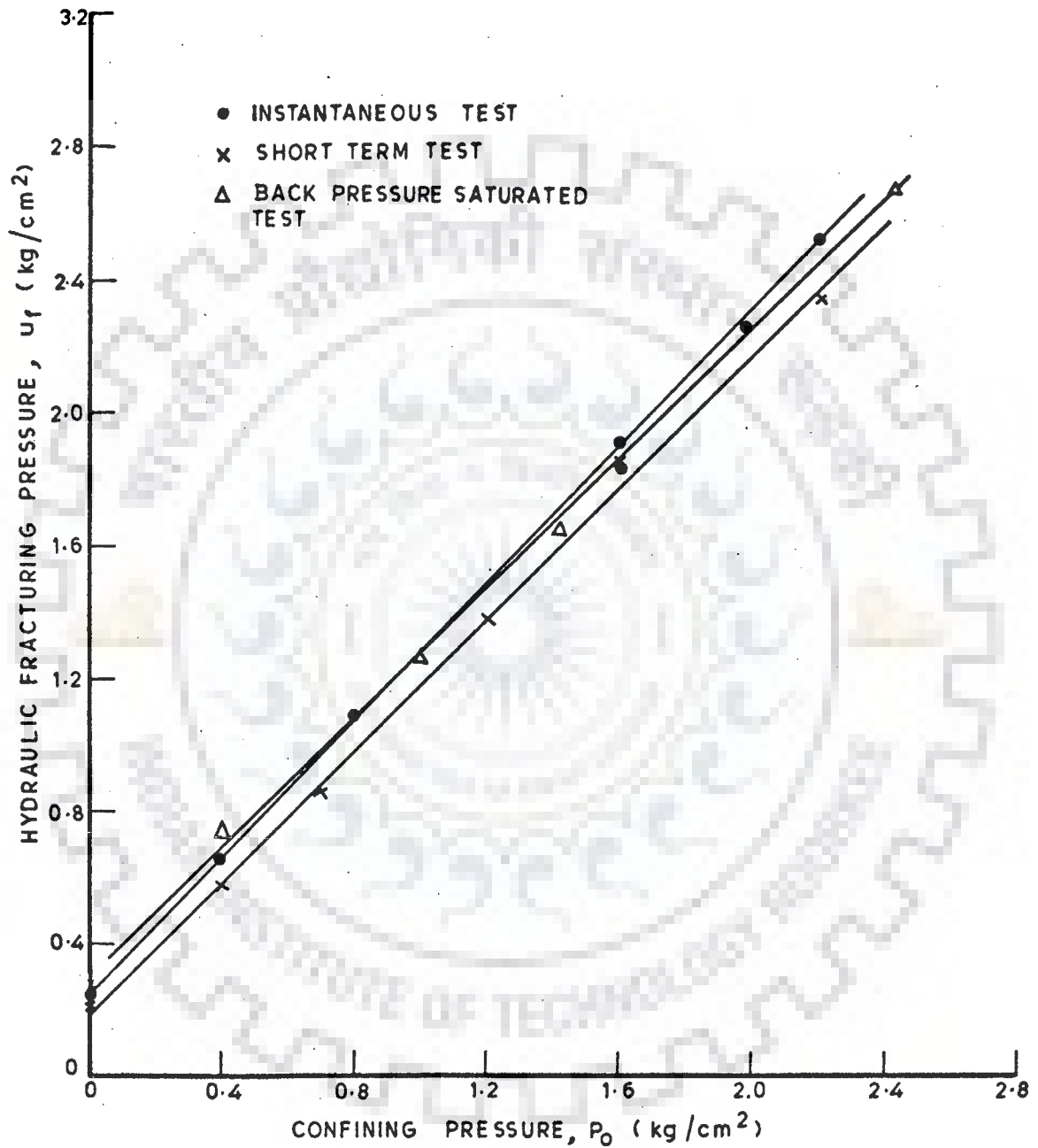
FIG. 5.5 _ COMPARISON OF u_f VS P_0 FOR BACK PRESSURE
SATURATED SPECIMENS WITH THOSE TESTED WITHOUT
BACK PRESSURE SATURATION

case upto 1.0 Kg/cm^2 confining pressure, and thereafter, the values are lower.

As expected the hydraulic fracturing pressure for back pressure saturated samples which were stressed to failure within about three minutes, are higher than those for short term tests conducted within about 12 minutes time, on conventionally saturated samples. Hence, it is inferred that the results of back pressure saturated specimens are nearly in agreement with those of instantaneous test results. Evidently there is no significant difference in test results obtained for the sample saturated under low heads or by back pressure saturation technique.

5.2.6 Anisotropic Pressure Application

The test results of anisotropic loading condition are presented in Fig. 5.6 as a plot of hydraulic fracturing pressure against total confining pressure. Two cases of anisotropic loading were examined with the ratio of vertical axial pressure to the lateral confining pressure as 1.25 and 1.50.

For comparison, the results of back pressure saturated specimens tested under uniform confining pressures are also reproduced in the same figure. The results for the two cases of anisotropic loading are close to each other. From the figure, it is seen that the slope of line m_o and vertical intercept for anisotropic loading is 0.98 and 0.20 Kg/cm^2 in comparison to the values of 0.97 and 0.30 Kg/cm^2 for uniform confining pressures. From this it could be seen that the slope of line remains
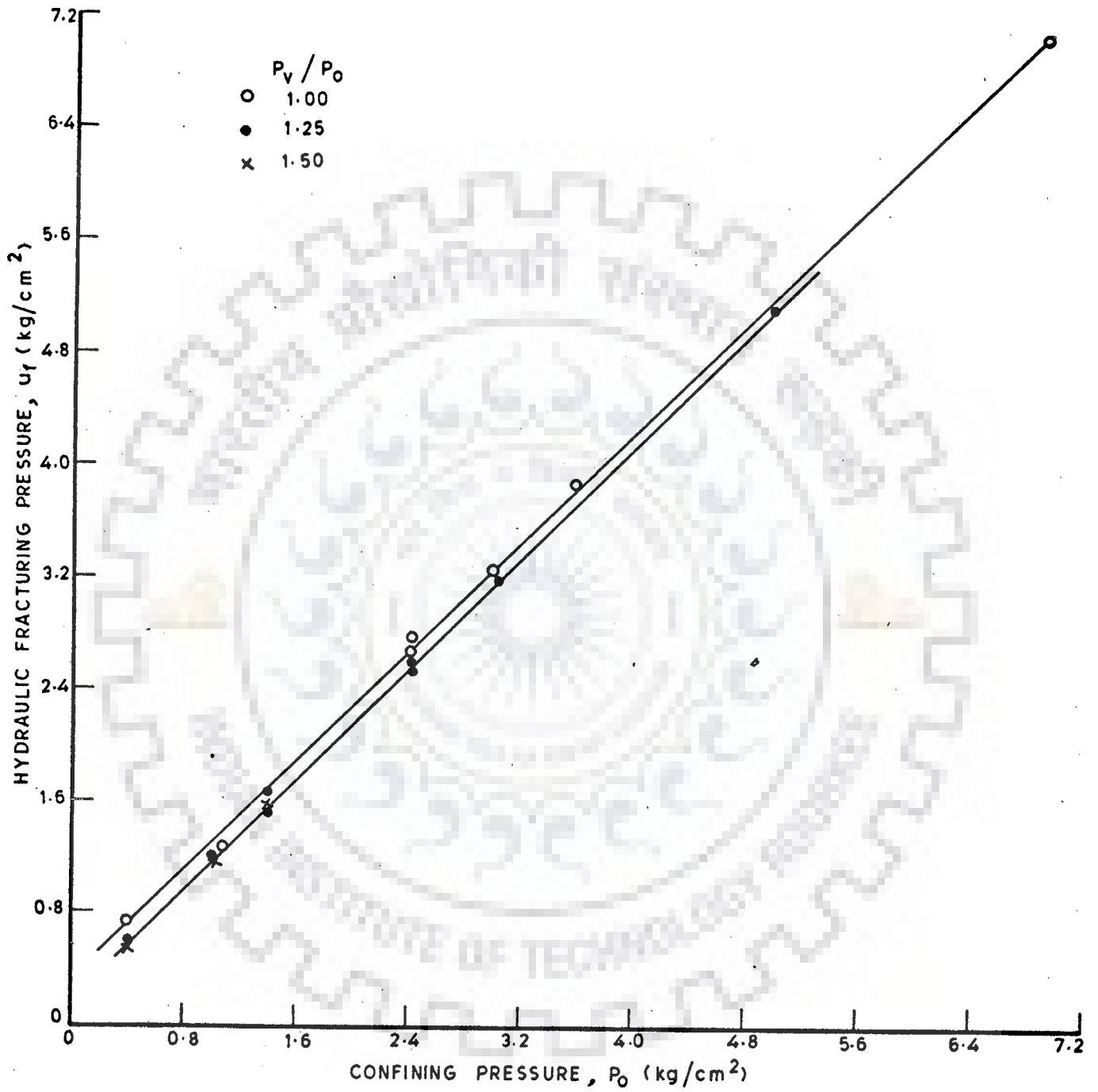
FIG. 5.6 _ VARIATION OF u_f VS P_o UNDER NON-ISOTROPIC LOADING CONDITION

unchanged, but the vertical intercept reduces for the anisotropic case in comparison to the case of uniform confining pressures.

In general it can be said that hydraulic fracturing pressure decreases with increase of the ratio of vertical axial pressure to the lateral confining pressure. This is also in agreement with the results based on theoretical analysis presented in Chapter 7. It was also seen during experimentation that in higher range of confining pressure, the soil under investigation could not resist axial load of 1.5 P_o. The specimen failed in bulging in the process of application of deviator stress, indicating that for the soil tested, the saturated specimen can not bear vertical loads of magnitude 1.5 P_o in the higher range of confining pressures.

5.2.7 Effect of Soil Characteristics

The analysis presented in the preceeding paragraphs, pertains to only one type of soil 'A'. The test results on type 'M' soil, are presented in Fig. 5.7, for u_f against P_o along with results for type 'A' soil as well. These results for both type of soils were obtained using back pressure saturation technique.

It is seen that the hydraulic fracturing pressure obtained for 'M' soil is slightly lower than soil 'A'. The values of slope and intercept for the two cases are listed in Table 5.1.
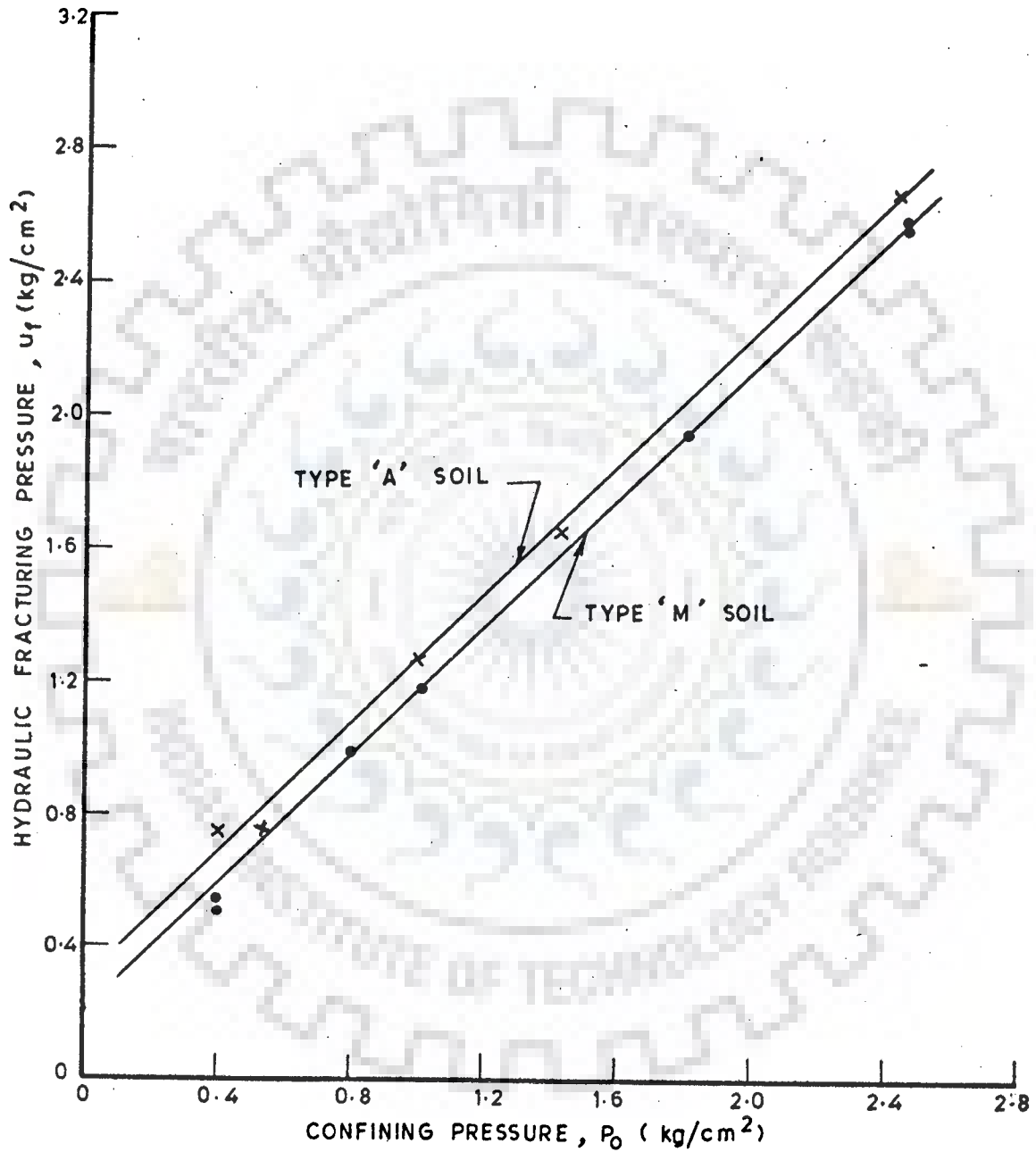
FIG. 5.7_ EFFECT OF VARIATION OF SOIL CHARACTERISTICS ON HYDRAULIC FRACTURING PRESSURE

TABLE 5.1   COMPARISON OF u_f VALUES FOR DIFFERENT
TYPE OF SOILS

| Soil | Characteristics | | Slope | Vertical inter-cept | Tensile stren-gth |
	LL	PI	m_o	$y_o (Kg/cm^2)$	(Kg/cm^2)
A	32.5	10.5	0.97	0.30	0.10
M	41.0	19.0	0.97	0.21	0.08

From the table, it could be seen that the slope of line for both type of soils is the same and is close to unity. The vertical intercept for 'M' type soil is lower than that of 'A' type soil. The tensile strength of 'M' type soil is also slightly less than that of 'A' type soil. However, the present investigation has not fully explored the effect of various soil properties in sufficient detail to come to a definite conclusion of their effect.

5.2.8   Constant Internal Pressure Application

The experimental observations obtained for hydraulic fracturing tests performed on back pressure saturated specimens using constant internal pressure application techniques are presented in Fig. 5.8. These plots are prepared for hydraulic fracturing pressure Vs confining pressures for both soil 'A' and soil 'M'. It is seen from the figure that the value of u_f is higher for soil 'A' compared to those obtained for soil 'M', as was observed previously (para 5.2.7).

The results of these tests are compared with those performed on back pressure saturated specimens under manually controlled condition in Fig. 5.8. It is seen from these plots that
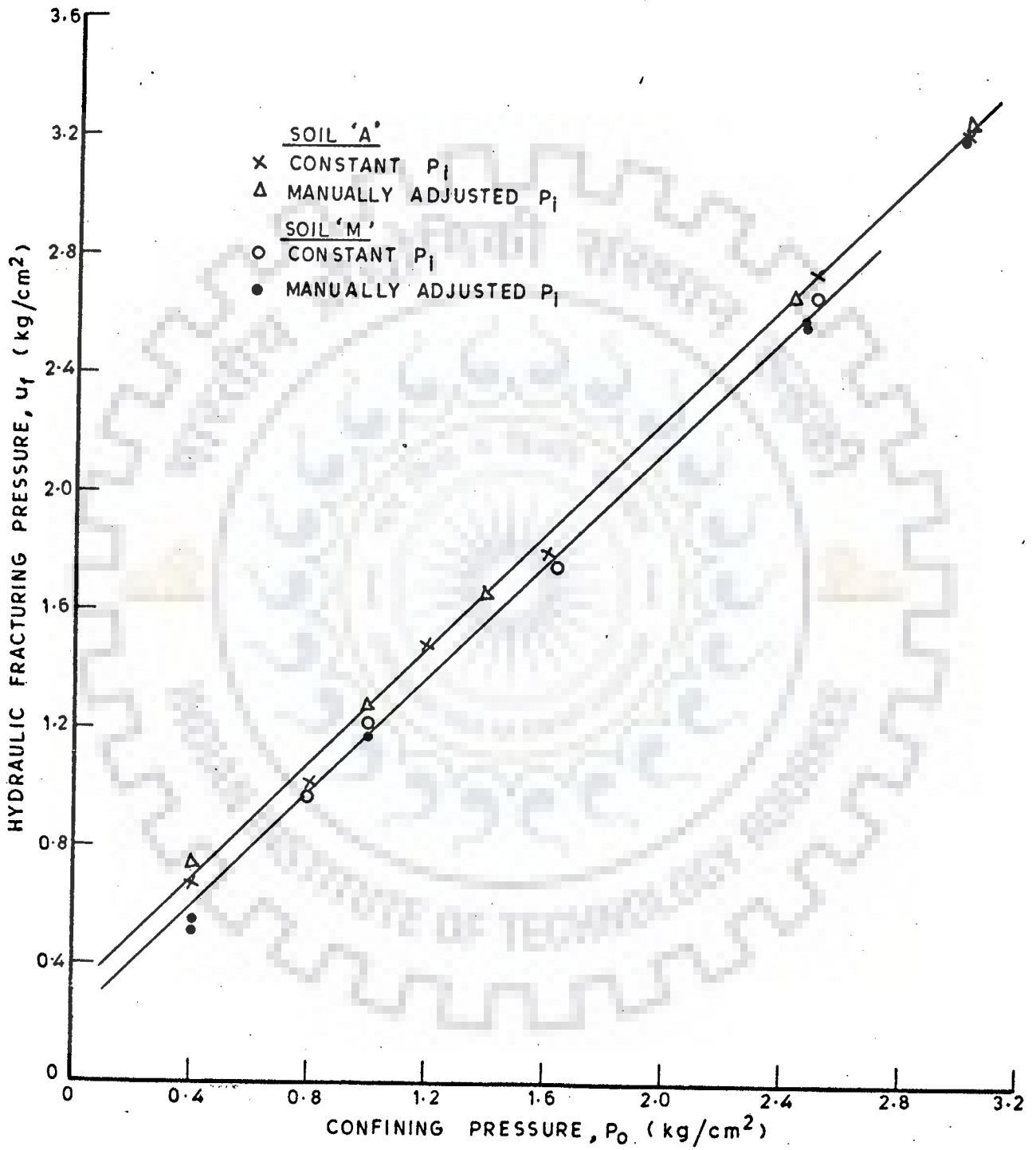
FIG. 5.8 _ VARIATION OF u_f VS P_0 FOR CONSTANT APPLICATION OF INTERNAL PRESSURE

for both type of soils, the results of manually controlled internal pressure application tests are in close agreement with the results of tests performed under constant internal pressure applications. This indicates that since saturation under back pressure was allowed for 24 hours at one particular pressure, sufficient water was absorbed by the specimen in earlier period of say 4-6 hours and very little pressure change took place during odd hours when manual control of pressure, could not be regulated. Hence, it can be concluded that so far as the prediction of u_f is concerned, it is insignificant whether unit IV with manual control of pressure is used or unit IVa with constant pressure self compensating mercury control system is used.

5.3 EFFECT OF DEGREE OF SATURATION

5.3.1 Evaluation of Degree of Saturation as a Function of Confining Pressure

For computing degree of saturation under various ranges of applied pressure, using equation 5.1, it is essential to know initial degree of saturation. Knowing specific gravity of the soil, initial void ratio and compactive moisture content, initial degree of saturation at -1% OMC, OMC and +1% OMC were calculated as 79, 84 and 89% respectively. In equation 5.1, the pressure P, is the same as confining pressure P_o, since internal pressure was also kept equal to P_o in the model testing utilizing back pressure saturation technique. Consequently, using the initial degree of saturation for specimens compacted

at OMC, the degree of saturation S, under various confining
pressures, were computed and the results are plotted in
Fig. 5.9, for P against S.

To measure the degree of saturation from experimental
data, the measurement of water intake by the soil specimen
during the process of saturation, and the minor volume changes
recorded throughout the advancement of experiments, were uti-
lized. Knowing the initial volumes of solid soil, water and
air, the volume of water in soil specimen and volume of voids
at any instant of time during the process of saturation under
each increment of applied back pressure was calculated. Hence,
the degree of saturation at any instant of time during experi-
mentation could be expressed as;

$$S = \frac{\text{initial volume of water + water intake by soil specimen}}{\text{initial volume of voids - Net volume change of soil specimen}} \qquad \text{.. (5.3)}$$

Degree of saturation at the end of each increment of
applied pressure is computed from experimental observation
using equation 5.3. These results are also plotted in
Fig. 5.9 in order to compare with those computed theoretically
using equation 5.1.

From Fig. 5.9, it is seen that upto an applied pre-
ssure of 0.5 Kg/cm^2, the degree of saturation obtained experi-
mentally is greater than that predicted theoretically using
equation 5.1 for the same increment of applied back pressure.
In the range of back pressure of 0.5 to 1.25 Kg/cm^2, the
experimental results are in close agreement with those pre-
dicted theoretically. But beyond 1.25 Kg/cm^2, the degree of
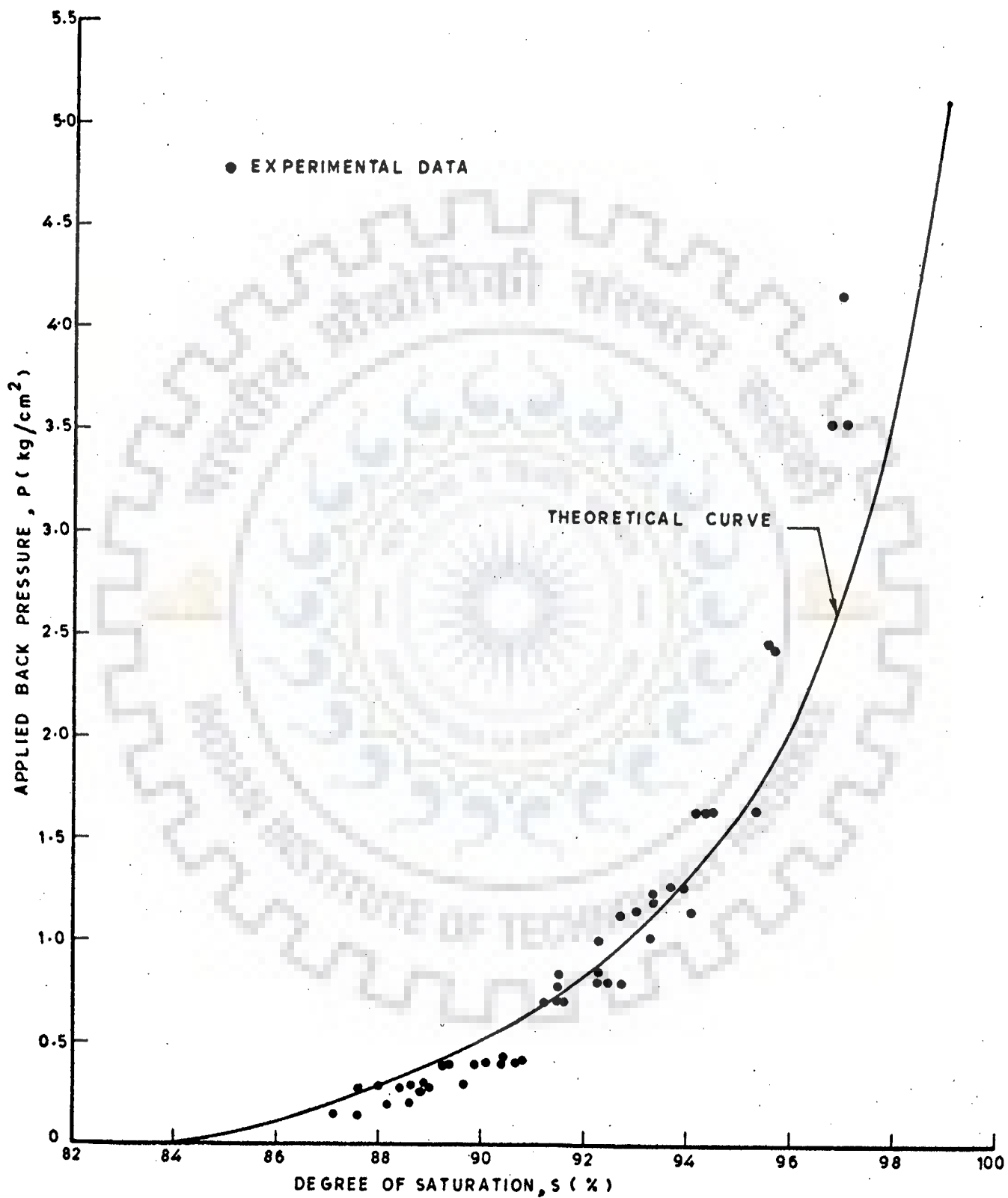
FIG. 5.9 _ RELATIONSHIP BETWEEN APPLIED BACK PRESSURE
AND DEGREE OF SATURATION

saturation obtained experimentally is lower than that obtained theoretically at the same increment of applied back pressure.

Lowe and Johnson[45] have reported that under low rate of back pressure application, equation 5.1 gives, the minimum pressure required for saturation, under no volume change condition. Black and Lee[10] also consistently found that equation 5.1 indicates the minimum amount of back pressure required to achieve full saturation. Thus the observation that above 1.25 Kg/cm^2, higher back pressures are required to attain a certain degree of saturation as compared to the values given by equation 5.1, is also supported by the work of earlier researchers. Regarding getting higher degree of saturation at low pressure, it may be due to experimental limitations as slight difference in estimating initial degree of saturation will affect the result because, the range of change of degree of saturation is very narrow. It is 84% at start and theoretically, it is 90% at 0.5 Kg/cm^2.

5.3.2 Hydraulic Fracturing Pressure Vs Degree of Saturation

To investigate the effect of degree of saturation on hydraulic fracturing pressure, the ratio of hydraulic fracturing pressure to total confining pressure against degree of saturation is plotted in Fig. 5.10, for conventionally saturated specimens tested at various rates of pressure application, as well as for back pressure saturated specimens. These test specimens were prepared at OMC with an initial degree of saturation at 84%. The values of hydraulic fracturing pressures are taken from the plot of u_f Vs P_o (Figs. 5.3 and 5.4), whereas
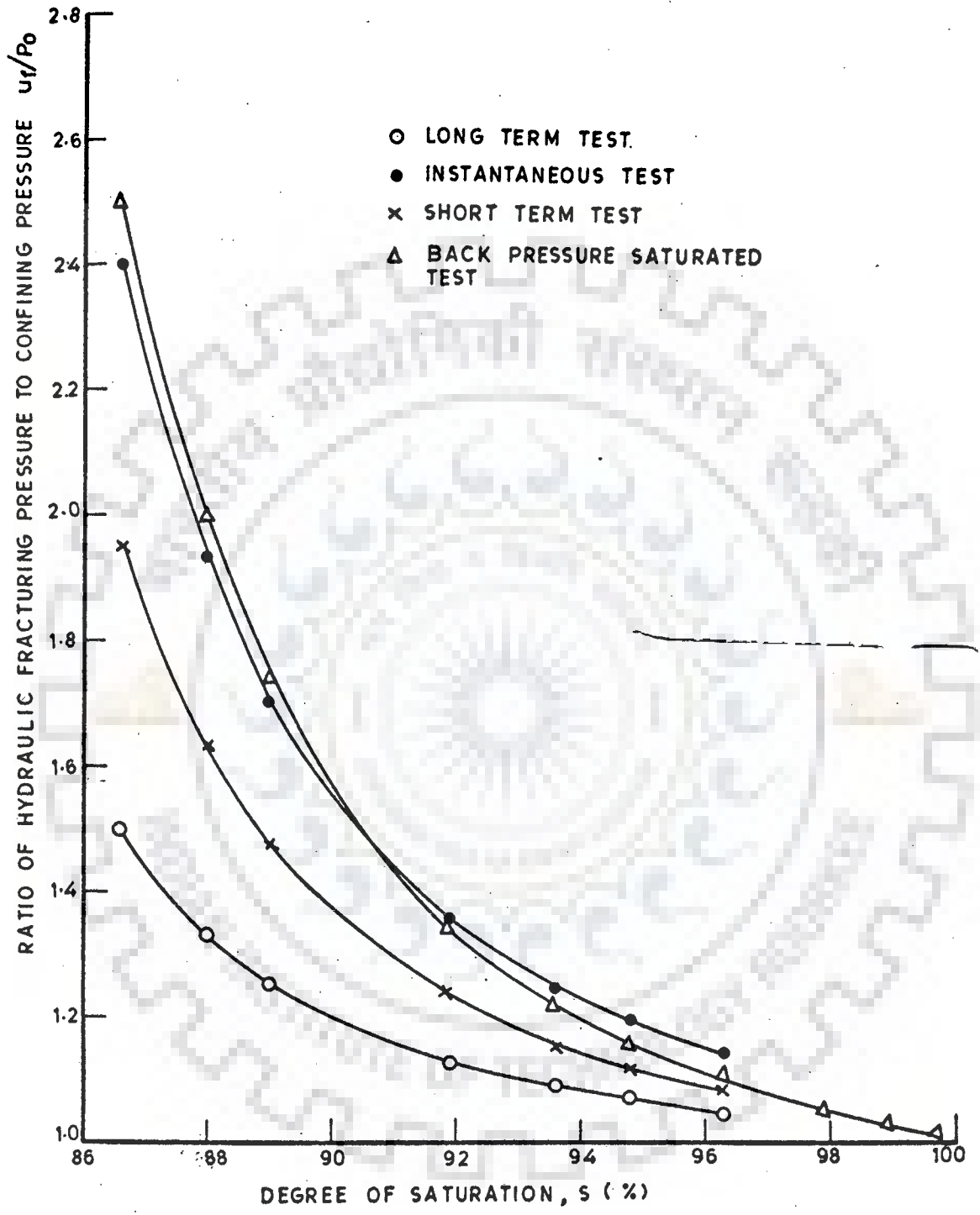
FIG. 5.10 _ EFFECT OF DEGREE OF SATURATION ON HYDRAULIC FRACTURING PRESSURE

the value of degree of saturation is taken for corresponding confining pressures from theoretical curve of P_o Vs S as shown in Fig. 5.9.

These curves show that as the degree of saturation increases, the ratio of hydraulic fracturing pressure to total confining pressure decreases. It is also seen that in case of instantaneous, short term and long term tests, for the same degree of saturation the values of u_f/P_o increases as the duration of test decreases. The reason may be attributed to the effect of rate of pressure application as discussed in para 5.2.4. The slightly higher value of u_f/P_o at lower degree of saturation in case of back pressure saturated test specimen is due to lower range of back pressure and lesser duration of specimens subjected to water which inturn could not achieve full saturation. Thus presence of negative capillary pressures resulted in higher value of hydraulic fracturing pressure. The basic effect in increasing u_f/P_o at low degree of saturation is primarily due to larger vertical intercept in straight line relationship of u_f and P_o. To demonstrate this, these results are reproduced in Fig. 5.11 as a plot between $\dfrac{u_f-P_o}{P_o}$ and S.

From these curves, it could be seen that at degree of saturation nearer or greater than 98%, u_f is approximately equal to P_o as the contribution of vertical intercept is minimised. These curves may be useful as design curves to estimate u_f for the known degree of saturation.
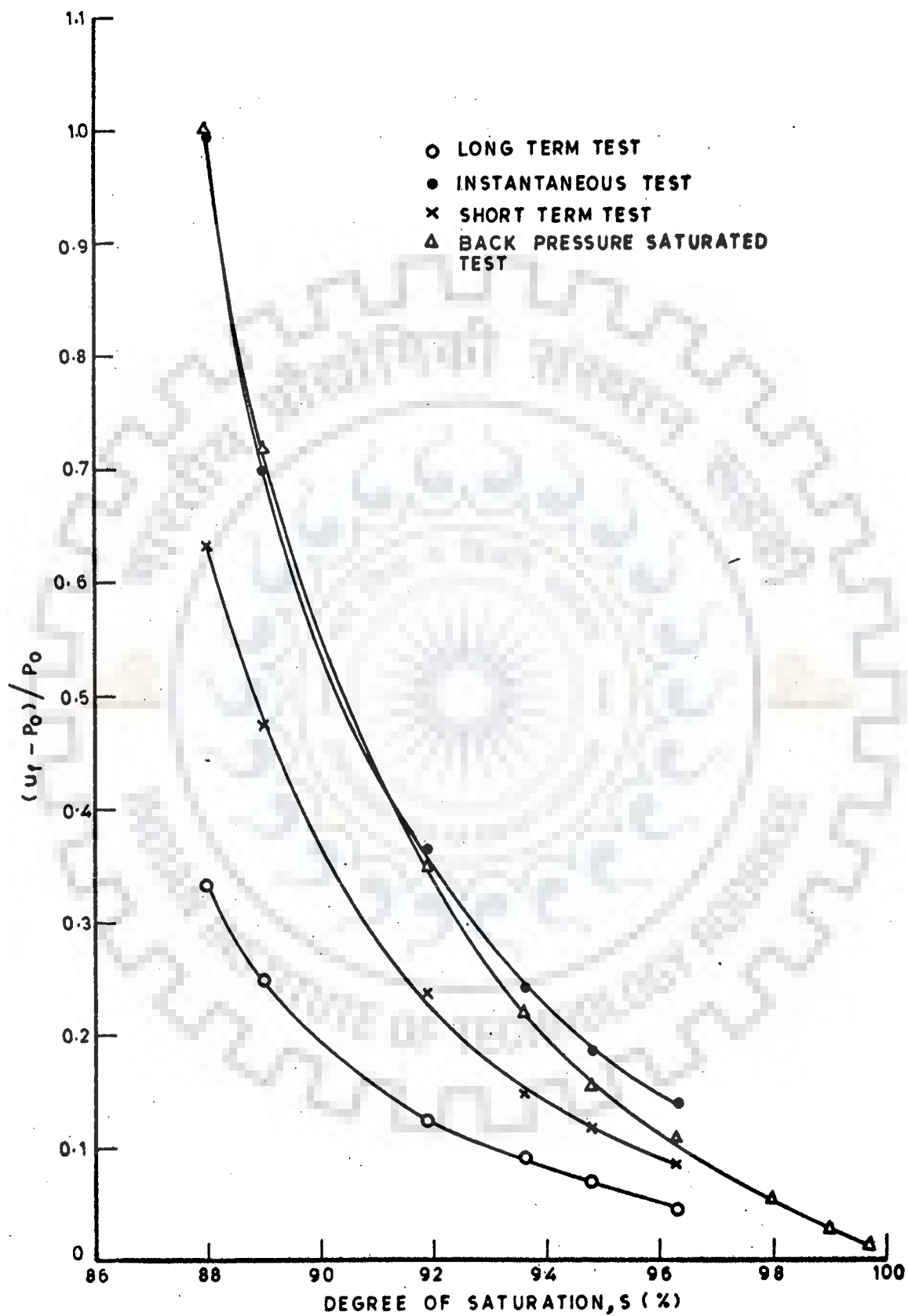
FIG. 5.11 _ VARIATION OF $(u_f - P_0)/P_0$ VS S FOR VARIOUS TYPE OF
HYDRAULIC FRACTURING PRESSURE APPLICATION

5.3.3 Pore Pressure as a Function of Degree of Saturation

The pore pressure measurement during back pressure saturation has been plotted on semi-log graph paper in Fig. 5.12 as a function of degree of saturation computed from water intake data recorded during experimentation of the specimen. It is seen that a logarithmic linear relationship exists between pore pressure (log.u) and S. The relationship found for the case studied is ;

$$\text{Log } u = 0.149 \ (S-84)-1.347 \qquad \qquad ..(5.4)$$

The empirical equation (5.4) is obtained from experimental data of saturated specimen, compacted at an initial degree of saturation of 84%.

5.4 REFRACTURING TESTS

In an earthen structure the possible reason for crack development during construction may be drying and shrinkage, improper compaction, differential settlement, earthquake, etc. The interesting point is that most of these cracks, remain as unseen pre-existing fine cracks in the dam body. Some of them may heal up due to wetting upon reservoir impounding, provided reservoir filling is done gradually and at a low rate. In healing of the cracks, the important aspect is that the soil should be prone to self-healing behaviour. The unhealed cracks would be wide opened by water penetrating through them due to water pressure of reservoir level and cause concentrated leaks. Therefore, the effect of pre-existing cracks are of considerable importance in investigation of hydraulic fracturing.
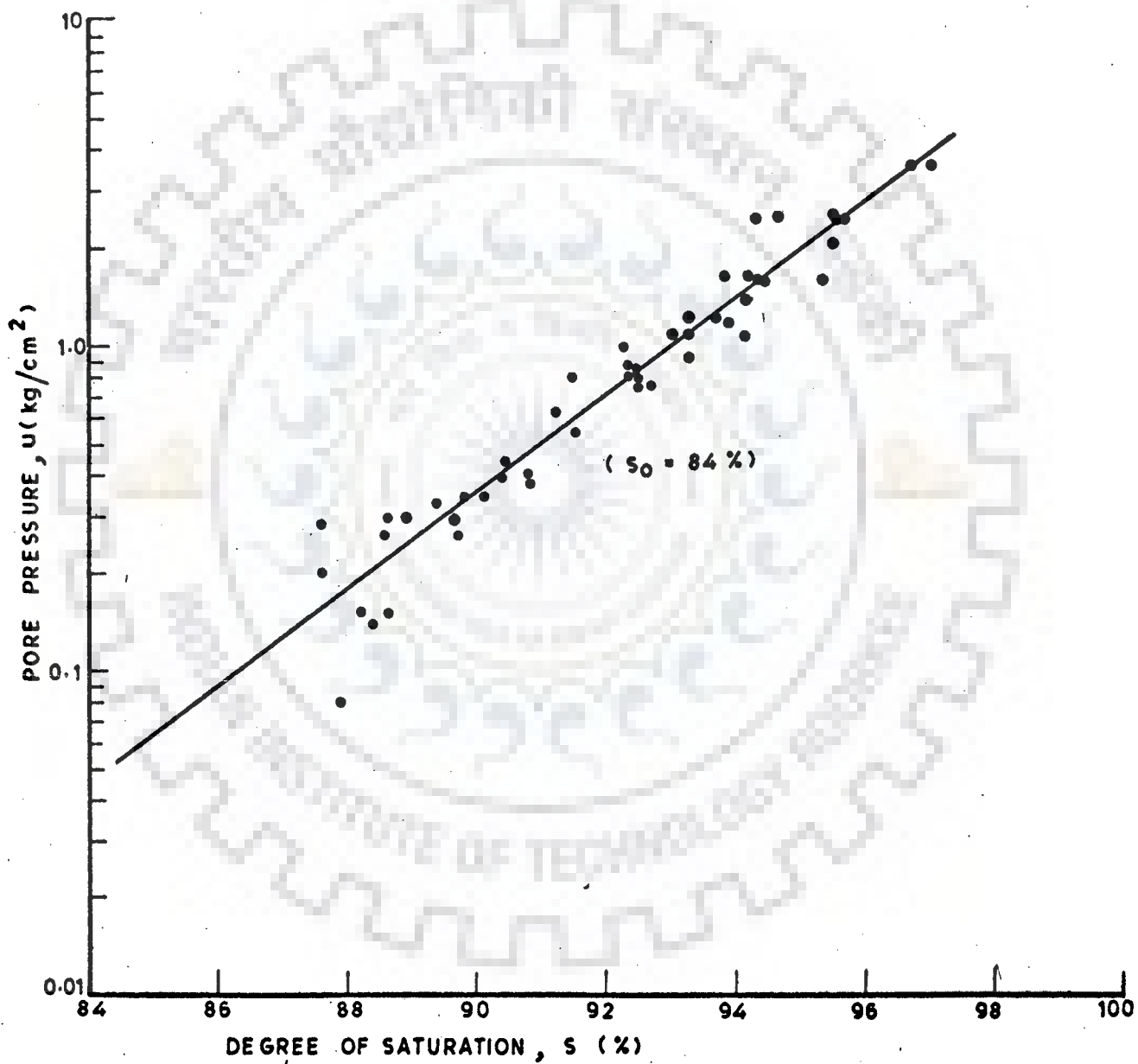
FIG. 5.12 – RELATIONSHIP BETWEEN PORE PRESSURE AND DEGREE OF SATURATION

To investigate the effect of pre-existing cracks on hydraulic fracturing pressure, refracturing tests were performed on back pressure saturated hollow cylindrical soil specimens, of type 'A' soil at confining pressure of 0.8 Kg/cm^2. On completion of saturation, internal pressure through the hollow of cylindrical soil specimen was increased linearly until fracture occurred and the fracturing pressure (u_f = 1.0 Kg/cm^2) and its subsequent reduction was recorded for some time. The soil sample remained under applied pressures overnight. It was observed that at the end of test, internal pressure was approximately equal to confining pressure. Next day, internal pressure was again linearly increased and the first refracturing pressure was recorded as 0.904 Kg/cm^2. Leaving the sample again overnight under the same confining pressure, following day, internal pressure was linearly increased until failure occurred. The second refracturing pressure was 0.891 Kg/cm^2. Thereafter, the internal pressure was reduced to half that of confining pressure, and the sample remained under pressures overnight. Next day, internal pressure was again linearly increased and third refracturing pressure was recorded as 0.959 Kg/cm^2. The technique of refracturing test was believed to roughly simulate a crack formed during construction (Jaworski et al[30] and Vaughan[69]).

The results of two refracturing tests are presented in Fig. 5.13 as Test I and II. From this figure, it is seen that initially sample (I) fractured at u_f = 1.0 Kg/cm^2. The following day, under same confining pressure of 0.8 Kg/cm^2, the specimen failed at 0.904 Kg/cm^2, indicating thereby that (i) healing to some extent had taken place and (ii) refracturing
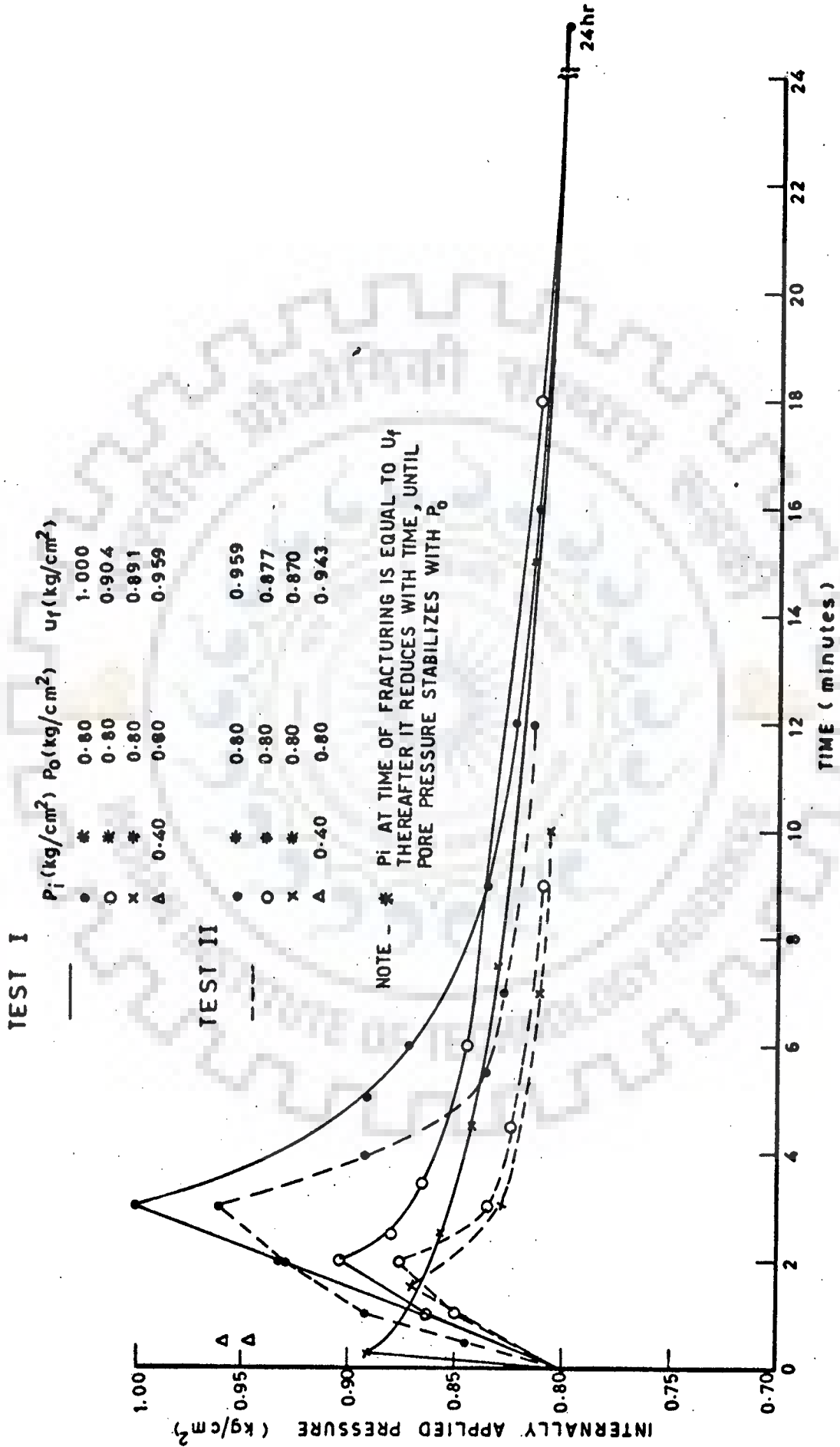
FIG. 5.13 — INTERNALLY APPLIED PRESSURE VS TIME FOR SPECIMENS SUBJECTED TO REFRACTURING PRESSURES

occurred at lower pressure than the initial one. After 48 hours of initial fracture, the refracturing pressure was reduced to 0.891 Kg/cm^2, which is again of the same order as was for test conducted after 24 hours of initial fracture. Maintaining the soil specimen with constant internal pressure of 0.4 Kg/cm^2 and confining pressure of 0.8 Kg/cm^2 for 24 hours the refracturing pressure recorded was 0.959 Kg/cm^2. This indicates that the third refracturing pressure(0.959 Kg/cm^2) is higher than the first refracturing of the specimen (0.904 Kg/cm^2), though lower than the initial fracturing pressure.

The reason may be attributed to the fact that in first and second refracturing tests, sample was under equal P_o and P_i for 48 hours, and slight healing of specimen occurred due to self-healing property of soil, while in last refracturing test, specimen remained under applied pressure of $P_o = 2P_i$, thus specimen got consolidated under high confining pressure and resulted in further healing of existing cracks which obviously require higher hydraulic pressure for refracturing. This shows that pre-existing cracks will heal after some time under high confining stresses, even for the low plasticity soil.

The results of refracturing tests and other tests performed for evaluation of hydraulic fracturing on hollow cylindrical soil specimens indicate that the pressure at which an existing crack fully closes over a period of time, is equal to confining pressure.

5.5 PATTERN OF CRACKS

To investigate the orientation of cracks, fractured specimens were taken out from triaxial cell in such a way that both external and internal pressures were slowly decreased to zero. On examining the fractured hollow cylindrical specimens, it was observed that many cracks were developed all-round the outer surface of the specimen. The direction of cracks was more or less vertical extending through full length of the specimen. The observed cracking pattern can be seen in Photo 4.5. The occurrence of vertical cracks is also supported by the theoretical analysis.

5.6 CONCLUSIONS

To determine hydraulic fracturing pressure in the laboratory on hollow cylindrical soil mass simulating confined borehole conditions, an experimental technique has been developed and improved upon continuously over a period of three years making provision for constant pressure application (both for external and internal), pore pressure measurement, volume change measurement, water intake measurement and back pressure saturation through the hollow of cylinder.

The test results confirm the findings of earlier researchers that a linear relationship exists between hydraulic fracturing pressure and confining pressure even for hollow cylindrical specimens. Further findings are as **below** :

(i)   The hydraulic fracturing pressure for partially saturated soil is greater than that for saturated soils.

(ii)   In case of saturated samples, hydraulic fracturing pressure reduces with increasing initial degree of saturation.

(iii) With increase in time of applications of pressure, the value of hydraulic fracturing pressure decreases.

(iv)   At lower range of confining pressure, back pressure saturation technique results in lower degree of saturation compared to conventionally saturated specimen at low head under long duration. As for this reason at low confining pressure, u_f value for back pressure saturated specimen is higher.

(v)   For the cases studied under anisotropic loading condition, the hydraulic fracturing pressure decreases with anisotropy upto ratio of 1.25, whereas thereafter the difference is negligible.

(vi)   The higher the tensile strength of soil, higher will be hydraulic fracturing pressure.

(vii) In higher range of degree of saturation higher back pressures are required to attain a certain degree of saturation as compared to the theoretical values computed by Lowe and Johnson's approach.

(viii) Generally vertical cracks were observed for all the hollow cylindrical specimens tested. This indicates that at borehole tests in the core of embankment dams with high fluid pressure, vertical cracks will develop all-round the boreholes.

CHAPTER - 6

ANALYSIS OF PORE PRESSURES

6.1 GENERAL

The hydraulic fracturing pressures have also been evaluated theoretically. For this purpose, it is necessary to carry out the stress analysis of the experimental model. In order to evaluate the effective stresses, the pore pressures which develop under steady state as well as transient conditions within the soil mass need to be analyzed. In this chapter, analysis of pore pressure has been carried out for evaluating the hydraulic fracturing pressure.

6.2 ANALYSIS OF SEEPAGE

Seepage through soil mass is an important aspect in many phases of engineering. Design of large hydraulic structures under complex field conditions where pore pressures play a significant role, is an important problem in the engineering field. High hydraulic pressures are generally encountered in problems related to dams and foundations, boreholes, grouting process etc. In these cases the determination of transient pore pressure assumes great significance. Failure or damage to the structure may occur in cases where the hydraulic pressure exceeds the existing stresses in the soil mass.

Generally numerical approaches are adopted for the determination of pore pressures under transient condition. Among the various numerical techniques, the finite difference and

finite element methods have played an important role in the
analysis of flow problems. For the analysis of flow through
permeable media, the finite difference approach has been used
extensively. However, solution for irregular boundary presents
some difficulties in the finite difference method. Finite ele-
ment technique is more general and is commonly used, being more
suitable for use with digital computers.

In the present investigation finite element technique
has been used for the evaluation of pore pressures under steady
state as well as transient conditions. The flow domain is the
experimental model consisting of a hollow cylindrical soil mass
subjected to external and internal pressures. Fig. 6.1 shows
the experimental model used for pore pressure analysis. The
flow domain represents a confined axisymmetric cylindrical per-
meable media to be analyzed for flow under steady state as well
as transient conditions.

For the solution of transient flow problem, the govern-
ing partial differential equation in polar coordinates can be
written as[35,71]:

$$K_r \left[\frac{\partial^2 \phi}{\partial r^2} + \frac{1}{r} \frac{\partial \phi}{\partial r} \right] + K_z \frac{\partial^2 \phi}{\partial z^2} = S_s \frac{\partial \phi}{\partial t} \qquad ..(6.1)$$

where K_r and K_z are the coefficients of permeability in radial
and vertical directions, ϕ the total potential head and t the
time parameter. Norrie and Vries[51] reported that S_s is the
effective porosity in case of free surface problems and it is
the specific storage in case of confined problems. Since in
the present investigation the flow domain is a confined flow
problem, thus S_s is considered as specific storage of the flow
problem.

The general assumptions encountered in the application of flow equation are enumerated below :

(i)   Flow is laminar and follows Darcy's law.

(ii)   Equation of continuity is applicable.

(iii)   Soil mass is isotropic and homogeneous.

(iv)   The soil particles are incompressible.

(v)   Effect of capillarity and surface tensions are neglected.

(vi)   Soil mass is fully saturated.

The boundary and initial conditions associated with equation (6.1) are :

$$\phi = \phi_i(t) \qquad \text{on } S_1$$
$$\phi = \phi_o \qquad \text{on } S_2 \qquad\qquad ..(6.2)$$
$$\frac{\partial \phi}{\partial n} = 0 \qquad \text{on } S_3$$

where S_1 is part of the boundary on which ϕ_i is prescribed, S_2 is part of boundary on which ϕ_o is prescribed and S_3 is the impervious boundary where flow normal to it is zero as shown in Fig. 6.1.

The basic differential equation governing seepage problem represented by equation 6.1 involves time as one of the parameters and is referred to as the transient or time dependent problem. If the time dependent term on the right hand side vanishes, the remaining part represents steady state seepage problem.

CROSS SECTION

PLAN
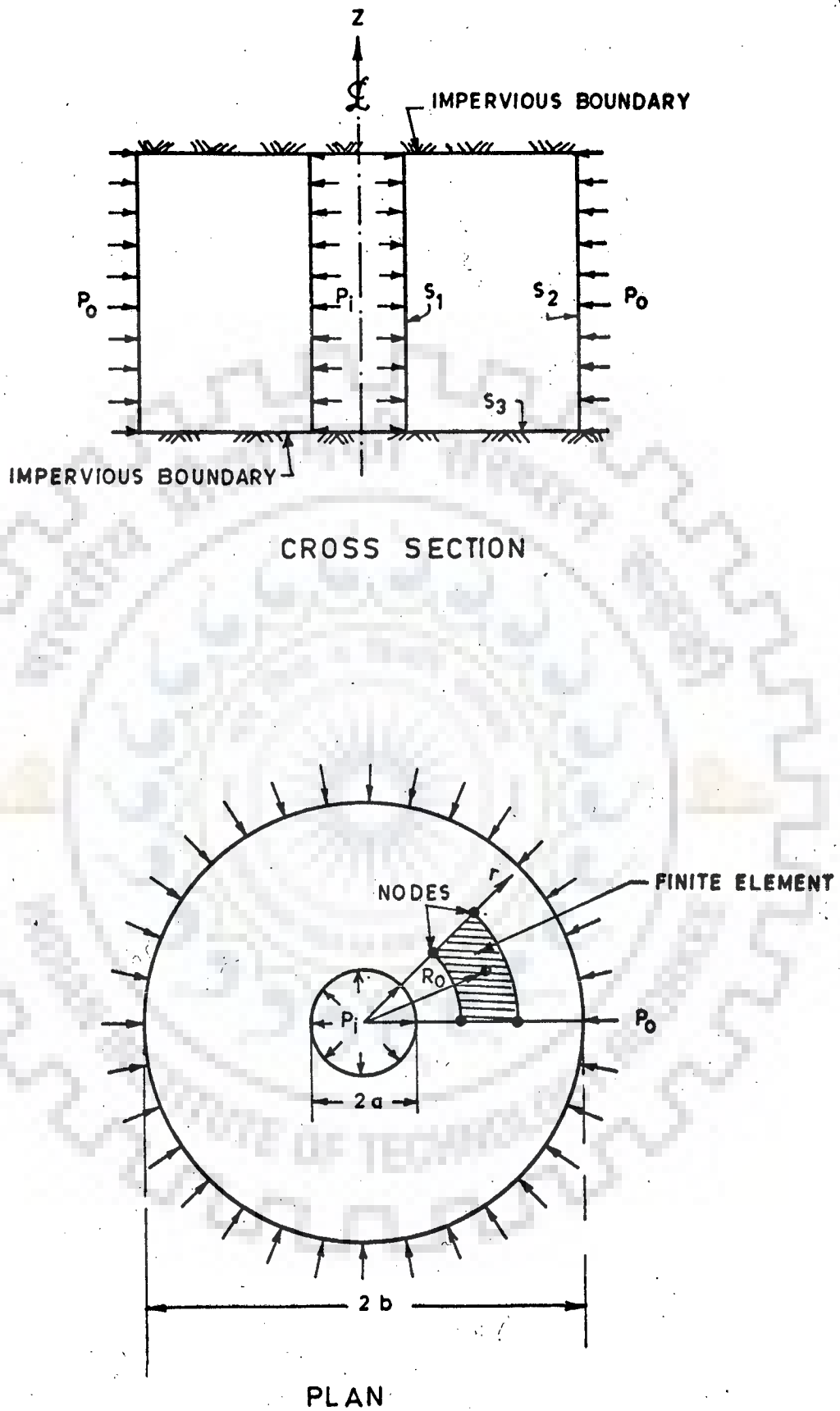
FIG. 6.1 _ SKETCH SHOWING HOLLOW CYLINDRICAL
SOIL SAMPLE

6.3 FINITE ELEMENT FORMULATION

The finite element method is well known and is described in the texts[14-16,52,72] and only some salient points are summarized here. The finite element technique consists of subdividing a given system into a discrete number of small regions of finite dimensions. Each small region is characterized as 'Finite Element' whose behaviour is easily understood. The original system is then rebuilt from such small elements to study the integrated behaviour. The differential equation describing the flow together with appropriate boundary conditions is recast into integral relations, whereas integrals are expressed as sum of the component integrals over individual elements. Using element interpolation functions, the integral relations are then approximated by a system of equations containing nodal values of flow variables as unknowns.

Following the steps of finite element technique[13,17, 53,73,74] equation 6.1 can be discretized using finite elements to give a matrix equation for each element as :

$$[G]^e\{\dot{\phi}_n\} + [H]^e\{\phi_n\} = \{0\} \quad ..(6.3)$$

where $[G]^e$ is the element characteristic (associated with specific storage) matrix, $[H]^e$ is the element characteristic (associated with permeability) matrix, $\{\phi_n\}$ is the nodal potential vector and dot defines differentiation with respect to time. For a finite element located in an axisymmetric flow domain as shown in Fig. 6.1, the elemental matrices can be written[26] as :

$$[H]^e = 2\pi \int_A [B]^T [R] [B] (R_o+r) \, drdz \quad ..(6.4)$$

$$[G]^e = 2\pi \, S_s \int_A [N]^T [N] \, (R_0 + r) \, dr dz \qquad ..(6.5)$$

where

$$[B] = \begin{bmatrix} \dfrac{\partial N_i}{\partial r} & \dfrac{\partial N_j}{\partial r} & \dfrac{\partial N_k}{\partial r} & \dfrac{\partial N_\ell}{\partial r} \\[2ex] \dfrac{\partial N_i}{\partial z} & \dfrac{\partial N_j}{\partial z} & \dfrac{\partial N_k}{\partial z} & \dfrac{\partial N_\ell}{\partial z} \end{bmatrix} \qquad ..(6.6)$$

$$[R] = \begin{bmatrix} k_r & 0 \\ 0 & k_z \end{bmatrix} \qquad ..(6.7)$$

and [N] is the matrix of shape functions, R_0 is the centeroid-al radial distance, r and z are the local coordinates in radial and axial directions respectively.

Consider a typical four noded rectangular element lo-cated in an axisymmetric flow domain as shown in Fig. 6.2. The distribution of potential head within the element can be expre-ssed in terms of nodal point heads as,

$$\begin{aligned} \{ \phi^e \} &= \sum_{i=1}^{4} N_i \, \phi_i \\ &= [N_i, \; N_j, \; N_k, \; N_\ell] \begin{Bmatrix} \phi_i \\ \phi_j \\ \phi_k \\ \phi_\ell \end{Bmatrix} \\ &= [N] \, \phi_n^{\;e} \end{aligned} \qquad ..(6.8)$$

where $\{ \phi_n \}^e$ are the nodal potential heads of the element and N_i, N_j, N_k and N_ℓ are the shape functions.

The shape functions for the element can be written as:

$$N_i = \tfrac{1}{4} (1 - \tfrac{r}{a}) (1 - \tfrac{z}{b})$$

$$N_j = \tfrac{1}{4} (1 + \tfrac{r}{a}) (1 - \tfrac{z}{b}) \qquad ..(6.9)$$

$$N_k = \tfrac{1}{4} (1 + \tfrac{r}{a}) (1 + \tfrac{z}{b})$$

$$N_\ell = \tfrac{1}{4} (1 - \tfrac{r}{a}) (1 + \tfrac{z}{b})$$

Element matrices associated with permeability and specific storage of material given by equations (6.4) and (6.5) can be obtained as follows, after performing exact integration.

$$
[H]^e = \frac{\pi}{3ab}
\begin{bmatrix}
2b^2R_0k_r + (2a^2R_0-a^3)k_z & -2b^2R_0k_r + a^2R_0k_z & -b^2R_0k_r - a^2R_0k_z & b^2R_0k_r - a^2R_0k_z \\
-2b^2R_0k_r + a^2R_0k_z & 2b^2R_0k_r + (2a^2R_0+a^3)k_z & b^2R_0k_r + (-2a^2R_0-a^3)k_z & -b^2R_0k_r - a^2R_0k_z \\
-b^2R_0k_r - a^2R_0k_z & b^2R_0k_r + (-2a^2R_0-a^3)k_z & 2b^2R_0k_r+(2a^2R_0+a^3)k_z & -2b^2R_0k_r + a^2R_0k_z \\
b^2R_0k_r + (-2a^2R_0+a^3)k_z & -b^2R_0k_r - a^2R_0k_z & -2b^2R_0k_r + a^2R_0k_z & 2b^2R_0k_r+(2a^2R_0-a^3)k_z
\end{bmatrix}
$$

$$..(6.10)$$

and

$$
[G]^e = \frac{2\pi abS_s}{9}
\begin{bmatrix}
4R_0-2a & 2R_0 & R_0 & 2R_0-a \\
2R_0 & 4R_0+2a & 2R_0+a & R_0 \\
R_0 & 2R_0+a & 4R_0+2a & 2R_0 \\
2R_0-a & R_0 & 2R_0 & 4R_0-2a
\end{bmatrix}
\quad ..(6.11)
$$

Where 2a and 2b specify the size of element.

With the evaluated matrices $[H]^e$ and $[G]^e$ for each finite element, the matrix equations for the complete system are obtained by systematic superposition as :

$$[G]\ \{\dot{\phi}\} + [H]\ \{\phi\} = \{0\} \qquad ..(6.12)$$

At the boundary nodal points, the pressure is defined and known. The equations given by equation (6.12) can be

rearranged corresponding to active and boundary nodal points as :

$$
\begin{bmatrix}
G_{11} & \vdots & G_{12} \\
(mxm) & \vdots & (mxq) \\
- - - & \vdots & - - - \\
G_{21} & \vdots & G_{22} \\
(qxm) & \vdots & (qxq)
\end{bmatrix}
\begin{Bmatrix}
\dot{\phi}_1 \\
(mx1) \\
- - - \\
\dot{\phi}_2 \\
(qx1)
\end{Bmatrix}
+
\begin{bmatrix}
H_{11} & \vdots & H_{12} \\
(mxm) & \vdots & (mxq) \\
- - - & \vdots & - - - \\
H_{21} & \vdots & H_{22} \\
(qxm) & \vdots & (qxq)
\end{bmatrix}
\begin{Bmatrix}
\phi_1 \\
(mx1) \\
- - - \\
\phi_2 \\
(qx1)
\end{Bmatrix}
=
\begin{Bmatrix}
0 \\
(mx1) \\
- - - \\
0 \\
(qx1)
\end{Bmatrix}
\quad ..(6.13)
$$

where q is the number of boundary nodal points on which the pressure is known and m is the number of points on which the pressure is to be computed.

Applying the boundary conditions equation (6.13) could be written as

$$
[G_{11}] \{\dot{\phi}_1\} + [H_{11}] \{\phi_1\} = -[G_{12}] \{\dot{\phi}_2\} - [H_{12}] \{\phi_2\}
$$
$$..(6.14)$$

For simplicity the matrix equation corresponding to the active nodal points given by equation (6.14) could be written as :

$$
[\bar{G}] \{\dot{\bar{\phi}}\} + [\bar{H}] \{\bar{\phi}\} = \{\bar{F}_{(t)}\} \qquad ..(6.15)
$$

where $\{\bar{F}_{(t)}\}$ is the vector of nodal forcing functions obtained after application of the boundary conditions and depends on transient condition where internal pressure is dependent on time.

6.4 SOLUTION SCHEME

6.4.1 Steady State Condition

When the time dependent term of equation (6.12) is zero, it gives the steady state condition of flow. For the steady

state condition the finite element equation for the system can be expressed as;

$$[H] \ \{\emptyset\} = \{0\} \qquad\qquad ..(6.16)$$

Applying the boundary conditions equation (6.16) can be expressed as ;

$$[H_{11}] \ \{\emptyset_1\} = -[H_{12}] \ \{\emptyset_2\} \qquad\qquad ..(6.17)$$

and the corresponding assembled matrix equations for the active nodal points can be written as ;

$$[\bar{H}] \ \{\bar{\emptyset}\} = \{\bar{F}_o\} \qquad\qquad ..(6.18)$$

where $\{\bar{F}_o\}$ is the matrix of nodal forcing function which depends on steady state condition in which the applied pressure is independent of time.

Equation (6.18) represents the system of linear algebraic equations to be solved for determination of pore pressure under steady state condition. Gaussian elimination technique has been adopted for the solution of these algebraic equations.

The steady state pore pressure distribution around axisymmetric hollow cylindrical soil media due to application of (i) external pressure with no internal pressure and (ii) internal pressure with no external pressure has been obtained and plotted in Fig. 6.4. The curves are prepared in dimensionless form for the ratio of pore pressure to peak applied pressure Vs ratio of radial distance to inner radius of the cylindrical soil mass.

6.4.2 Transient Condition

Equation (6.15) can be integrated with respect to time. For the solution of this time dependent problem, Crank-Nickolson recurrence method[11,12,29] is adopted. This scheme is an implicit method which is unconditionally stable[65]. Crank-Nickolson recurrence approach reduces the time dependent equations into a system of linear algebraic equations with unknown potentials at later time intervals. To apply the solution scheme, time is divided into a series of time increments Δt, assuming that the initial conditions of the problems are known. Hence the following approximation can be used[11,54,56].

$$\dot{\phi}_{\Delta t/2} = \frac{\phi_{\Delta t} - \phi_0}{\Delta t}$$

and

$$\phi_{\Delta t/2} = \frac{\phi_{\Delta t} - \phi_0}{2}$$

$$F_{\Delta t/2} = \frac{F_{\Delta t} - F_0}{2}$$

..(6.19)

In equation (6.19), $\phi_{\Delta t}$ and $\phi_{\Delta t/2}$ are unknowns. Substituting values of $\dot{\phi}_{\Delta t/2}$, $\phi_{\Delta t/2}$ and $F_{\Delta t/2}$ from equation (6.19) into equation (6.15), at time $\Delta t/2$, the following equation is obtained,

$$([\bar{H}] + \frac{2}{\Delta t} [\bar{G}]) \{\vec{\phi}_{\Delta t}\} = (\{\bar{F}_{\Delta t}\} + \{\bar{F}_0\}) - ([\bar{H}] - \frac{2}{\Delta t} [\bar{G}] \{\vec{\phi}_0\}$$

..(6.20)

Equation (6.20) represents the system of linear algebraic equations to be solved at various time intervals. Gaussian elimination technique has been adopted for the solution of these algebraic equations.

6.5 INVESTIGATION OF PARAMETERS AFFECTING THE TRANSIENT FLOW

The main parameters involved in the study of transient flow problems are permeability, specific storage of the flow domain, type and rate of pressure application and the time step of integration. The effect of these parameters in the analysis of non-steady axisymmetric flow through permeable media has been studied as follows ;

6.5.1 Coefficient of Permeability and Specific Storage of Flow Media

The correct evaluation of coefficient of permeability K, and specific storage S_s is quite difficult in case of fine grained soils from conventional laboratory experimentation. The coefficient of permeability in the range of 10^{-6} cm/sec or less has been reported for cohesive soils[5,66]. However, experiments were conducted in the laboratory for the fine grained soil used in this investigation in order to evaluate its permeability, and the average value of K in the range of 4×10^{-7} cm/sec has been obtained. Experiments for determination of specific storage are rather more difficult and limited information is available even in case of cohesionless soils. To the knowledge of the author, no information has been reported so far for the measurement of specific storage of cohesive soils. The evaluation of specific storage involves many parameters and can be expressed as[47,71];

$$S_s = \gamma_w (C_s + n C_w) \qquad \qquad ..(6.21)$$

where γ_w is the unit weight of water, C_s is the compressibility

of the soil skeleton (i.e. the reciprocal of bulk modulus of the soil) and C_w is the compresibility of water (i.e. the reciprocal of bulk modulus of water) and n is the porosity of the soil.

The average value of porosity for the soil tested has been determined as 33.5 percent. The compressibility of water and soil depend on their bulk modulus. The bulk modulus of water is generally accepted as 20×10^3 Kg/cm^2 [43], while evaluation of bulk modulus of soil depends on many parameters, such as existing state of stresses to which soil mass is subjected, type and properties of soil mass and nature of load deformation characteristics of soil. A value of bulk modulus of 500 Kg/cm^2 has been adopted[22,36,59] for the core material of many existing dams, using more or less the same type of soil as used for the experimental work, presented in this thesis. Assuming bulk modulus of soil skeleton as 500 Kg/cm^2, porosity 33.5 percent and bulk modulus of water as 20×10^3 Kg/cm^2, the specific storage has been found to be about 2×10^{-6} 1/cm. Gambolati[20] showed that the use of S_s as a constant for saturated media is justified as long as vertical strain is less than 5%. A normalized factor η, defined as the ratio of coefficient of permeability to the specific storage of the soil medium is calculated as 12 cm^2/minute which has been adopted for analyzing the seepage flow behaviour of the soil under investigation.

In order to study the effect of the coefficient of permeability and specific storage on pore pressure development within the soil mass, the value of η has also been varied between 1 and 120 for the same applied pressure.

6.5.2 Effect of Rate of Application of Hydraulic Pressure

In order to investigate the effect of rate of pressure application analytically, the hydraulic pressure has been linearly increased on the inner surface of the hollow cylindrical soil mass in time duration τ from initial value of zero as shown in Fig. 6.3. The value of τ has been varied between 0.1 and 2.5 minutes for the same applied pressure. The slope of the curve in Fig. 6.3, indicates the rate of pressure application.

6.5.3 Time Step of Integration

Effect of time step of integration (Δt) has been studied by varying $\tau/\Delta t$ from 10 to 100. The percentage of pore pressure development at middle thickness of hollow cylindrical soil mass for each integration time step is presented in Table (6.1) at various time instants for τ equal to one minute. The results indicate that the pore pressure distribution for $\tau/\Delta t$ equal to 20 gives quite accurate results at all the time instants and has been adopted for the present investigation.

TABLE 6.1   PERCENTAGE OF PORE PRESSURE DEVELOPMENT AT MIDDLE THICKNESS OF HOLLOW CYLINDRICAL SOIL MASS

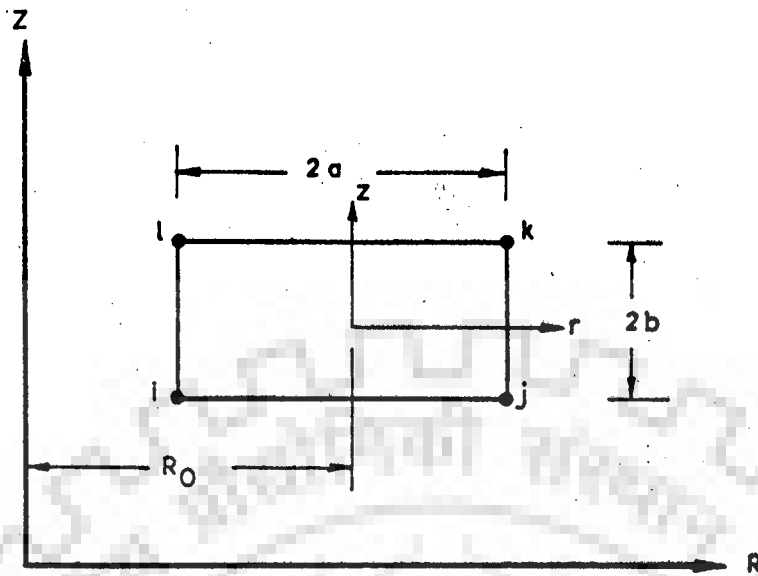| $\tau/\Delta t$ \ t	0.2	0.5	1.0	1.5	2.0	2.5	3.0
100	1.38	8.00	21.50	27.33	27.69	27.71	27.71
20	1.38	7.99	21.49	27.34	27.69	27.71	27.71
10	1.30	7.97	21.50	27.36	27.69	27.71	27.71

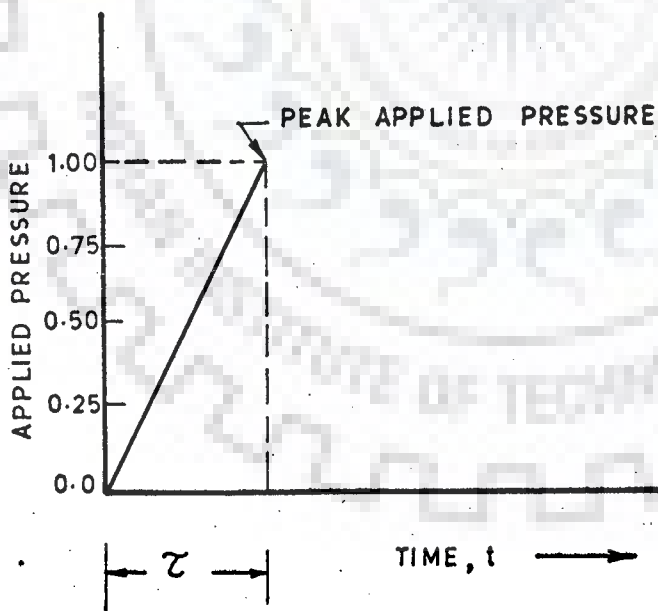FIG. 6·2 _ TYPICAL 4 NODED LINEAR ELEMENT

FIG. 6·3 _ DIAGRAMMATIC REPRESENTATION OF
PRESSURE APPLICATION
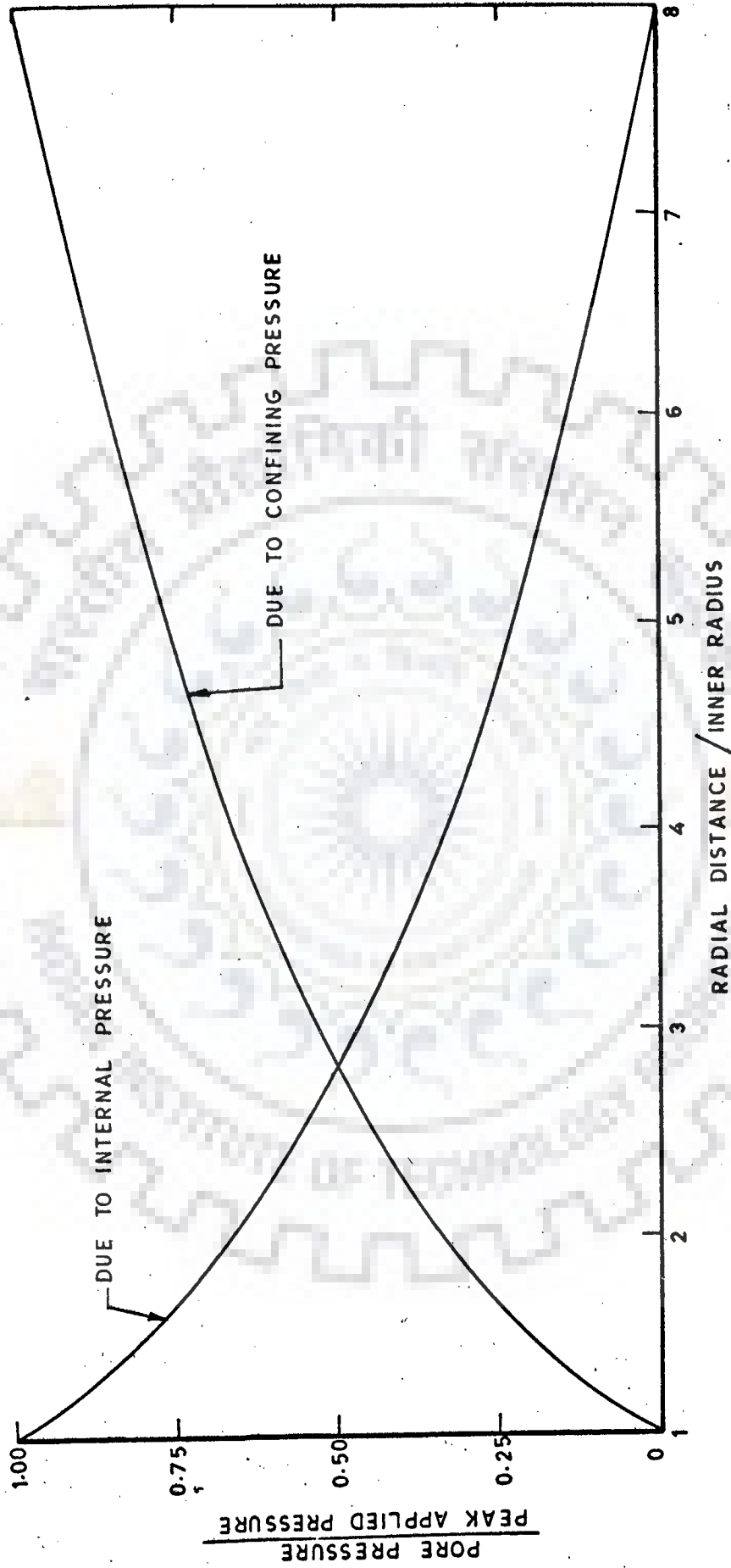
FIG. 6.4 — VARIATION OF PORE PRESSURE WITH RADIAL DISTANCE OF HOLLOW CYLINDRICAL SOIL MASS AT STEADY STATE CONDITION

6.6 ANALYSIS AND DISCUSSIONS

In this section the results of various parameters affecting transient flow as computed theoretically are presented. The solution for transient condition has been obtained, considering zero internal pressure at time, t = 0. For the conditions where pore pressures are not zero at the initial time, the steady state pore pressures would be added to the transient pore pressures to get total pore pressure at any time under consideration.

To study the effect of variation of η, curves of pore pressure development to the peak applied pressure vs time due to applied interial pressure are plotted at a radial distance of 5 percent from inner surface and at the middle thickness of hollow cylindrical soil mass in Figs. 6.5 and 6.6 respectively. These curves show that as the value of η increases, the time required to achieve steady state condition decreases. This indicates that as material becomes more porous, the time required for the achievement of steady state condition is less and pressure stabilizes at a faster rate.

Figs. 6.7 and 6.8 show the effect of rate of internal pressure application on the pore pressure development at a radial distance of 5 percent from the inner surface of the soil cylinder and its middle thickness respectively. It is noted from the figures that as rate of application of pressure increases, the time required to achieve steady state pressure decreases. The pore pressure is developed at a faster rate at the points, closer to the inner surface, as expected, compared to the middle thickness of the hollow cylindrical soil mass. It is also seen

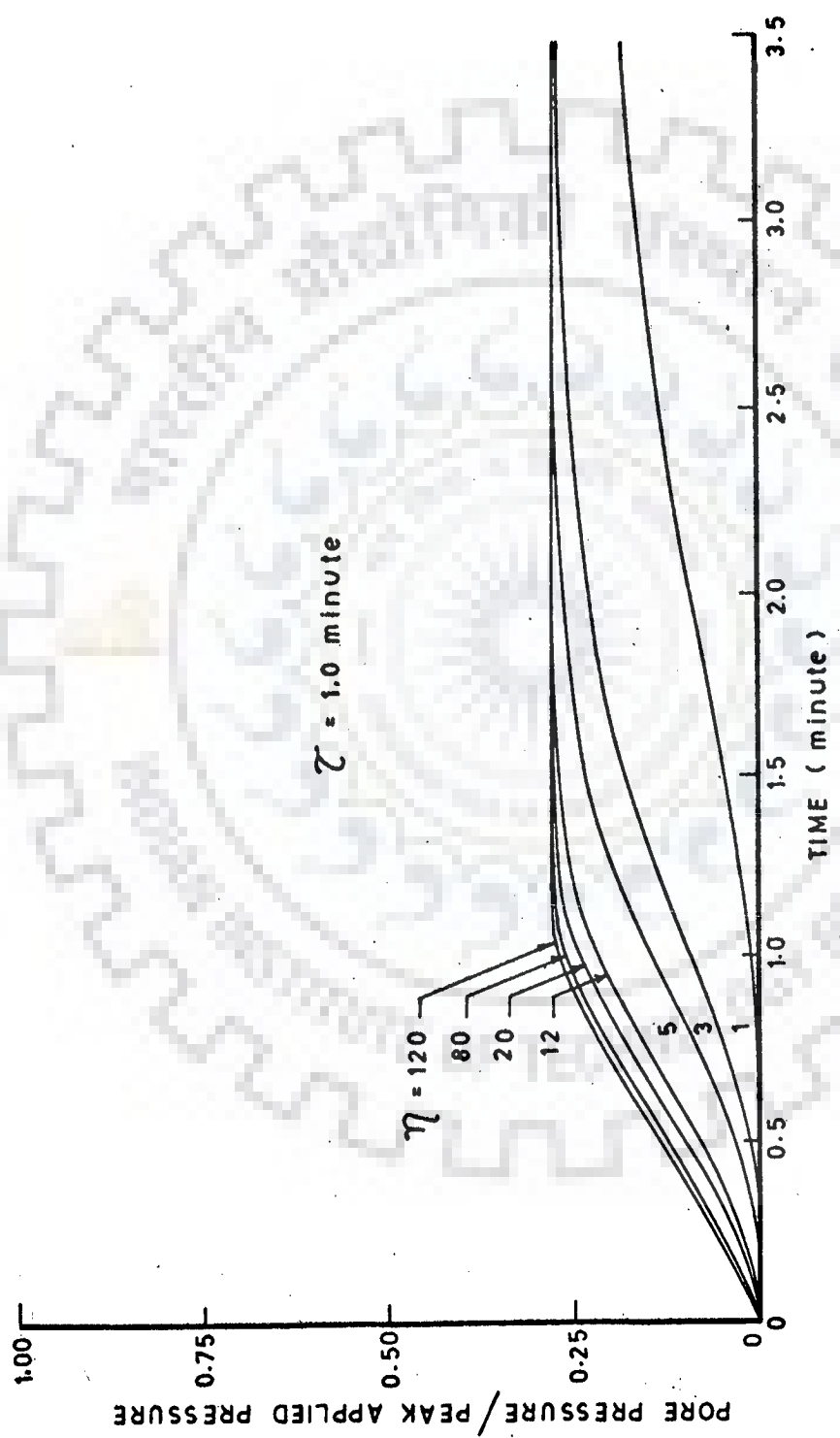FIG. 6.6 _ VARIATION OF PORE PRESSURE WITH TIME AT MIDDLE THICKNESS OF HOLLOW CYLINDRICAL SOIL MASS
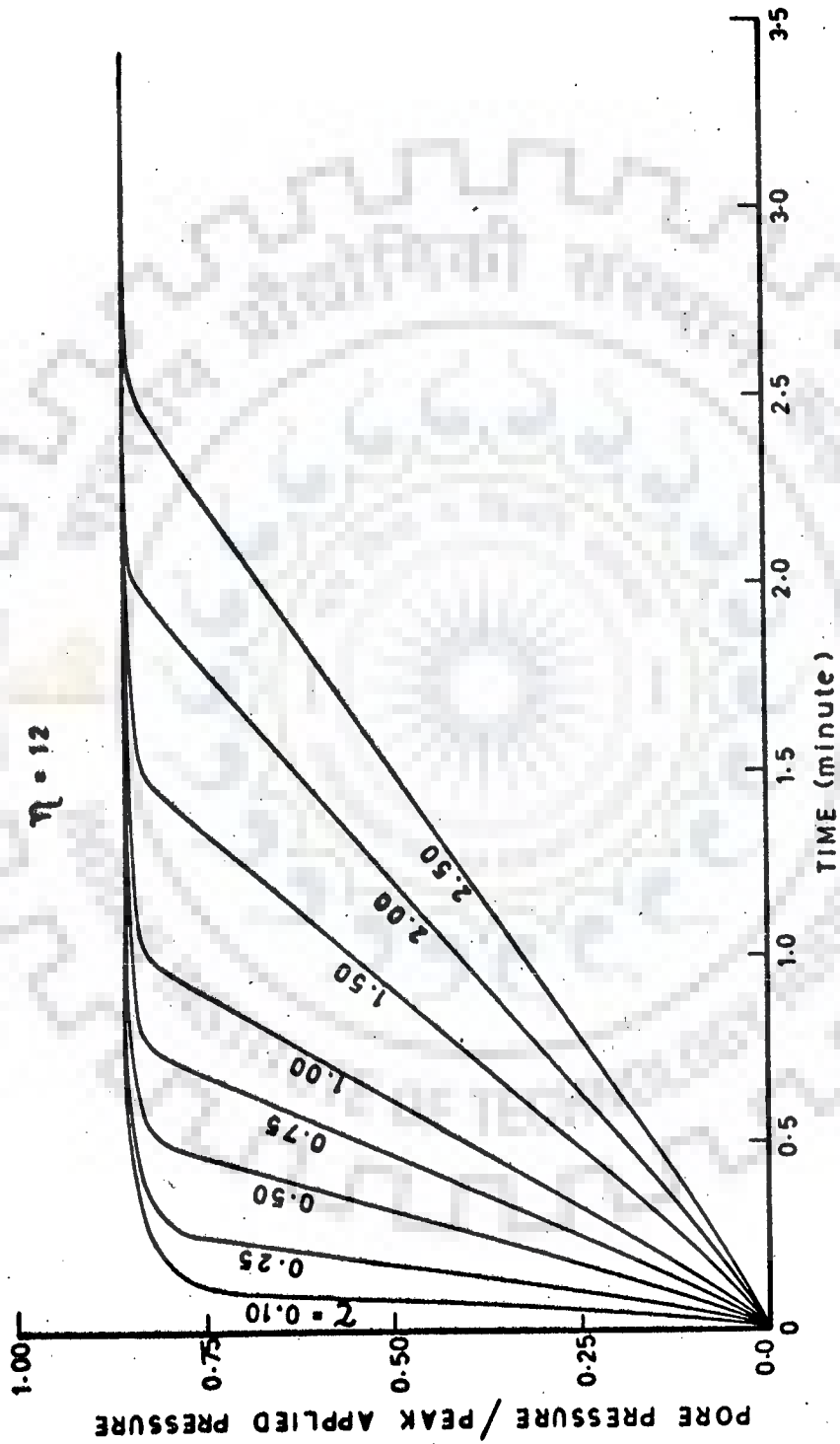
FIG. 6.7 – VARIATION OF PORE PRESSURE WITH TIME AT 5% RADIAL DISTANCE FROM INNER SURFACE OF HOLLOW CYLINDER FOR VARIOUS RATES OF PRESSURE APPLICATION
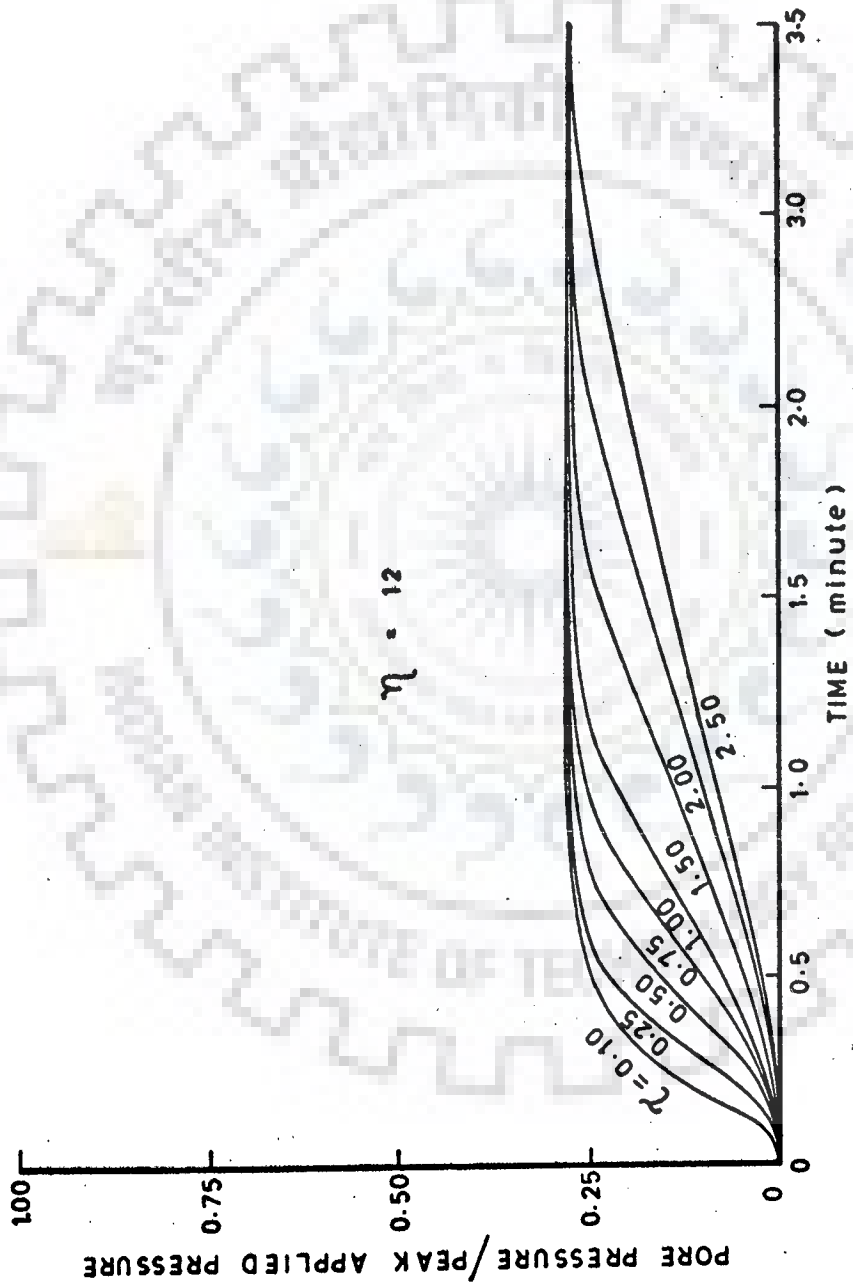
FIG. 6.8 – VARIATION OF PORE PRESSURE WITH TIME AT MIDDLE THICKNESS OF HOLLOW CYLINDRICAL SOIL MASS FOR VARIOUS RATES OF PRESSURE APPLICATION

from the figures that the steady state pore pressure developed
at 5 % radial distance from the inner surface of hollow cylin-
der is of the order of 86 % of the applied internal pressure,
while it is about 28 % at its middle thickness.

Fig. 6.9 shows the variation of pore pressure vs time
at various points along the radial distance of hollow cylindri-
cal soil mass. These curves further clarify the nature of pore
pressure development at various points. The time required for
achievement of steady state pore pressure increases with in-
crease of radial distance. At radial distance of 5 % from the
inner surface, the steady state pore pressure is 86 % of the
applied internal pressure and is obtained an 1.4 minutes, while
at a distance of 75 % from the inner surface, 12 % pore pressure
is obtained, at a time of 3.5 minutes, whereas internal pressure
was applied at a time period of, τ = 1.0 minutes. Thus the
higher pore pressure at points closer to inner surface of hollow
cylindrical soil mass is more critical for the crack develop-
ment or failure within the soil mass.

Variation of pore pressure development along radial
distance from the inner surface of hollow cylindrical soil mass
due to applied internal pressure is presented in Fig. 6.10 for
τ = 1.0 minutes and η = 12. Curves are drawn in dimensionless
form for the ratio of pore pressure to peak applied pressure
vs ratio of radial distance to the inner radius of the model
hollow cylindrical soil specimen used for experimental investi-
gations, at various time instants. It is seen that beyond the
time interval equal to τ, the rate of pore pressure development
along radial distance decreases with increase of time. It is
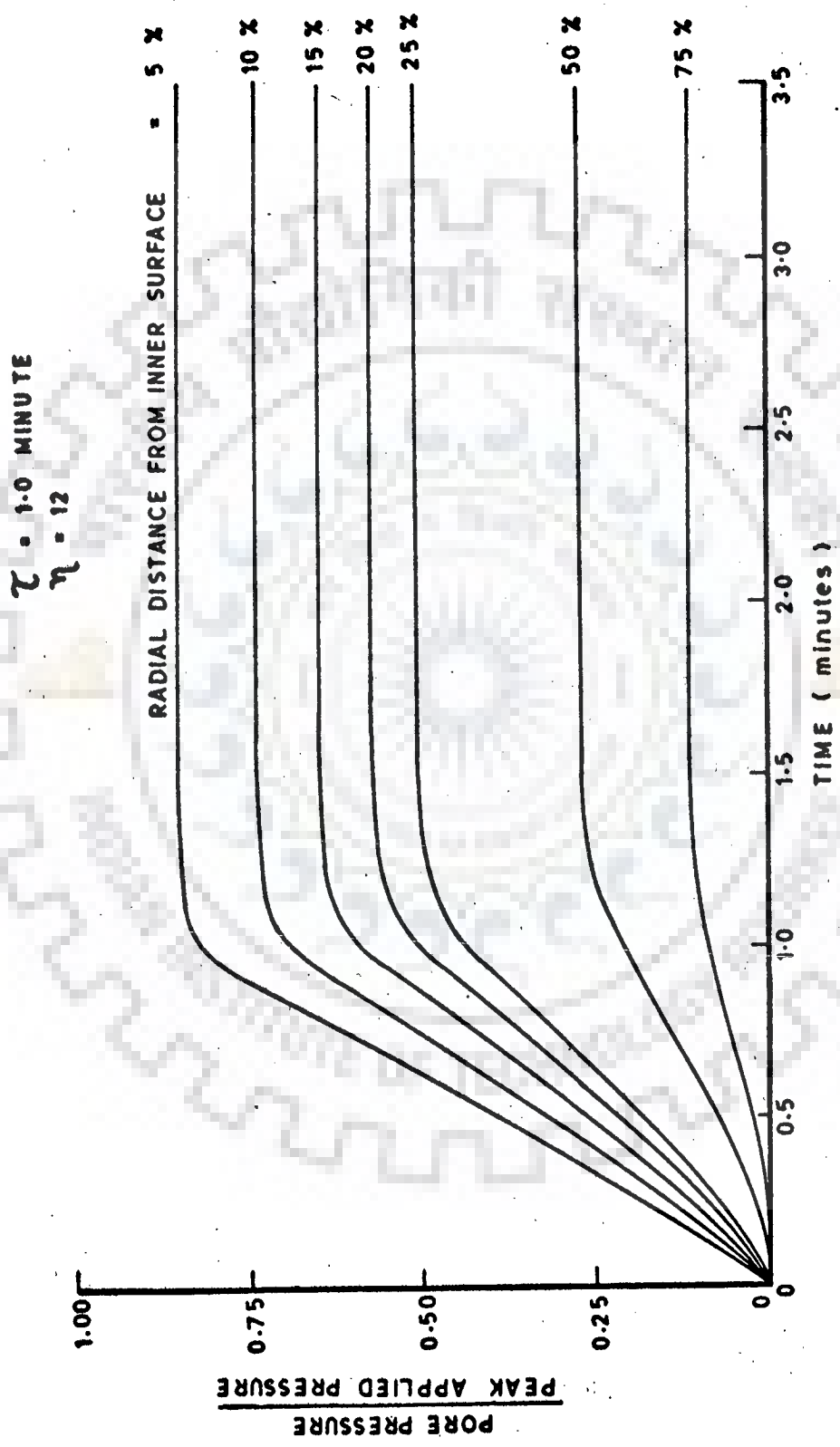
FIG. 6.9 - VARIATION OF PORE PRESSURE WITH TIME AT DIFFERENT POINTS
FROM INNER SURFACE OF HOLLOW CYLINDRICAL SOIL MASS

obvious that during pressure application, transient pore pressure develops faster and **afterwards** the rate of pore pressure development decreases, until steady state condition is achieved. The plots show that as a radial distance increases from the inner surface of hollow cylindrical soil mass, the value of pore pressure development decreases at decreasing rate.

For the model investigated, pore pressure development could be predicted from such curves at any point and instant of time along the radial distance knowing rate of internal pressure application. Similar curves are presented in Figs. 6.11 to 6.16 for τ values of 0.5, 0.75, 2.0, 3.0, 7.0 and 12.0 minutes, taking $\eta = 12$. These curves are used in Chapter 7, for prediction of pore pressure development under transient condition, in order to evaluate hydraulic fracturing pressure for actual experimental series presented in Chapter 4.

Since curves of Figs. 6.10 to 6.16 are prepared for dimensionless parameters, curves of this type could be prepared for various rates of application of hydraulic pressure and different η values to cover various types of material and rates of pressure application for actual field conditions. Such curves can be used as design curves for determination of pore pressure development at various locations and instant of times in the soil mass.

$$\tau = 1.0 \text{ MINUTE}$$

$$\eta = \frac{K}{S_s} = \frac{\text{COEFFICIENT OF PERMEABILITY}}{\text{SPECIFIC STORAGE}} = 12$$

t = 1.0 (minute)

STEADY STATE

0.9
0.8
0.7
0.6
0.5
0.4
0.3
0.2
0.1

RADIAL DISTANCE / INNER RADIUS

PORE PRESSURE / PEAK APPLIED PRESSURE

1.00 0.75 0.50 0.25 0.0
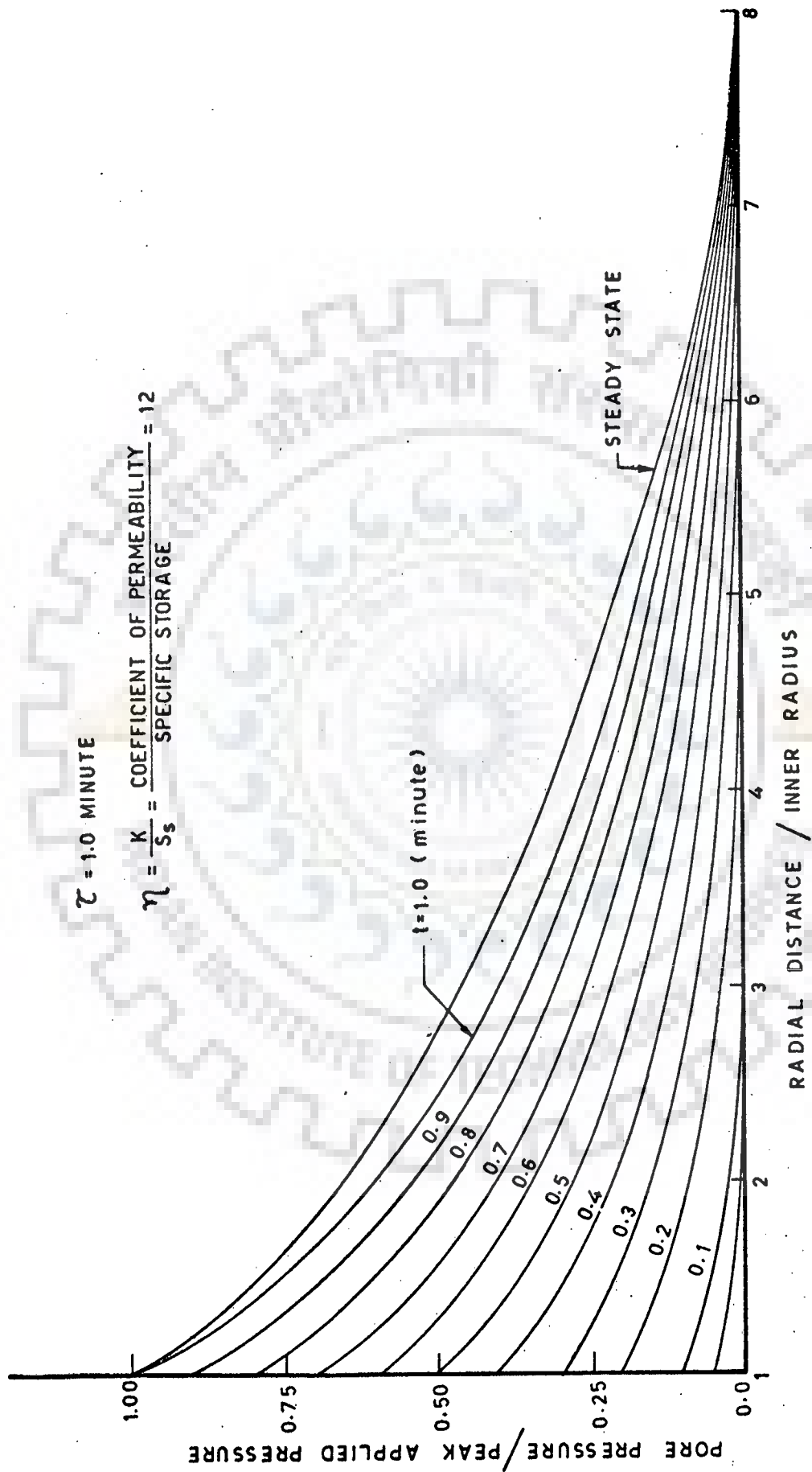
FIG. 6.10 - VARIATION OF PORE PRESSURE WITH RADIAL DISTANCE OF HOLLOW CYLINDRICAL SOIL MASS AT VARIOUS TIME INSTANTS
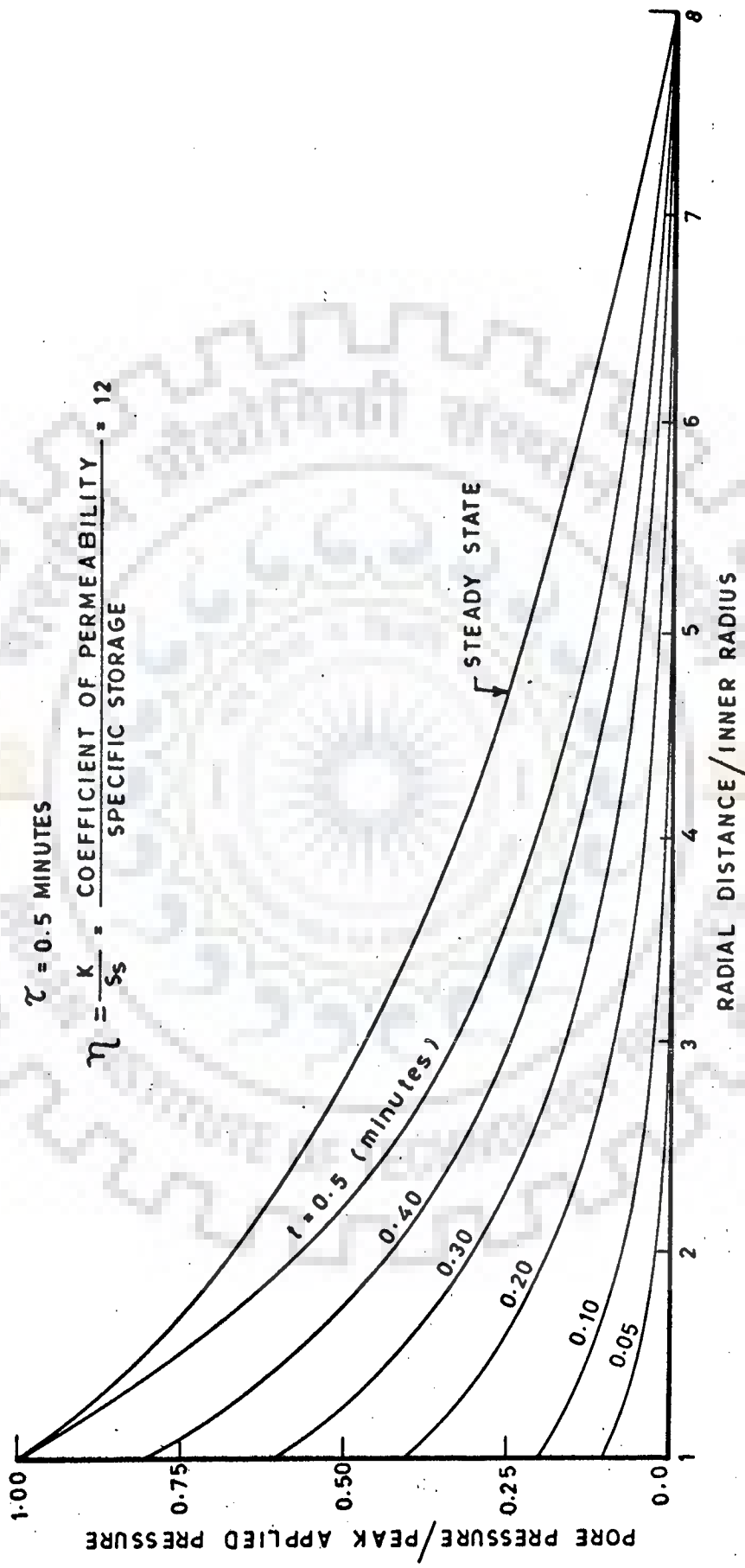
FIG. 6.11 – VARIATION OF PORE PRESSURE WITH RADIAL DISTANCE OF HOLLOW CYLINDRICAL SOIL MASS AT VARIOUS TIME INSTANTS

130

$\tau = 0.75$ MINUTES

$\eta = \dfrac{K}{S_s} = \dfrac{\text{COEFFICIENT OF PERMEABILITY}}{\text{SPECIFIC STORAGE}} = 12$

STEADY STATE

$t = 0.75$ (minutes)

0.70

0.60

0.50

0.40

0.30

0.20

0.10

RADIAL DISTANCE / INNER RADIUS

PORE PRESSURE/PEAK APPLIED PRESSURE
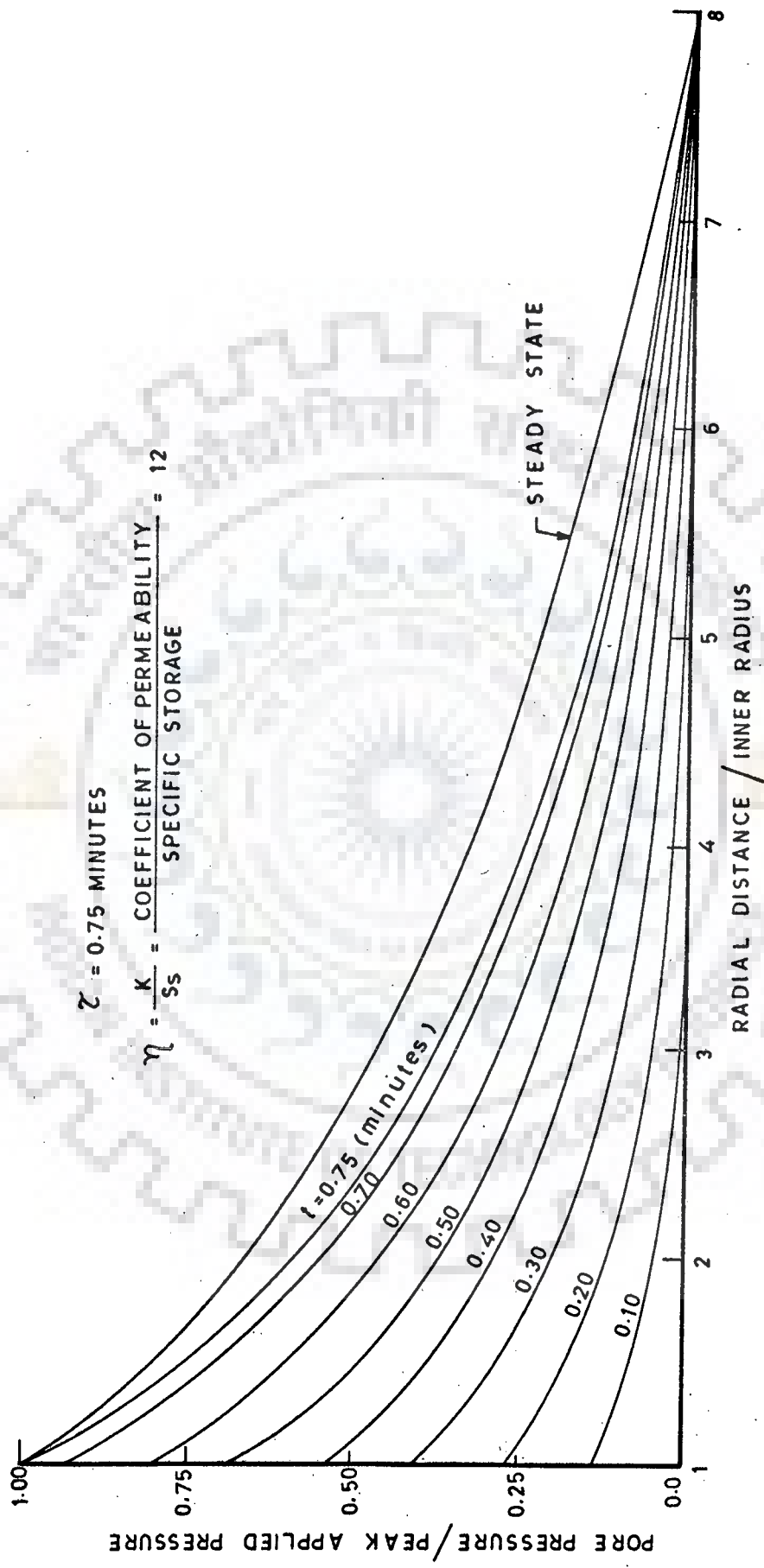
FIG. 6.12 — VARIATION OF PORE PRESSURE WITH RADIAL DISTANCE OF HOLLOW CYLINDRICAL SOIL MASS AT VARIOUS TIME INSTANTS

131
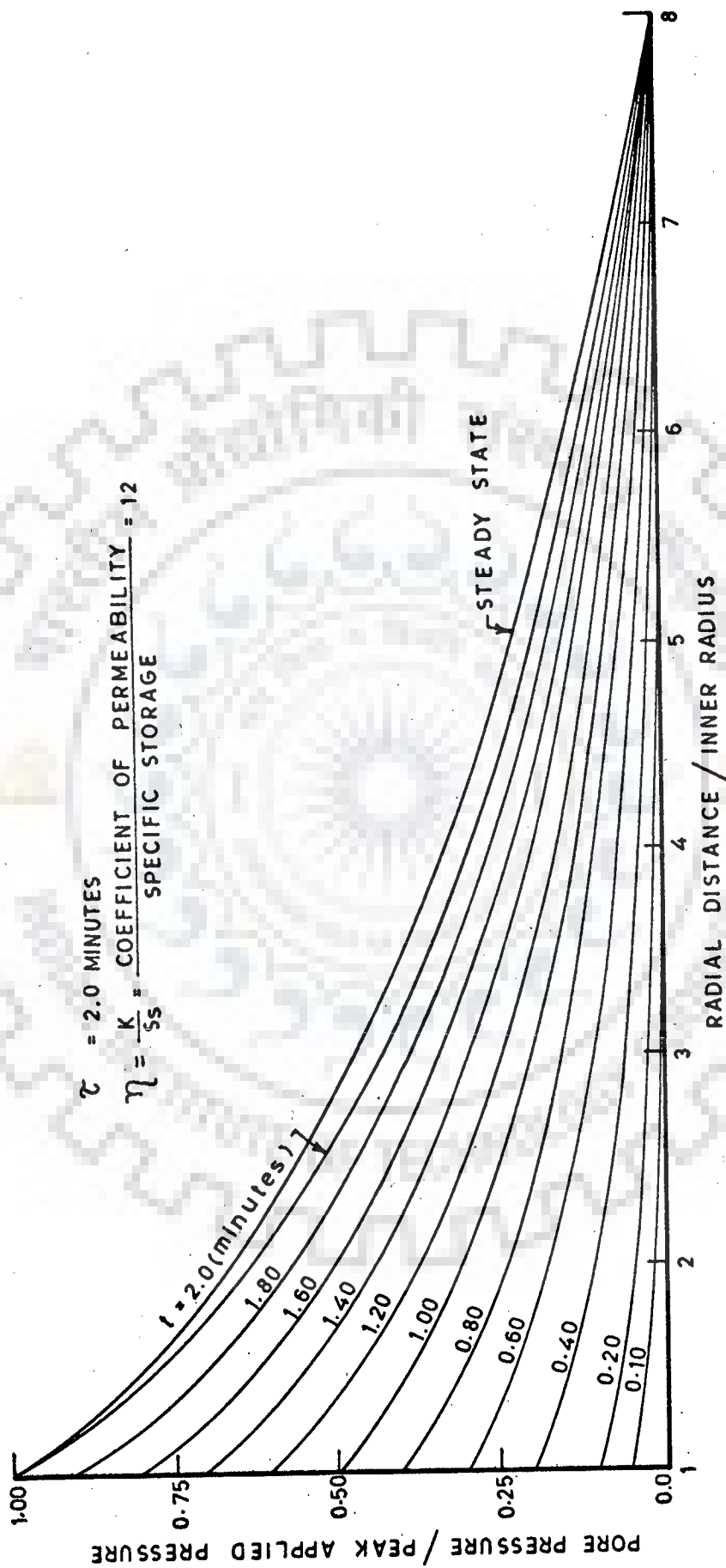
FIG. 6.13 - VARIATION OF PORE PRESSURE WITH RADIAL DISTANCE OF HOLLOW CYLINDRICAL SOIL MASS AT VARIOUS TIME INSTANTS
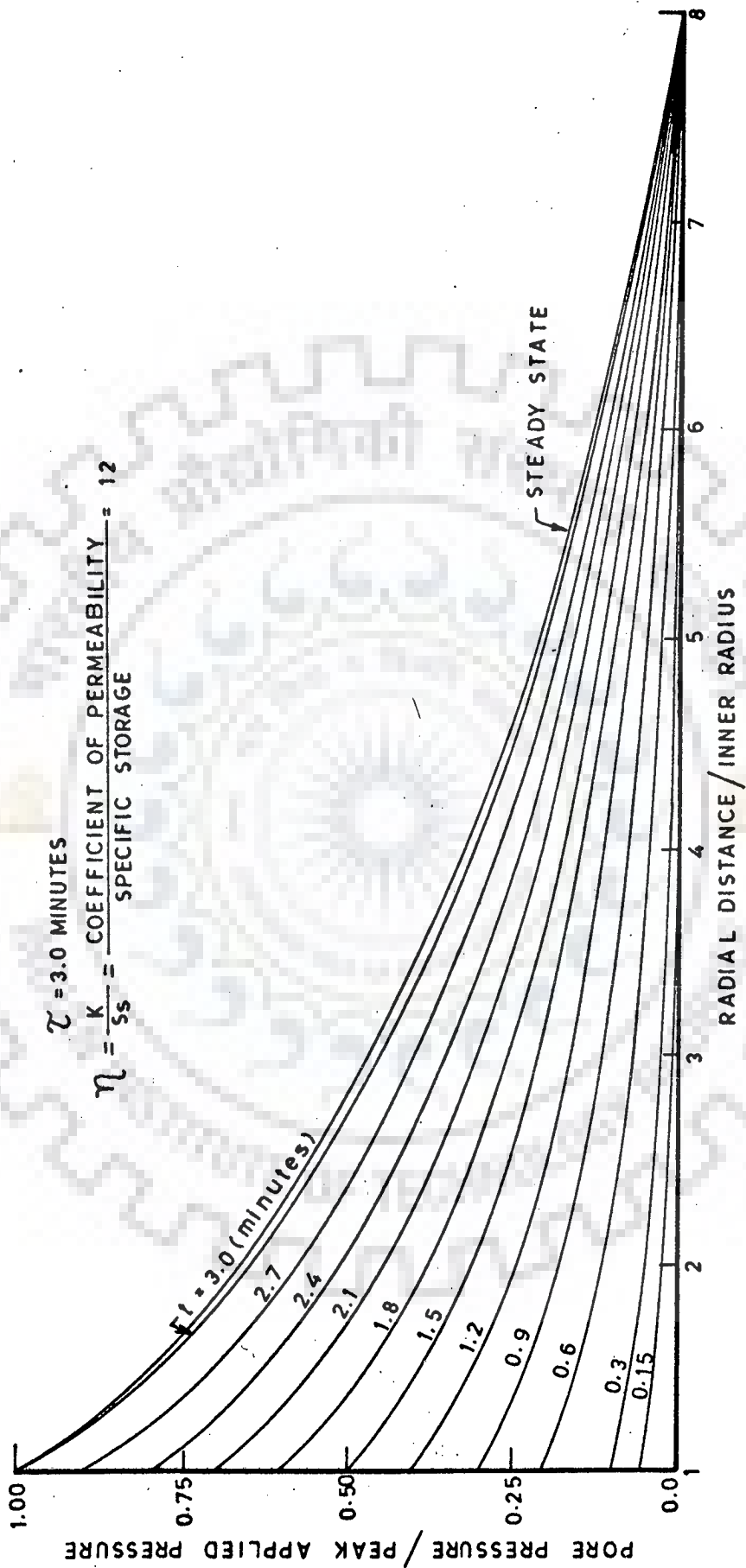
FIG. 6.14.– VARIATION OF PORE PRESSURE WITH RADIAL DISTANCE OF HOLLOW CYLINDRICAL SOIL MASS AT VARIOUS TIME INSTANTS
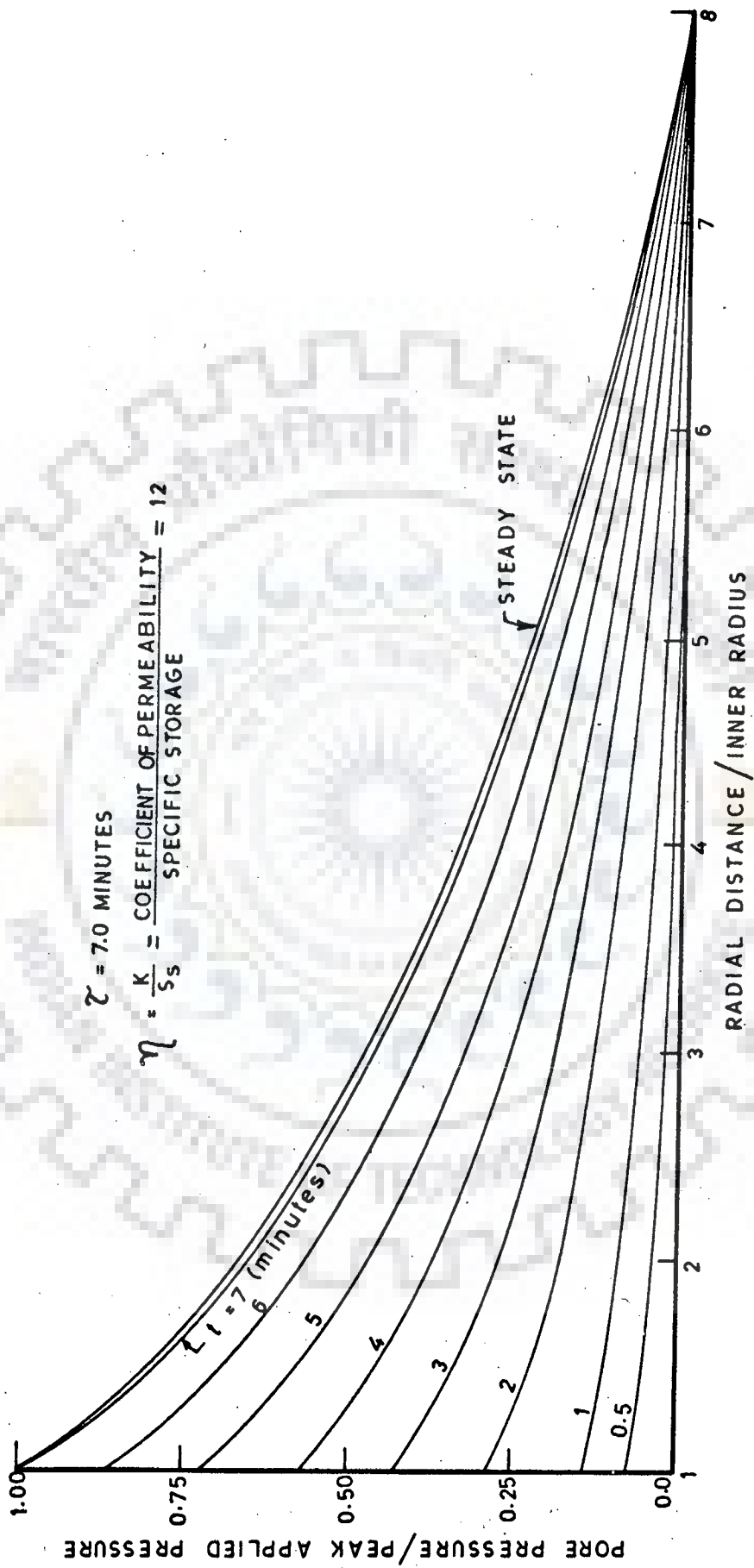
FIG. 6.15 – VARIATION OF PORE PRESSURE WITH RADIAL DISTANCE OF HOLLOW CYLINDRICAL SOIL MASS AT VARIOUS TIME INSTANTS
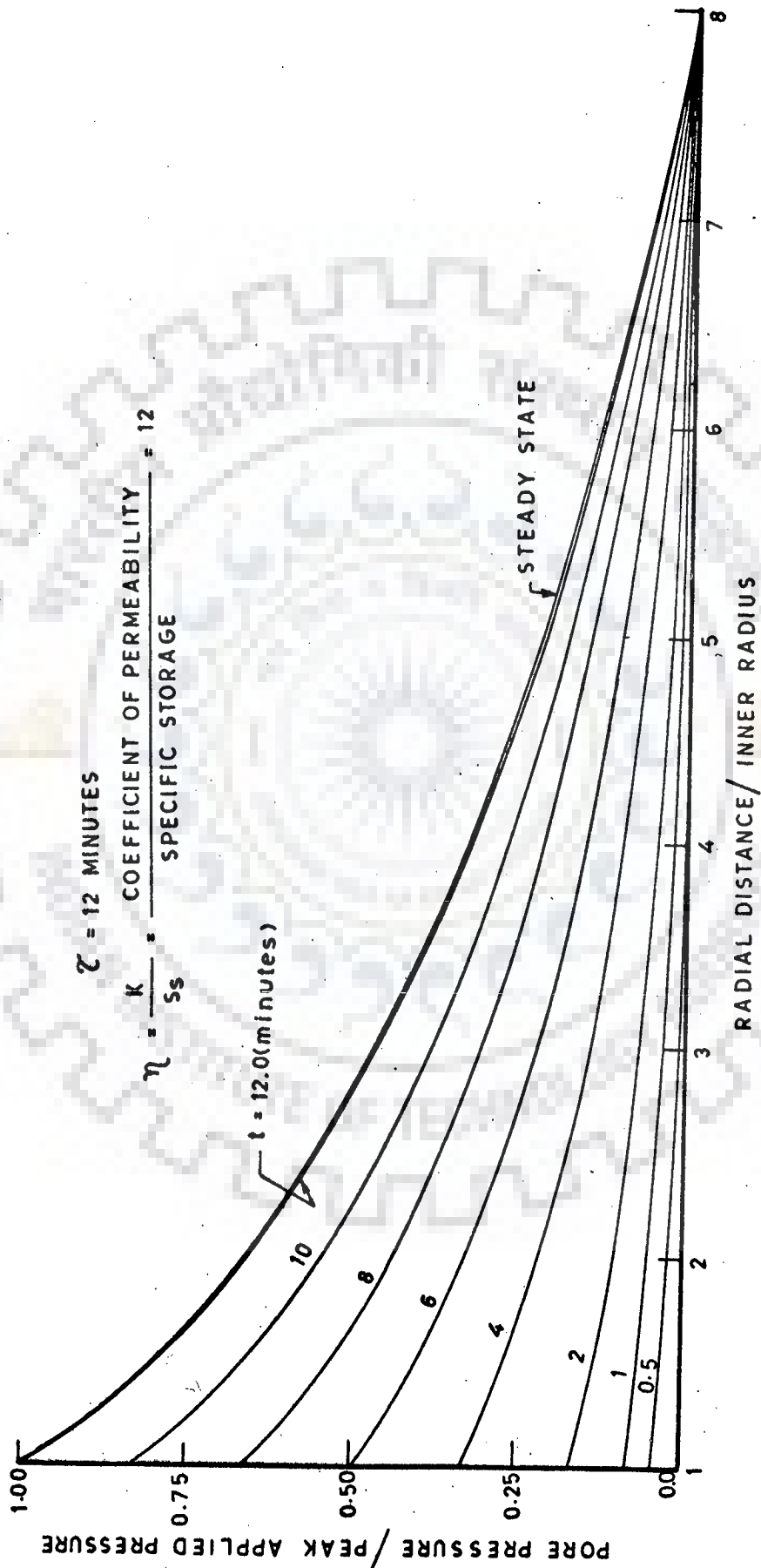
FIG. 6.16 – VARIATION OF PORE PRESSURE WITH RADIAL DISTANCE OF HOLLOW CYLINDRICAL SOIL MASS AT VARIOUS TIME INSTANTS

6.7 CONCLUSION

A technique for evaluating pore pressures in an axisymmetric flow domain under transient and steady state conditions has been presented. Design curves for the prediction of pore pressure under transient condition for the model confined borehole condition are presented. Similar curves can be prepared to cover different rates of hydraulic pressure application and various types of soil for actual field conditions.

CHAPTER - 7

THEORETICAL INVESTIGATION OF HYDRAULIC FRACTURING

7.1 GENERAL

In order to corroborate the experimental results of hydraulic fracturing, theoretical analysis for the experimental model has been carried out. From the theoretical approach, stresses have been obtained in the hollow cylindrical soil mass subjected to uniform pressures on the inner and outer surfaces of the hollow cylinder, and critical condition of the stresses worked out to evaluate the hydraulic fracturing pressure.

It is assumed that hydraulic fracturing will take place when the effective stress in the soil mass is tensile and equals the tensile strength of the soil. Potential occurrence of hydraulic fracturing has been examined considering the following cases:

(a)   Investigation of hydraulic fracturing around the model soil specimen under uniform confining pressures.

(b)   Expression based on Mohr-Coulomb Failure criterion has been derived for hydraulic pressure required to induce fracture around boreholes under uniform confining pressures as well under anisotropic condition of the pressure application.

(c)   Employing Mohr-Coulomb failure criterion, the concept of critical radius has been utilized to investigate the potential occurrence of hydraulic fracturing under;

(i)   steady state pore pressure development and

(ii)   transient condition of pore pressure development.

Expressions have been obtained for evaluating hydraulic pressure which cause fracture in the soil mass under transient pore pressure development for the following cases;

(a)   Specimens saturated without application of back pressure and tested for hydraulic fracturing under various rates of pressure application.

(b)   Specimens saturated utilizing the back pressure saturation technique and then tested for evaluation of hydraulic fracturing.

7.2   STRESS ANALYSIS

Theoretical analysis of stresses in the model is based on the thick cylinder theory. The finite element analysis carried out[30] using linear as well as nonlinear behaviour of the soil for investigation of hydraulic fracturing around boreholes indicated that the nonlinear behaviour of soil has only a small effect on the hydraulic fracturing pressure and the values of u_f are quite insensitive to the properties of the soil with the exception of tensile strength of the soil. Thus stresses have been obtained in hollow cylindrical soil mass used in experimental investigations considering the elastic behaviour of the soil. Fig. 7.1 shows plan view of the model hollow cylindrical soil specimen under applied internal and external pressures. These applied pressures will cause stresses in radial as well as tangential directions. Considering compressive stresses as positive, the radial and tangential (hoop) stresses could be obtained[68] as follows :
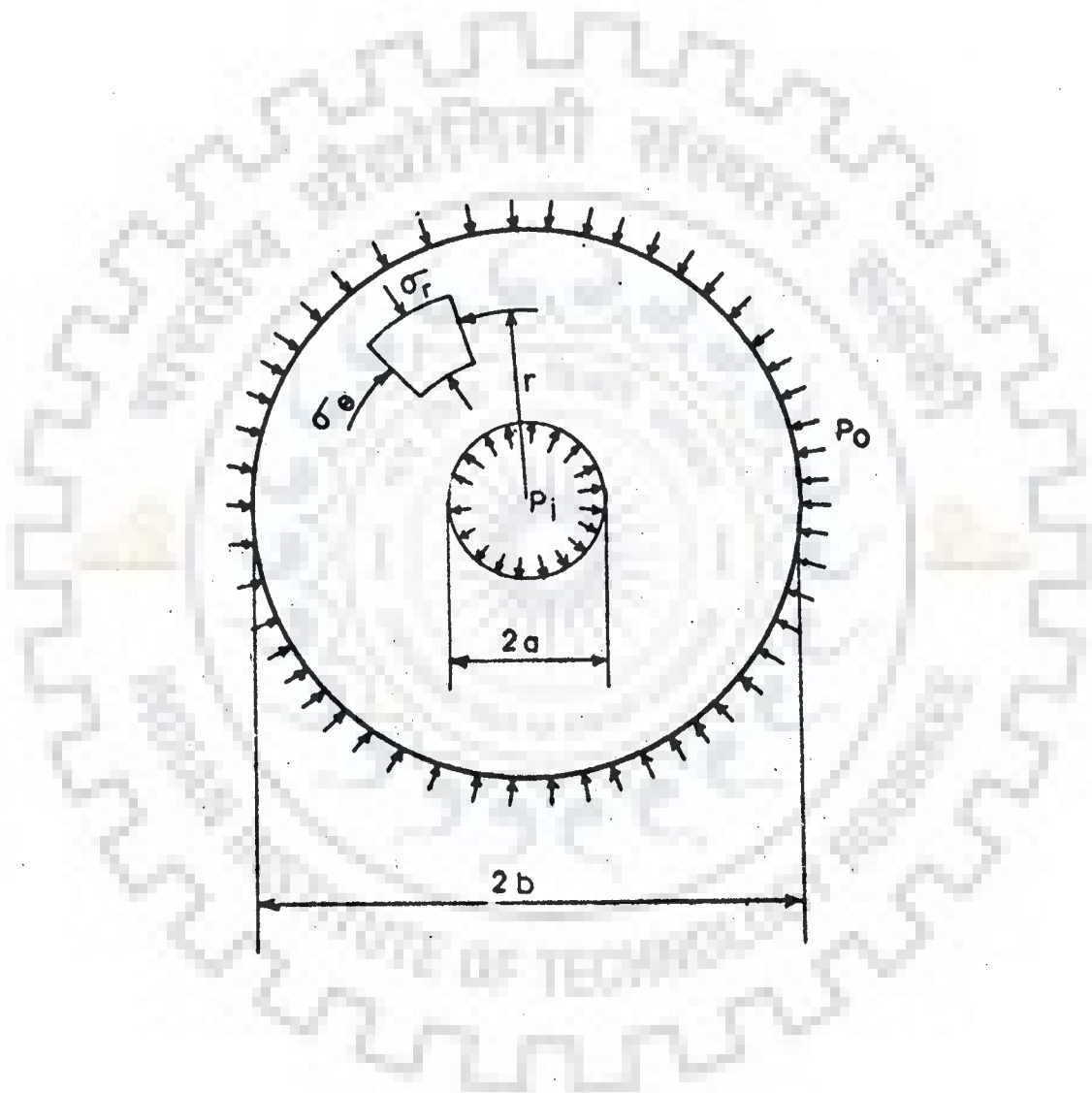
FIG.7·1· STRESS CONDITION AROUND A HOLLOW
CYLINDRICAL CAVITY SUBJECTED TO UNIFORM
INTERNAL AND EXTERNAL PRESSURES.

$$\sigma_r = \frac{P_o b^2 - P_i a^2}{(b^2 - a^2)} - \frac{(P_o - P_i)a^2 b^2}{r^2(b^2 - a^2)} \qquad ..(7.1)$$

$$\sigma_\theta = \frac{P_o b^2 - P_i a^2}{(b^2 - a^2)} + \frac{(P_o - P_i)a^2 b^2}{r^2(b^2 - a^2)} \qquad ..(7.2)$$

where σ_r is the radial stress, σ_θ the tangential stress, P_o and P_i are the external and internal applied pressures respectively, a and b are the inner and outer radii of the cylinder and r is the radial distance at which stresses are evaluated.

To study the variation of stresses in the model soil sample under the action of applied internal and external pressures separately, equations (7.1) and (7.2) under the action of applied external pressure could be written as ;

$$\sigma_r = \frac{P_o b^2}{(b^2 - a^2)} (1 - \frac{a^2}{r^2}) \qquad ..(7.3)$$

$$\sigma_\theta = \frac{P_o b^2}{(b^2 - a^2)} (1 + \frac{a^2}{r^2}) \qquad ..(7.4)$$

The variation of these stresses is shown in Fig. 7.2, wherein curves are prepared for σ_r and σ_θ Vs ratio of radial distance to inner radius of the cylindrical soil mass. These curves indicate that external pressure always results in compressive stresses in the radial as well as tangential directions of the soil cylinder.

In order to study the effect of internal pressure on the variation of radial and tangential stresses, the expressions for σ_r and σ_θ under the action of internal pressure could be expressed as follows;

P₀ = 1.0 kg/cm²
P₀ = 0.0 kg/cm²

σ_θ

σ_r

INNER SURFACE

RADIAL DISTANCE / INNER RADIUS

TOTAL STRESSES, σ_r AND σ_θ (kg/cm²)

FIG. 7.2 — VARIATION OF TOTAL RADIAL AND TANGENTIAL STRESS VS RADIAL DISTANCE DUE TO APPLICATION OF EXTERNAL PRESSURE

$$\sigma_r = \frac{P_i \, a^2}{(b^2 - a^2)} \left(\frac{b^2}{r^2} - 1\right) \qquad \qquad ..(7.5)$$

$$\sigma_\Theta = \frac{-P_i \, a^2}{(b^2 - a^2)} \left(\frac{b^2}{r^2} + 1\right) \qquad \qquad ..(7.6)$$

The variation of σ_r and σ_Θ based on equations (7.5) and (7.6) are plotted in Fig. 7.3 for σ_r and σ_Θ Vs ratio of radial distance to inner radius of the soil cylinder. These curves indicate that σ_r is compressive stress and σ_Θ a tensile stress. The tangential stress is maximum at the inner surface of the soil cylinder.

To study the combined effect of application of external pressure and internal pressures on σ_r and σ_Θ. The total radial and tangential stresses are computed using equations (7.1) and (7.2) and plotted in Figs. 7.4 and 7.5. These plots are prepared for radial and tangential stresses Vs ratio of radial distance to inner radius of the soil cylinder. These curves are obtained by superimposing the values of σ_r and σ_Θ obtained for various values of internal pressure on the values obtained due to application of constant external pressure. The plots show that σ_r is compressive stress increasing with increase of P_i while σ_Θ is compressive at beginning and decreasing with increase of internal pressure.

7.3 ANALYSIS OF HYDRAULIC FRACTURING

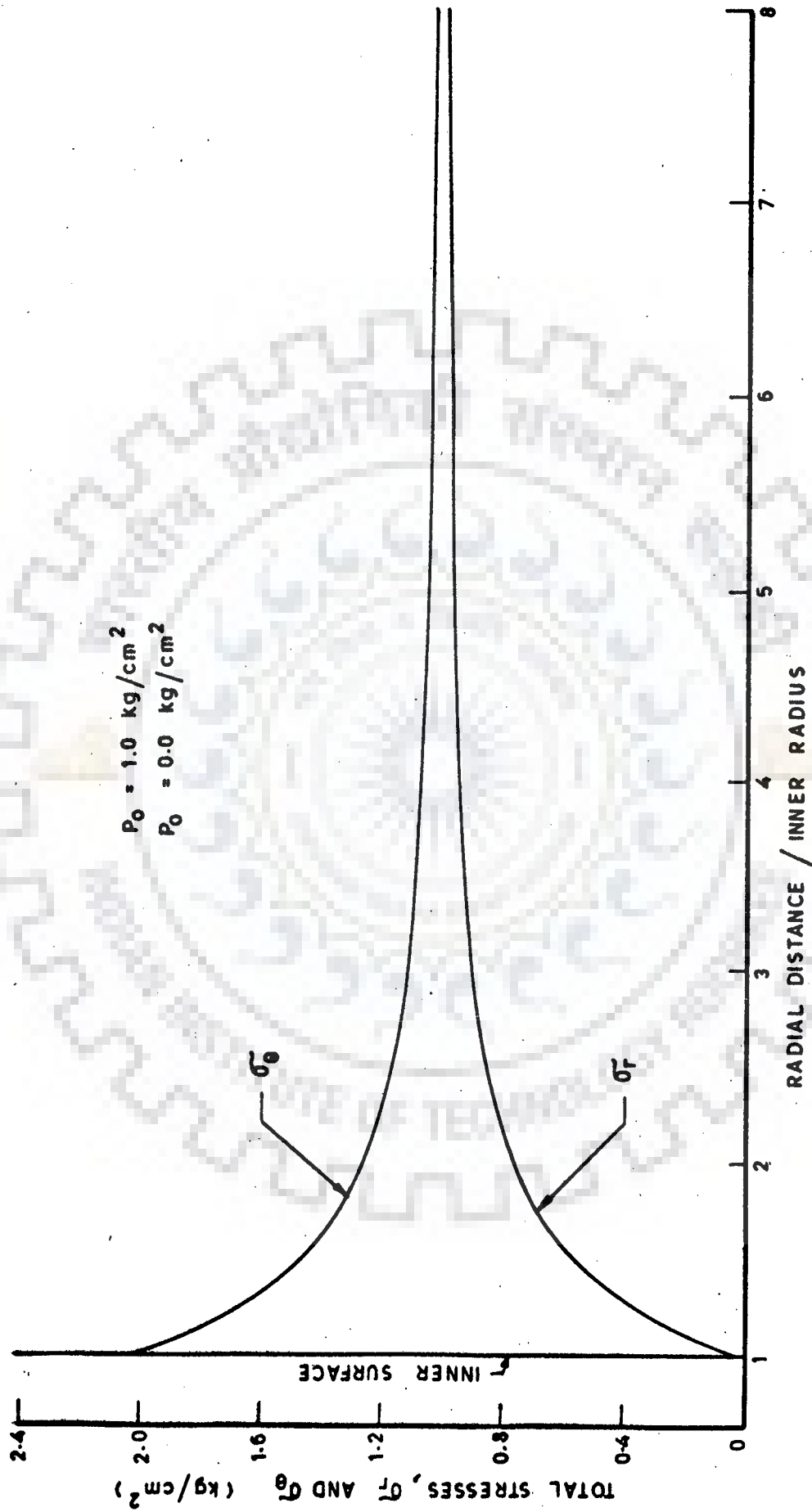To evaluate the potential occurrence of hydraulic fracturing in soil mass, it is essential to evaluate effective
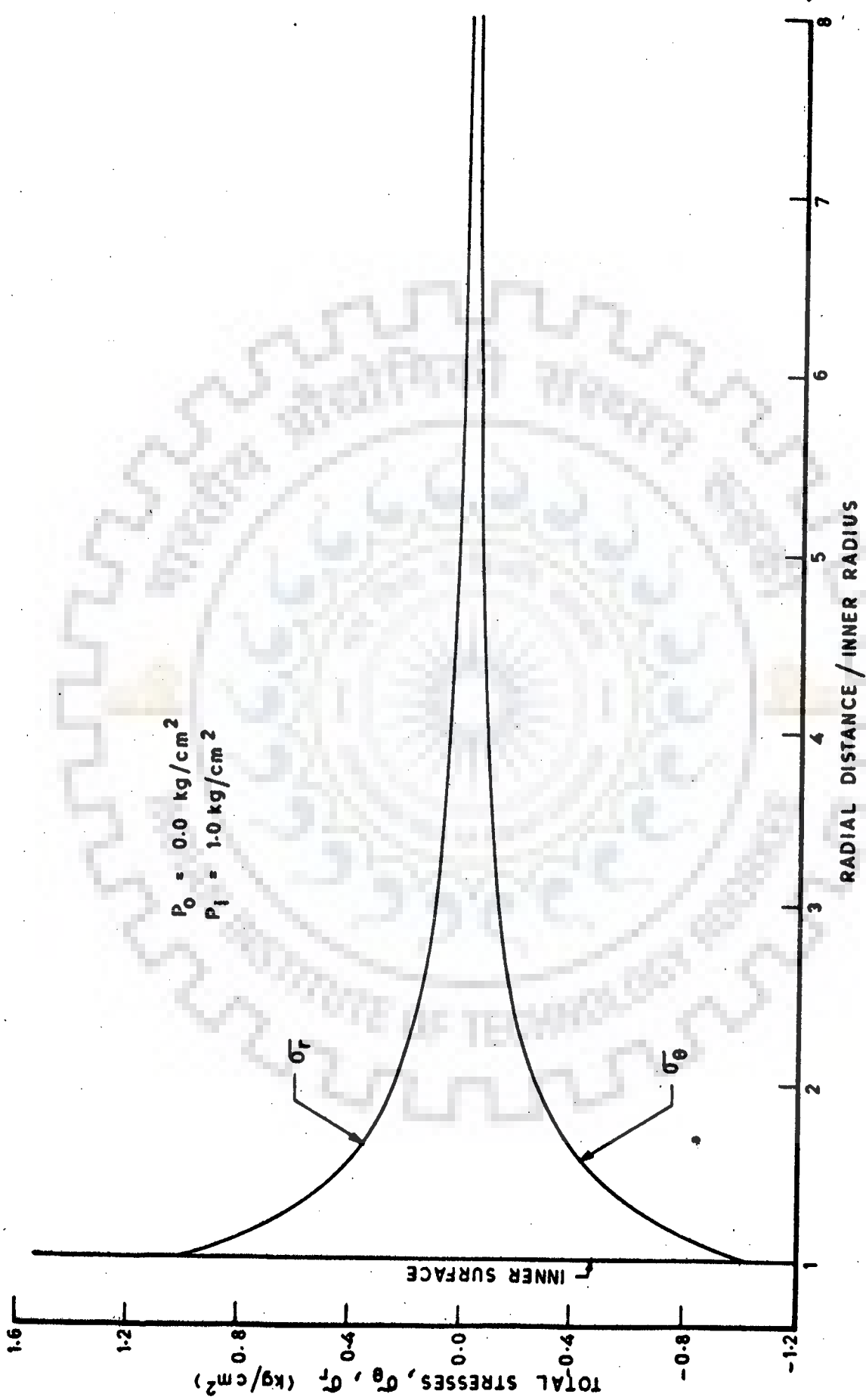
FIG. 7.3 — VARIATION OF TOTAL RADIAL AND TANGENTIAL STRESSES VS RADIAL DISTANCE DUE TO APPLICATION OF INTERNAL PRESSURE
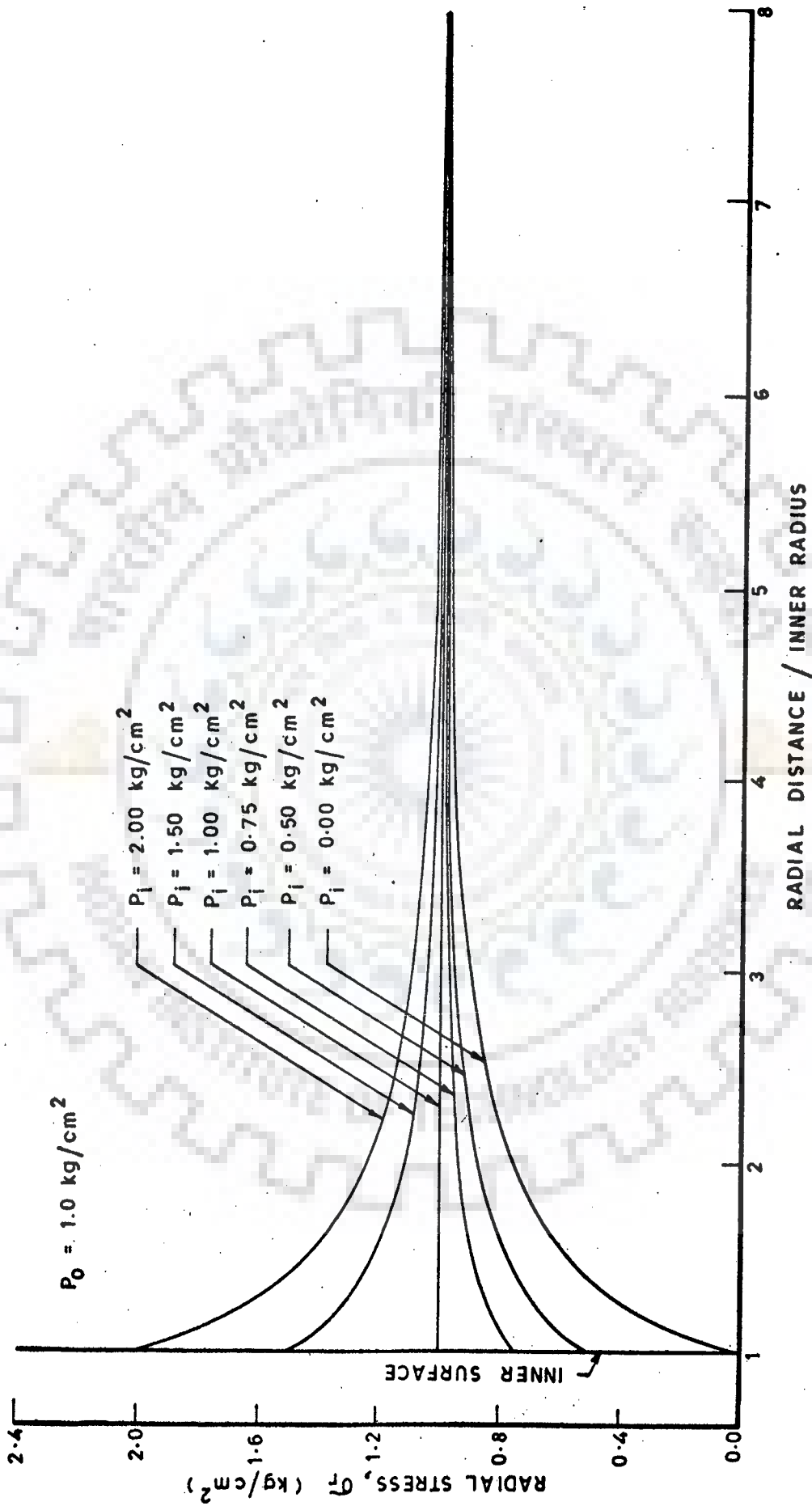
FIG. 7.4 _ VARIATION OF TOTAL RADIAL STRESS VS RADIAL DISTANCE

RADIAL DISTANCE / INNER RADIUS

RADIAL STRESS, σ_r (kg/cm^2)

INNER SURFACE

$P_0 = 1.0$ kg/cm^2

$P_i = 2.00$ kg/cm^2
$P_i = 1.50$ kg/cm^2
$P_i = 1.00$ kg/cm^2
$P_i = 0.75$ kg/cm^2
$P_i = 0.50$ kg/cm^2
$P_i = 0.00$ kg/cm^2

2.4 2.0 1.6 1.2 0.8 0.4 0.0

1 2 3 4 5 6 7 8
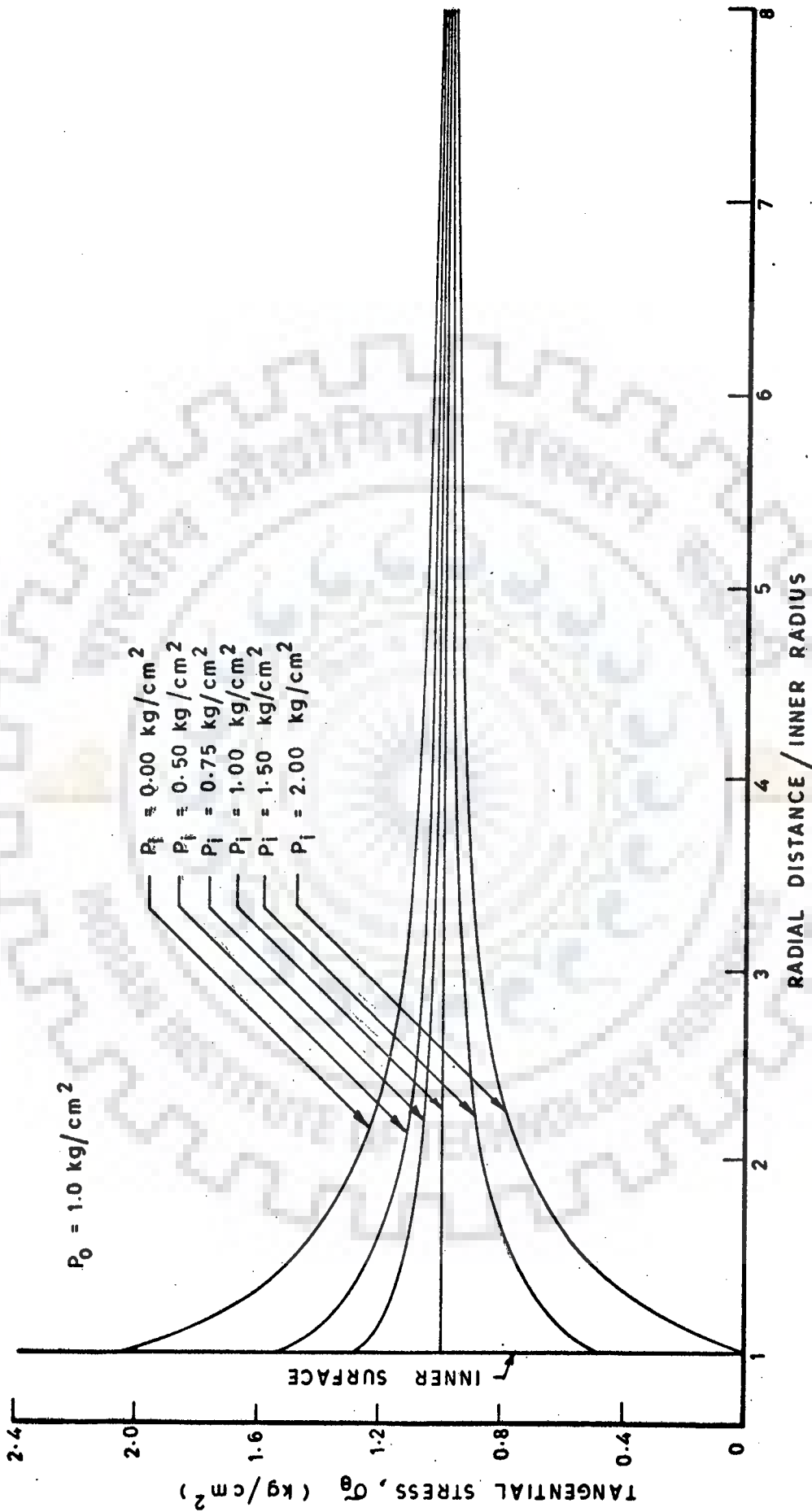
FIG. 7.5 - VARIATION OF TOTAL TANGENTIAL STRESS VS RADIAL DISTANCE

stresses in the soil mass, For the conventionally saturated specimens, i.e. for the case where external pressure P_o, was zero before performing hydraulic fracturing test, thereafter, confining pressure was increased linearly and maintained for sufficient time in order to achieve steady state pore pressure and afterwards, internal pressure was linearly increased to cause fracturing of the soil specimen. The pore pressure evaluated analytically and presented in Fig. 6.4 have been utilized to find out the effective stresses. In order to examine the variation of effective stresses for various values of P_i while P_o is constant, total tangential and radial stresses were calculated from equations (7.1) and (7.2) respectively, along the radial distance and the pore pressure at corresponding locations were obtained from Fig. 6.4.

The curves for effective radial and tangential stresses Vs radial distance are plotted in Figs. 7.6 and 7.7 respectively. These curves are prepared for P_o = 1.0 Kg/cm^2 but P_i varying from 0.5 to 1.5 Kg/cm^2. From these curves it could be seen that the maximum tensile stress for radial stress is 0.2 Kg/cm^2, for P_i = 1.5 Kg/cm^2, whereas for tangential stress, tensile stress increases to 1.0 Kg/cm^2 for corresponding value of P_i. This shows that the most critical condition for the occurrence of hydraulic fracturing is due to tangential stress.

Considering combined effect of external pressure as well as internal pressure at critical condition at the inner surface of the hollow cylinder (r=a), equation (7.2) for tangential stress can be rewritten as ;

147
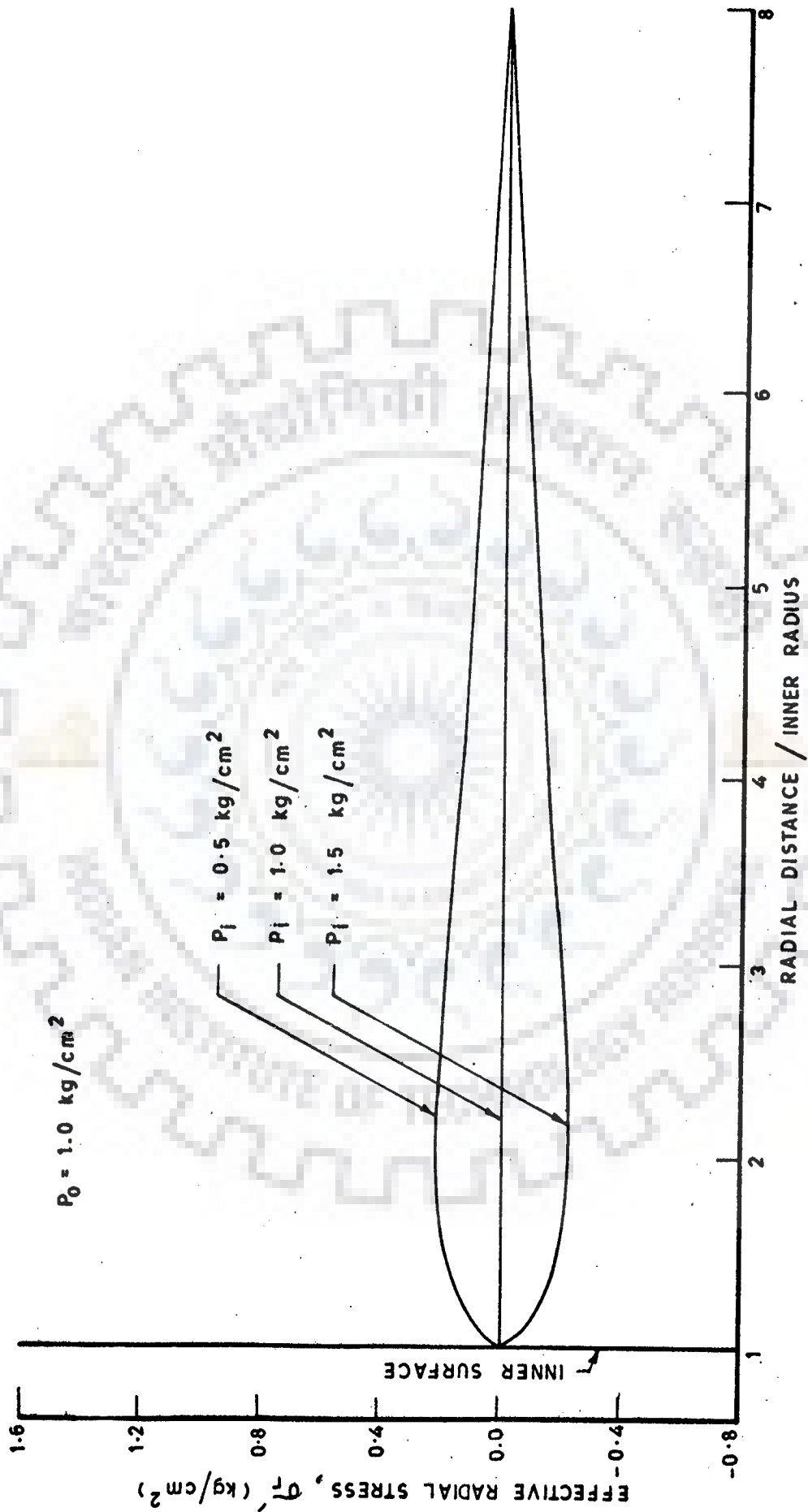
FIG. 7.6 – VARIATION OF EFFECTIVE RADIAL STRESS VS RADIAL DISTANCE
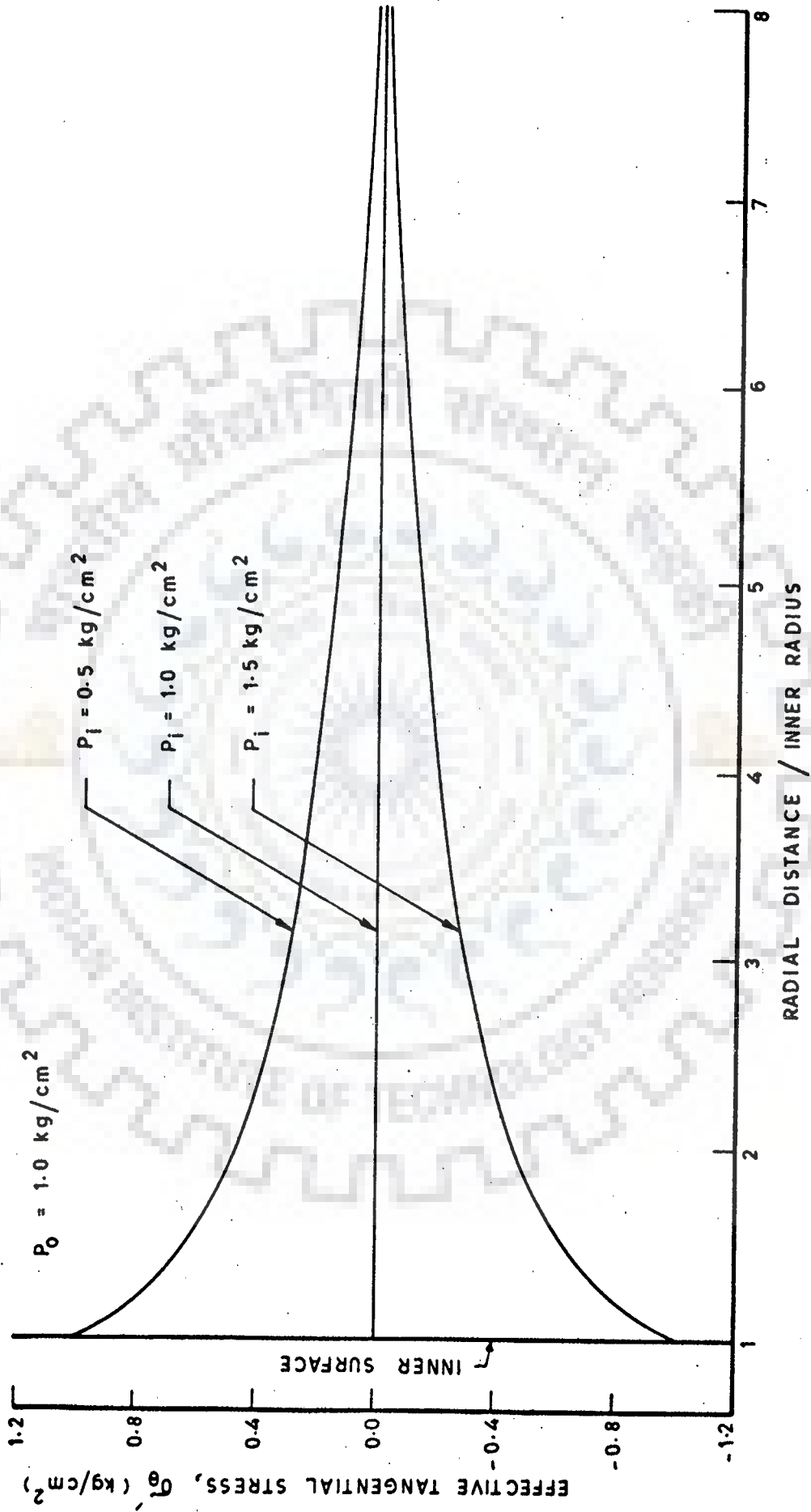
FIG. 7.7 – VARIATION OF EFFECTIVE TANGENTIAL STRESS VS RADIAL DISTANCE

148

$$\sigma_\theta = \frac{2\,P_o\,b^2}{(b^2-a^2)} - \frac{P_i(a^2+b^2)}{(b^2-a^2)} \qquad ..(7.7)$$

The effective stresses at the inner surface will be equal to the difference between the total stress and the internally applied water pressure,

$$\sigma'_\theta = \sigma_\theta - P_i \qquad ..(7.8)$$

Hence, substituting equation (7.7) into equation (7.8), the expression for effective tangential stress at the inner surface can be expressed as;

$$\sigma'_\theta = \frac{2\,P_o\,b^2}{(b^2-a^2)} - \frac{P_i(a^2+b^2)}{(b^2-a^2)} - P_i \qquad ..(7.9)$$

Assuming that for the occurrence of hydraulic fracturing, effective stress of the soil becomes tensile and equals to tensile strength of the soil σ_t, then

$$\sigma'_\theta = -\sigma_t \qquad ..(7.10)$$

At the initiation of hydraulic fracturing at inner surface of the hollow cylindrical soil mass, the internal pressure P_i, is equal to the hydraulic fracturing pressure, u_f. Substituting for σ'_θ from equation (7.10) into equation (7.8) and replacing P_i by u_f, the expression for evaluation of hydraulic fracturing pressure can be obtained as ;

$$u_f = P_o + \frac{\sigma_t}{2}\left(\frac{b^2-a^2}{b^2}\right) \qquad ..(7.11)$$

Equation (7.11) shows that the hydraulic pressure depends upon the initial state of stresses, dimensions of the soil mass and the tensile strength of the soil. Hydraulic fracturing

pressure computed theoretically based on equation (7.11) has been plotted in Fig. 7.8 for the experimentally tested soil specimens of type 'A' soil having, $\sigma_t = 0.1$ Kg/cm^2, b = 5.08 cm and, a = 0.635 cm, but with various values of P_o. From the figure it is seen that hydraulic fracturing is a linear function of confining pressure and occurs at a pressure greater than confining pressure, as was the case of experimental investigation.

7.4 USE OF MOHR-COULOMB FAILURE CRITERIA FOR EVALUATION OF HYDRAULIC FRACTURING

The stresses which develop in the soil mass are limited by the strength of the soil. The well known failure criterion applied for problems of geotechnical engineering is Mohr-Coulomb failure criterion. Mohr stress circle is independent of the nature of the medium, but depends only on the state of stresses at a point while Mohr-strength envelope depends on the property of the soil being tested.

In this analysis the failure stresses are those obtained from Mohr-Coulomb failure criterion for brittle material and it is assumed that Mohr-Coulomb strength envelope follows the straight line path in compression as well as in tension.

To evaluate the conditions of stresses in relation to strength of the soil, considering a soil mass subjected to plane stress condition, Mohr stress circles and Mohr-Coulomb failure envelope are drawn in Fig. 7.9. In this figure $\overline{OM}$ represents the uniaxial ultimate strength of material in
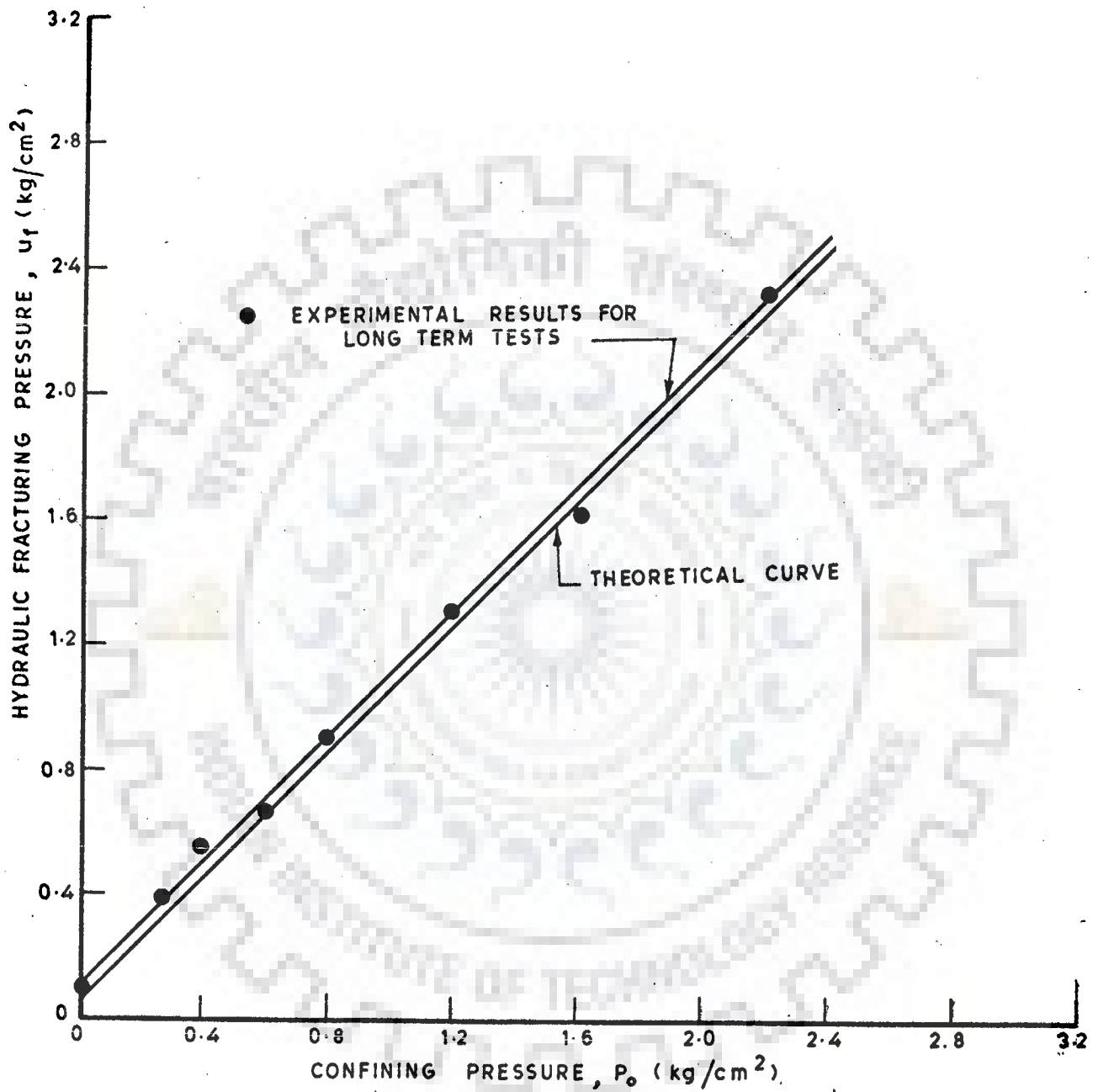
FIG. 7.8 _ RESULTS OF THEORETICAL ANALYSIS AND EXPERIMENTAL INVESTIGATION OF HYDRAULIC FRACTURING

tension σ_t, and $\overline{OG}$ represents the uniaxial ultimate strength of material in compression σ_c, then for any value of major and minor principal stresses σ_1' and σ_3' respectively[67], failure stresses could be obtained by drawing a circle with diameter $\overline{KH}$ and tangent to the strength envelope $\overline{NS}$. The following geometrical expression can be derived using the similarity of triangles LJE and LIF.

$$\frac{\dfrac{\sigma_1' - \sigma_3' - \sigma_t}{2}}{\dfrac{\sigma_c - \sigma_t}{2}} = \frac{\dfrac{\sigma_1' + \sigma_3' + \sigma_t}{2}}{\dfrac{\sigma_c + \sigma_t}{2}} \qquad ..(7.12)$$

where σ_1' and σ_3' are algebraic quantities. This equation could be further simplified as follows;

$$\frac{\sigma_1'}{\sigma_c} - \frac{\sigma_3'}{\sigma_t} = 1 \qquad ..(7.13)$$

In order that the stresses induced in the soil mass are consistent with the strength of the soil as obtained from the Mohr-Coulomb criteria, the above expression must be satisfied.

From Mohr-Coulomb failure criterion shown in Fig. 7.9, the following expression can be obtained;

$$\sin \theta' = \frac{\dfrac{\sigma_c}{2}}{c' \cot\theta' + \sigma_c/2} \qquad ..(7.14)$$

or

$$\sigma_c = \frac{2 c' \cos\theta'}{1 - \sin\theta'} \qquad ..(7.15)$$

where c' is the cohesion and θ' the effective angle of internal friction of the soil.

At the inner surface of hollow cylinder, the pore water pressure is equal to the applied internal pressure. Thus, the expression for effective principal stresses could be written as;

$$\sigma_1' = \sigma_1 - P_i \qquad \qquad ..(7.16)$$

$$\sigma_3' = \sigma_3 - P_i \qquad \qquad ..(7.17)$$

As discussed earlier the condition of stresses are critical at inner surface of the hollow cylindrical specimen and the crack would initiate at inner surface of the cylinder. Thus the internal pressure P_i at the time of crack initiation is equal to the hydraulic fracturing pressure, u_f. Substituting values of σ_1' and σ_3' from equations (7.16) and (7.17) and value of σ_c from equation (7.15) into equation (7.13) and simplifying for u_f,

$$u_f = \frac{(\sigma_3 + \sigma_t)2c'\cos\theta' - \sigma_1\sigma_t(1-\sin\theta')}{2c'\cos\theta' - \sigma_t(1-\sin\theta')} \qquad ..(7.18)$$

Equation (7.18) thus gives a general expression to obtain the hydraulic pressure required to initiate the crack at inner surface of hollow cylinder. It shows that hydraulic fracturing pressure is a function of soil strength parameters and the maximum and minimum principal stresses acting on the soil mass.

Under experimental conditions simulated in the laboratory, cylindrical specimen is subjected to all-round confining pressure and uniform internal pressure through the hollow of the specimen. Thus in cylindrical specimen, all radial planes are planes of symmetry and shear stresses acting on these planes will be equal to zero. Since the shear stresses acting
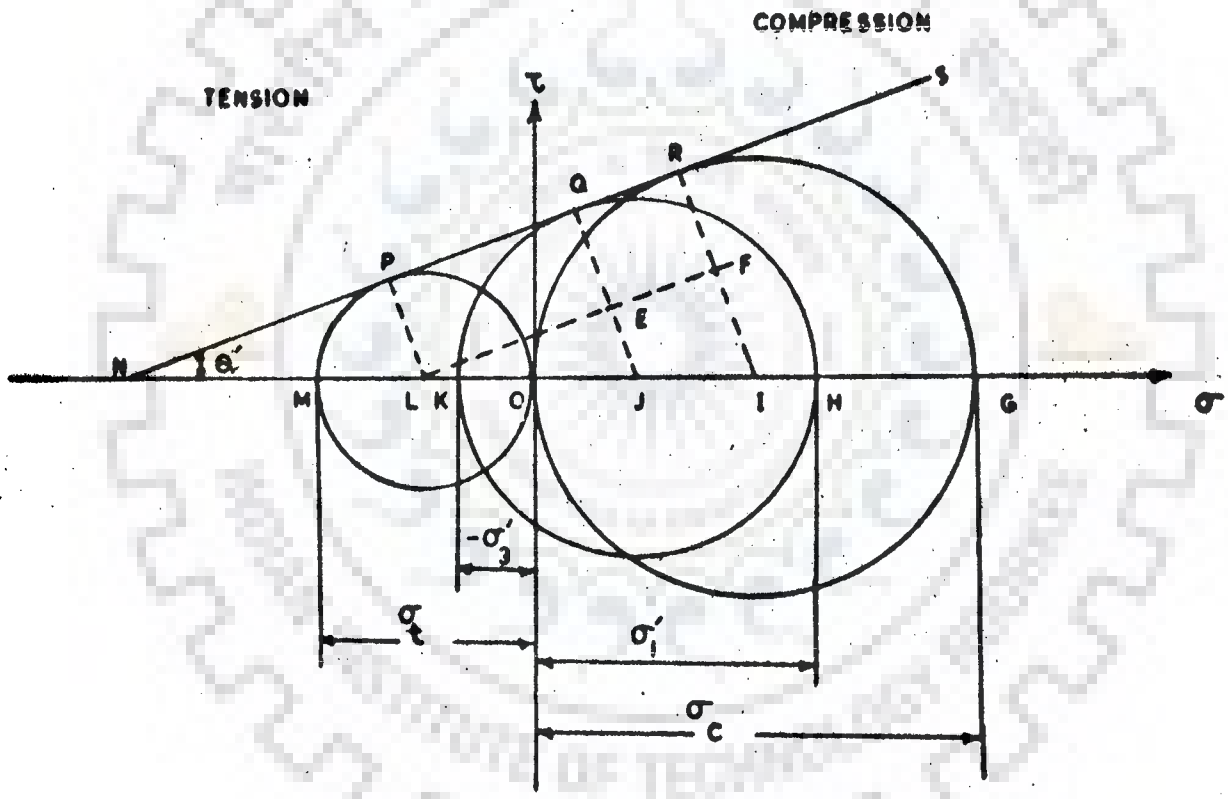
FIG. 7·9 - MOHR STRESS CIRCLES AND MOHR - COULOMB
STRENGTH ENVELOPE.

on two mutually perpendicular planes are always equal due to complementary nature of the shear stress, the shear stresses on any circumferential plane will also be equal to zero, the latter being perpendicular to the radial planes. Thus the radial stress, circumferential stress and the vertical stress could be the three principal stresses acting on the hollow cylindrical specimen, subjected to internal pressure and all-round confining pressure.

The application of equation (7.18), to actual experimental cases has been investigated in the following paragraphs.

7.4.1 Uniform Confining Pressures

If a hollow cylindrical soil mass is subjected to uniform all-round confining pressure as well as internal pressure in a triaxial test it has been shown[24] that the most critical condition at the stage of occurrence of hydraulic fracturing, where $P_i > P_o$, is due to tangential stress. Maximum stress acting at inner surface of the hollow cylinder is the radial stress while the minimum stress acting at inner surface is the tangential stress.

From equations (7.1) and (7.2) if $r = a$ and $P_i = u_f$, then;

$$\sigma_r = u_f \qquad \qquad ..(7.19)$$

and

$$\sigma_\theta = \frac{2 P_o b^2}{(b^2 - a^2)} - u_f \frac{(a^2 + b^2)}{(b^2 - a^2)} \qquad ..(7.20)$$

Substituting equations (7.19) and (7.20) into equation (7.18) for $\sigma_1 = \sigma_r$ and $\sigma_3 = \sigma_\theta$ and simplifying for u_f,

$$u_f = P_o + \frac{\sigma_t}{2} \left(\frac{b^2-a^2}{b^2}\right) \qquad \qquad ..(7.21)$$

Equation (7.21) is same as equation (7.11) and the same conclusions can be drawn.

7.4.2 Anisotropic Application of Pressure

The vertical stress σ_z, acting at a point in a soil mass is generally greater than the horizontal stress. In order to consider this condition, it is assumed that the hollow cylindrical soil specimen is subjected to inner pressure P_i, all-round confining pressure P_o, and the vertical stress σ_z, where $\sigma_z = \lambda P_o$. For $\lambda = 1$, the governing major and minor principal stresses are σ_r and σ_θ respectively, as shown in previous section. For λ sufficiently greater then unity, σ_z will be greater than σ_r, so the major principal stress would be σ_z instead of σ_r and the minor principal stress σ_θ. Equation (7.18) can be written as;

$$u_f = \frac{\left(P_o \frac{2b^2}{(b^2-a^2)} + \sigma_t\right) 2c' \cos\theta' - \lambda P_o \sigma_t (1-\sin\theta')}{2c' \cos\theta' \left(\frac{2b^2}{(b^2-a^2)}\right) - \sigma_t (1-\sin\theta')} \qquad ..(7.22)$$

Equation (7.22) is general expression for evaluation of hydraulic fracturing at inner surface of the hollow cylindrical soil mass subjected to non-isotropic pressure application. Equation (7.22) is plotted for u_f against P_o in Fig. 7.10 for various values of λ. These plots show that for the model cylindrical soil specimen used in this investigation, u_f value decreases with increase of λ.
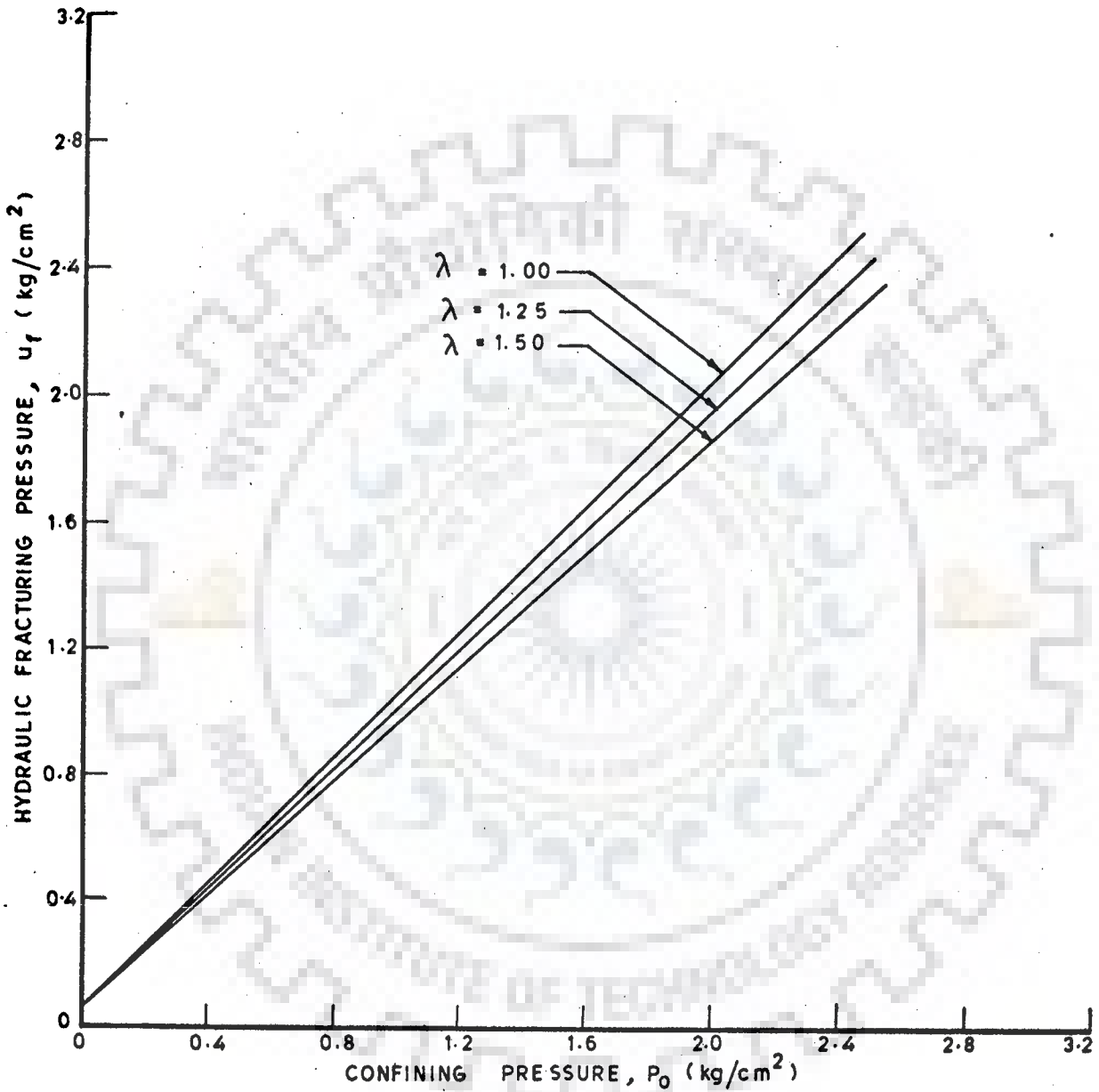
FIG. 7.10 _ EFFECT OF NON-ISOTROPIC APPLICATION OF LOADING
ON HYDRAULIC FRACTURING PRESSURE

7.5 THE CONCEPT OF CRITICAL RADIUS

7.5.1 Stress Analysis

Generally the stresses developed in soil mass are limited by the strength of the soil, using concept of Mohr-Coulomb failure criterion for the stress development around an axisymmetric cylindrical soil mass, the Mohr-Coulomb failure crtierion in terms of polar coordinates can be written as;

$$|\sigma_\theta - \sigma_r| = (\sigma_\theta + \sigma_r) \sin\theta + 2c \cos\theta \qquad \cdots (7.23)$$

Jaworski et al[30] have indicated that the above relation indicates the largest value of $(\sigma_\theta - \sigma_r)$ consistent with the strength of the soil. They have discussed the concept of critical radius r_c, at which the stresses in soil are equal to those given by Mohr-Coulomb failure criterion. Critical radius can be defined by substituting equations (7.3) and (7.4) into equation (7.23) and simplifying for r. This gives the critical radius r_c as;

$$r_c = \left[\frac{P_o a^2 b^2}{P_o b^2 \sin\theta + (b^2 - a^2) c \cos\theta} \right]^{1/2} \qquad \cdots (7.24)$$

The maximum tangential stress will develop at the critical radius and can be obtained by substituting equation (7.24) into equation (7.4).

$$\sigma_{\theta max} = \frac{P_o b^2 (1 + \sin\theta)}{(b^2 - a^2)} + c \cos\theta \qquad \cdots (7.25)$$

The tangential stress at a radius greater than the critical radius can be obtained from equation (7.4) and the tangential stresses less than the critical radius may be obtained

by substituting equation (7.3) into equation (7.23) as follows;

$$\sigma_\theta = \frac{\frac{P_o\, b^2}{(b^2-a^2)}(1 - \frac{a^2}{r^2})(1 + \sin\theta) + 2c\,\cos\theta}{(1 - \sin\theta)} \quad ..(7.26)$$

The variation of σ_θ along the radial distance of soil cylinder for the typical confining pressures of 1.0 Kg/cm^2 is shown in Fig. 7.11.

To determine the variation of tangential stress resulting from an increase in the water pressure inside the hollow cylindrical soil specimen, tangential stress due to application of internal pressure has been computed using equation (7.6). Using superposition the tangential stress distribution can be determined by adding the stress resulting from an application of long term applied external pressure to the stress distribution resulting from increase of water pressure inside the hollow cylinder as shown in Fig. 7.11. It is seen that due to application of P_i the stress picture in soil mass changes. Tangential stress are maximum at a radial distance governed by Mohr-Coulomb failure criterion, called the critical radius. These curves show that as P_i increases the value of σ_θ decreases and it even becomes tensile at inner surface of the hollow cylinder. These plots indicate that due to negative nature of stress at inner surface of the soil cylinder redistribution of stresses may take place, but the failure of soil mass would occur only if the applied internal pressure increases the effective tangential stresses at critical radius beyond the tensile strength of the soil.

The effective tangential stress σ_θ', at critical radius may be expressed as;
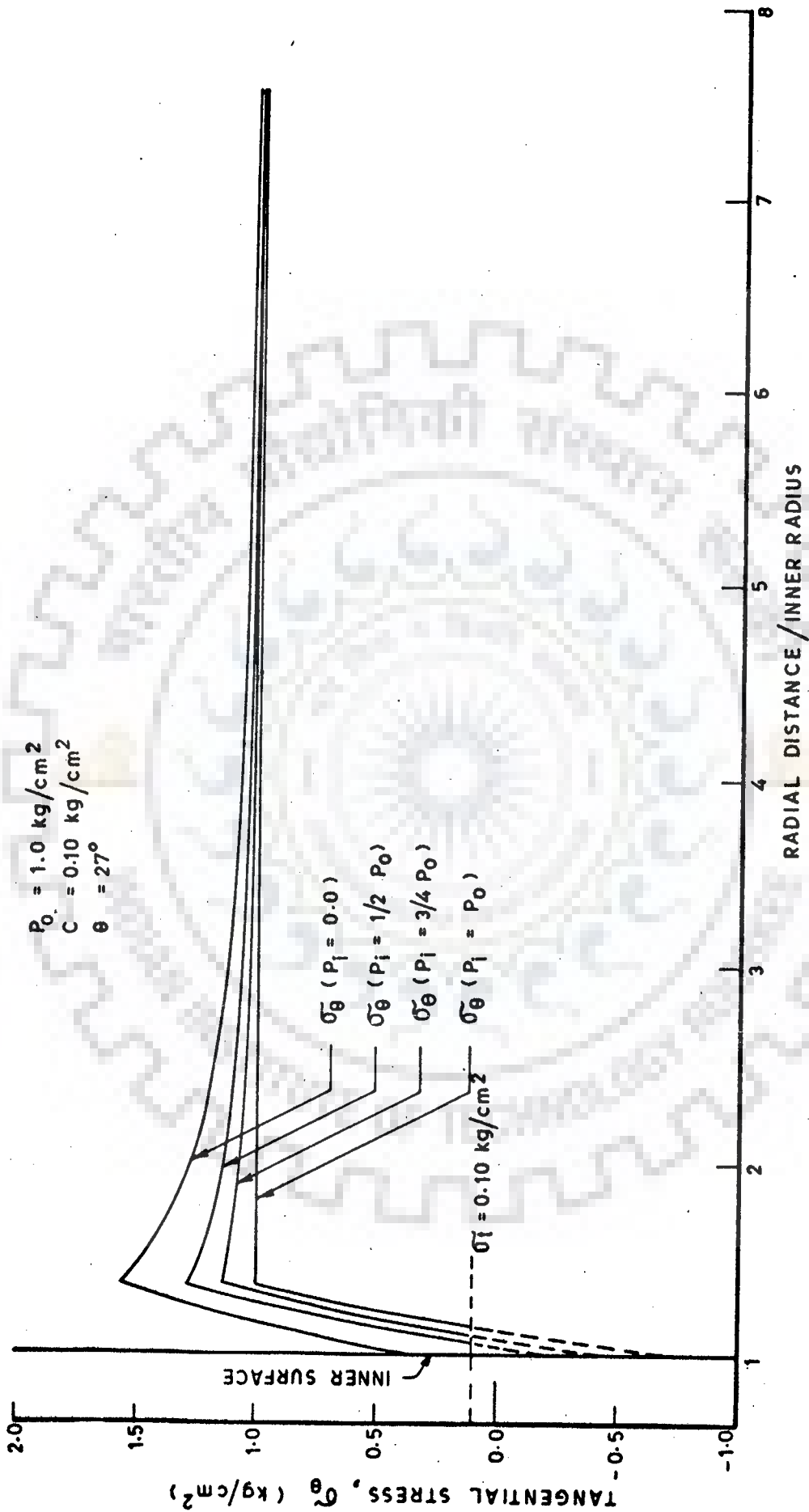
FIG. 7.11 – DISTRIBUTION OF TANGENTIAL STRESS ALONG RADIAL DISTANCE OF HOLLOW CYLINDRICAL SOIL MASS

$P_0 = 1.0$ kg/cm^2
$C = 0.10$ kg/cm^2
$\theta = 27°$

σ_θ ($P_i = 0.0$)
σ_θ ($P_i = 1/2\ P_0$)
σ_θ ($P_i = 3/4\ P_0$)
σ_θ ($P_i = P_0$)

$\sigma_i = 0.10$ kg/cm^2

INNER SURFACE

RADIAL DISTANCE/INNER RADIUS

TANGENTIAL STRESS, σ_θ (kg/cm^2)

$$\sigma'_\theta = \sigma_{\theta_0} \text{ (due to } P_o) + \sigma_\theta \text{(due to } P_i) \text{ - Pore pressure developed in soil mass}$$

$$..(7.27)$$

The confining pressure P_o, is constant at time of conducting tests of hydraulic fracturing. Thus the tangential stress at critical radius due to P_o is constant for a specific value of P_o and given soil. Assuming that P_i is applied in a short period of time then its effect on evaluation of critical radius r_c, will be negligible and same r_c values can be adopted as found out for P_o using equation (7.24). The tangential stress at critical radius, may however vary slightly due to the application of P_i and equation (7.27) can be rewritten as;

$$\sigma'_\theta = \sigma_{\theta_0} + \alpha P_i - u \qquad ..(7.28)$$

and

$$\alpha = \frac{-a^2}{(b^2 - a^2)} \left(1 + \frac{b^2}{r_c^2}\right) \qquad ..(7.29)$$

where σ_{θ_0} is the tangential stress due to P_o, α is the factor which depends on critical radius and dimensions of the soil cylinder and determines the stress due to P_i and u is the pore pressure.

The effective stresses as obtained from equation (7.28), when compared with the tensile strength of the soil under study will enable us to assess the potential of hydraulic fracturing.

7.5.2 Application for Evaluation of Hydraulic Fracturing

The pore pressure distribution along radial distance of hollow cylindrical soil mass as found analytically in Chapter 6 for steady state as well as transient conditions, has been

utilized for stress analysis of experimental model specimen tested for hydraulic fracturing. Effective stresses under steady state as well as transient conditions have been evaluated for investigation of potential occurrence of hydraulic fracturing.

Various series of hydraulic fracturing tests performed on hollow cylindrical soil specimens have been analysed for prediction of potential of hydraulic fracturing.

7.5.2.1 Instantaneous Tests

In this series of tests saturated soil specimen were first subjected to confining pressure and afterwards the internal pressure was applied (Para 4.2.3) and linearly increased to cause failure of the soil specimen. Instantaneous tests were carried out in which the duration of application of internal pressure for inducing hydraulic fracturing varied from half to one minute. Thus the total pore pressure would be the sum of the pore pressure due to P_o and the pore pressure developed under transient condition due to P_i, i.e.

$$u = \text{Pore pressure developed} + \text{Pore pressure developed}$$

u = Pore pressure developed + Pore pressure developed
    due to P_o under steady   due to P_i under transient
    state condition   condition   ..(7.30)

Therefore, the existing pore pressure in soil mass at start of the hydraulic fracturing test at any point in the soil mass will be equal to u_o (pore pressure developed due to P_o under steady state condition) and the pore pressure developed under transient condition due to application of P_i which can be predicted from design curves (Figs. 6.10 - 6.16). Thus equation

(7.30) can be expressed as;

$$u = u_o + \beta \, P_i \qquad \qquad ..(7.31)$$

where β is the fraction of pore pressure developed in the soil mass as a function of P_i under transient condition at the location and instant of time under consideration.

In order to evaluate the hydraulic fracturing pressure required to induce cracking in soil mass, water pressure inside the hollow cylindrical soil mass was uniformly increased until failure occurred. Thus in equation (7.31) P_i at failure can be replaced by u_f.

The expression for effective tangential stress as given in equation (7.28) can be simplified by replacing P_i by u_f and introducing equation (7.31). Thus,

$$\sigma'_\theta = \sigma_{\theta_o} - u_f \, (\beta - \alpha) - u_o \qquad \qquad ..(7.32)$$

It is assumed that hydraulic fracturing will take place when the effective stress in the soil mass reduces to negative equal to tensile strength of the soil. Therefore, substituting σ'_θ equal to σ_t in equation (7.32), the expression for hydraulic fracturing pressure under transient condition can be simplified as[27];

$$u_f = \frac{\sigma_{\theta_o} + \sigma_t - u_o}{\beta - \alpha} \qquad \qquad ..(7.33)$$

Equation (7.33) indicates that u_f is a function of initial state of stresses, tensile strength of the soil and the pore pressure.

For the experiments performed, the hydraulic fracturing pressure at various values of confining pressure under transient

conditions are computed theoretically using equation (7.33), for an average tensile strength of the soil as 0.10 Kg/cm^2, and results are plotted in Fig. 7.12 for hydraulic fracturing pressure u_f, against confining pressure P_o.

7.5.2.2 Short Term Tests

In this series of experiments, similar procedure was followed to prepare hollow cylindrical specimen for conducting hydraulic fracturing tests. The only difference is in duration of performing hydraulic fracturing tests. In these experiments water pressure causing fracture was increased linearly in a period of about 12 minutes, depending upon the range of confining pressures.

For theoretical computation of hydraulic fracturing pressure, equation (7.33) could be used as such, the only difference is that β values should be obtained from corresponding design curves where internal pressures are applied in time periods of up to 12 minutes. Using equation (7.33), hydraulic fracturing pressures are calculated for actual experimental cases and shown in Fig. 7.13. The plots are prepared for hydraulic fracturing pressure u_f, against confining pressure P_o.

7.5.2.3 Long Term Tests

Long term tests were performed on saturated specimens, where firstly confining pressure was applied, and thereafter, internal pressure was increased in incremental steps over a total period varying from 3 hours to 24 hours depending upon the range of confining pressures.. Thus due to long duration of
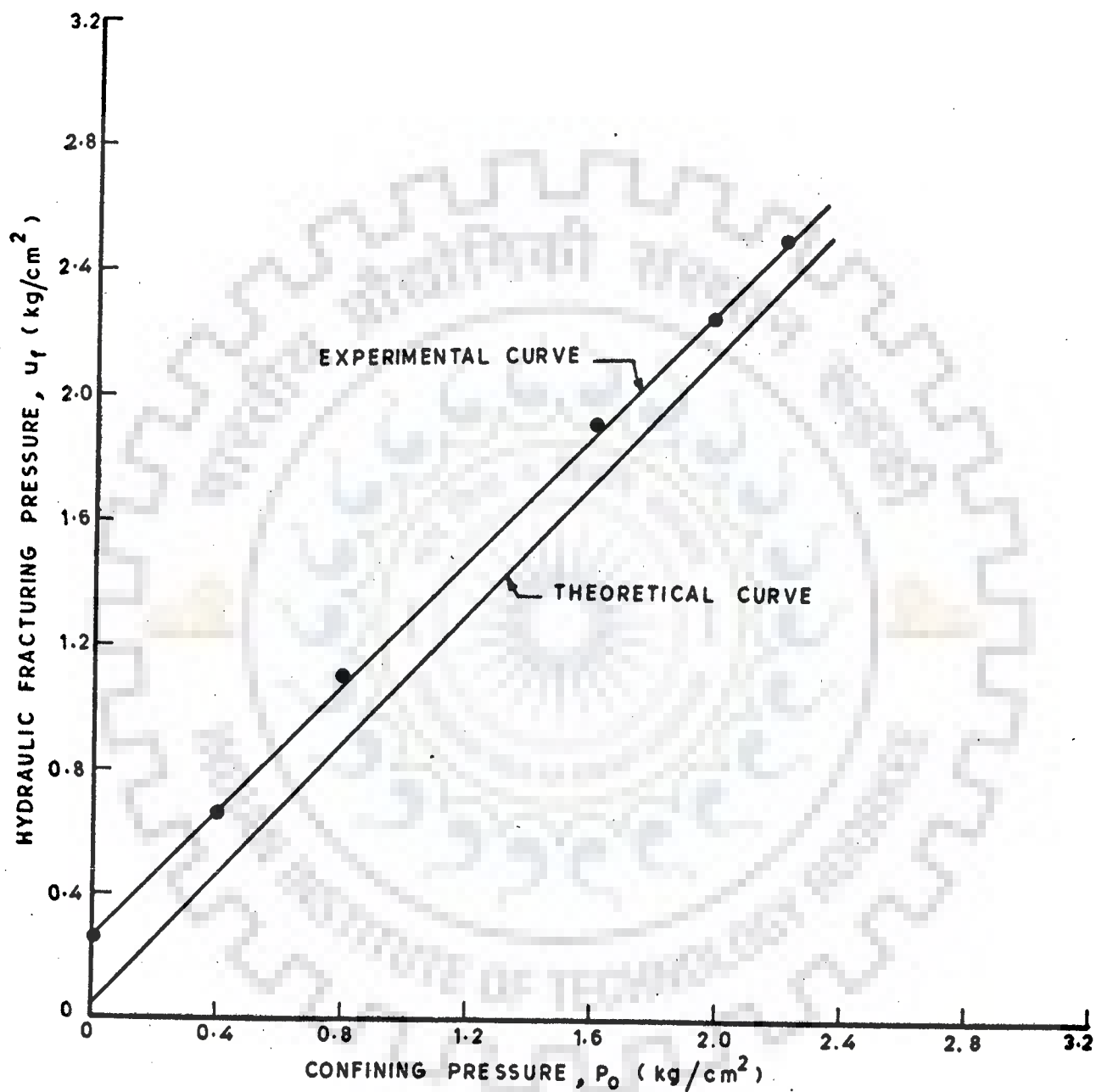
FIG. 7.12 _ VARIATION OF HYDRAULIC FRACTURING PRESSURE
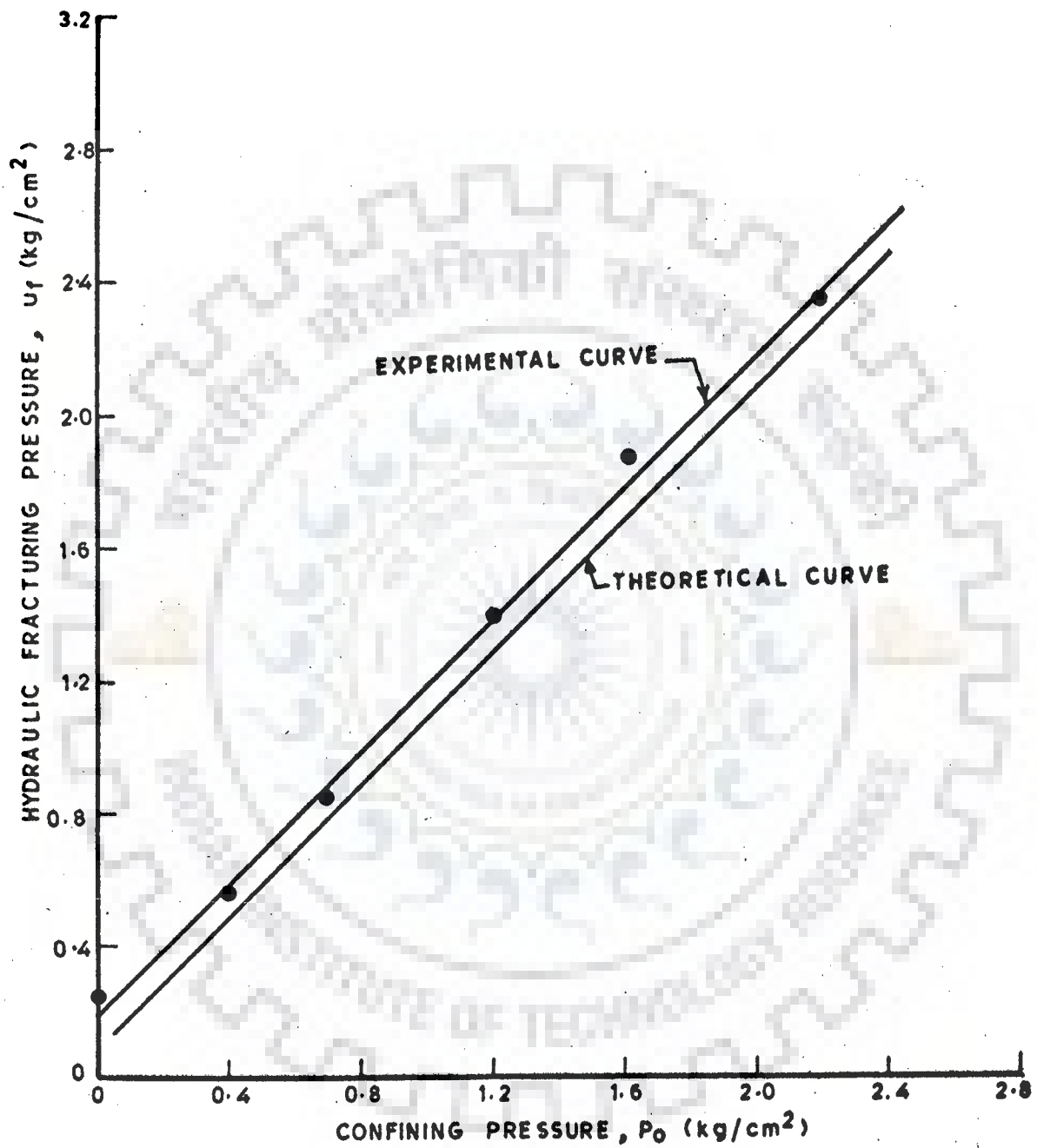VS CONFINING PRESSURE FOR INSTATANEOUS TESTS

FIG. 7.13 _ VARIATION OF HYDRAULIC FRACTURING PRESSURE
VS CONFINING PRESSURE FOR SHORT DURATION
TESTS

testing the pore pressure development due to internally applied pressure in soil specimen will stabilize and achieve steady state condition. Therefore the expression for evaluation of hydraulic fracturing pressure, i.e. equation (7.33), could be used as such. In this expression the coefficient β, under steady state condition due to application of internal pressure could be obtained from Fig. 6.4.

The values of hydraulic fracturing pressure u_f computed theoretically for this condition are plotted in Fig. 7.14 against confining pressure P_o.

7.5.2.4 Back Pressure Saturated Specimens

In the series of tests performed with the use of back pressure saturation technique, the soil mass is saturated under simultaneously applied confining pressure and internal pressure of equal increments. At the time of conducting hydraulic fracturing test, the soil mass is under equal internal and external pressure. The pore pressure under steady state condition would be equal to applied pressures. Under transient condition the only change in pore pressure would be due to increase of P_i which can be predicted from design curves. Therefore, equation (7.30) for this condition can be rewritten as;

$$u = P_o + \beta (P_i - P_o) \hspace{2cm} ..(7.34)$$

For the back pressure saturated specimens Fig. 7.5 indicates that at the start of hydraulic fracturing test where P_o is equal to P_i, the tangential stress is equal to P_o at all the points in the soil mass. The only change in stress will be due to increase of P_i, in order to induce hydraulic fracture.

Therefore, equation (7.27) for this condition can be **written** as;

$$\sigma'_\theta = P_o + \alpha (P_i - P_o) - u \qquad ..(7.35)$$

substituting equation (7.34) into equation (7.35) and replacing P_i by u_f and equating effective tangential stress equal to tensile strength of the soil, the expression for u_f can be simplified as;

$$u_f = P_o + \frac{\sigma_t}{(\beta - \alpha)} \qquad ..(7.36)$$

Hydraulic pressures required for crack initiation under various confining pressures are computed using equation (7.36) and plotted in Fig. 7.15 for u_f against P_o.

7.5.3 Analysis and Discussions

It is seen from the foregoing analysis that hydraulic fracturing pressure is a function of existing state of stress, geometery of the borehole and the strength parameters of the soil.

The application of analytical studies to actual experimental conditions (Figs. 7.12 to 7.15) indicate that hydraulic fracturing pressure is a linear function of confining stress.

In order to compare the application of theoretical criteria developed for evaluation of hydraulic fracturing pressure under transient condition to various actual experimental cases, theoretical plots of u_f Vs P_o, Figs. 7.12 to 7.15 are reproduced in Fig. 7.16. It is seen that the value of hydraulic fracturing pressure u_f increases as the duration of conducting hydraulic fracturing tests decreases. This may be attributed to lower
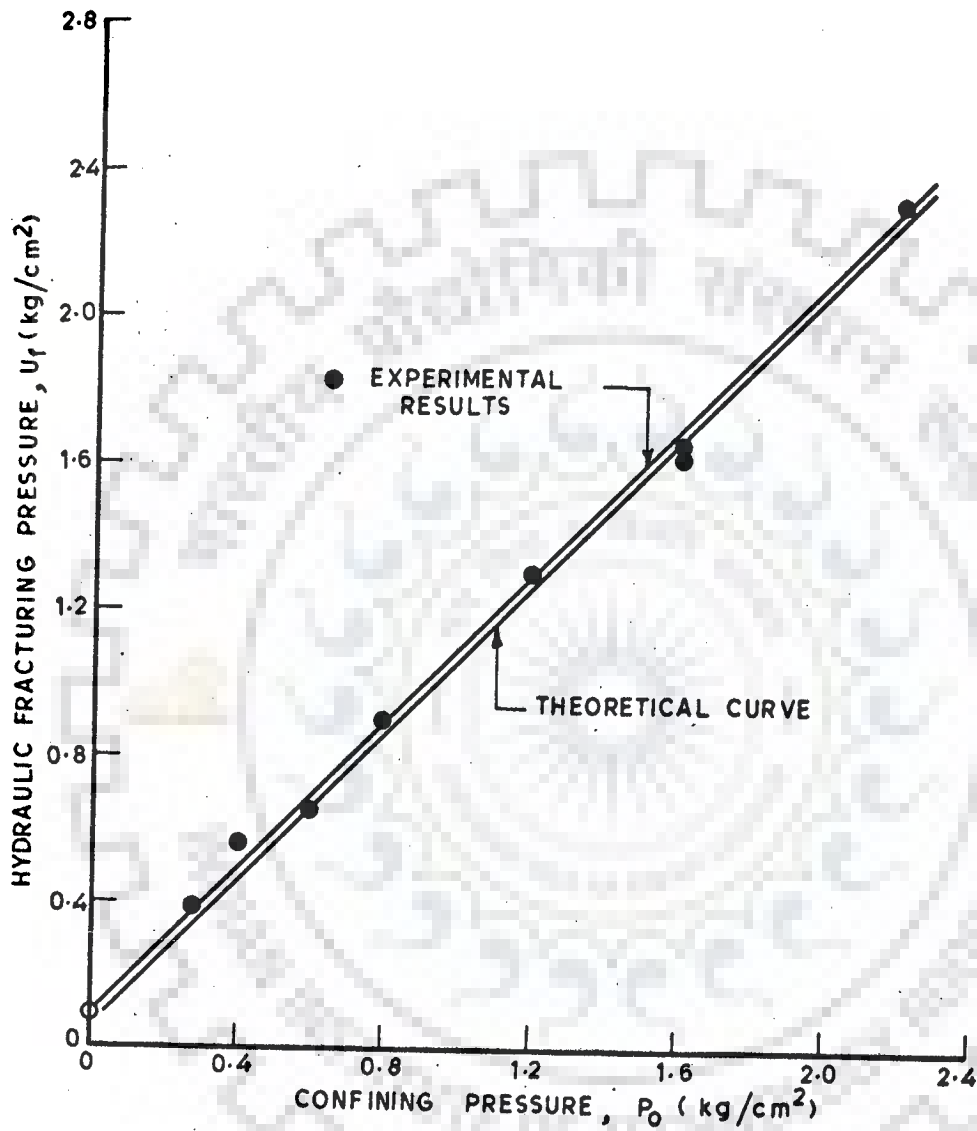
FIG. 7.14 _ VARIATION OF HYDRAULIC FRACTURING PRESSURE
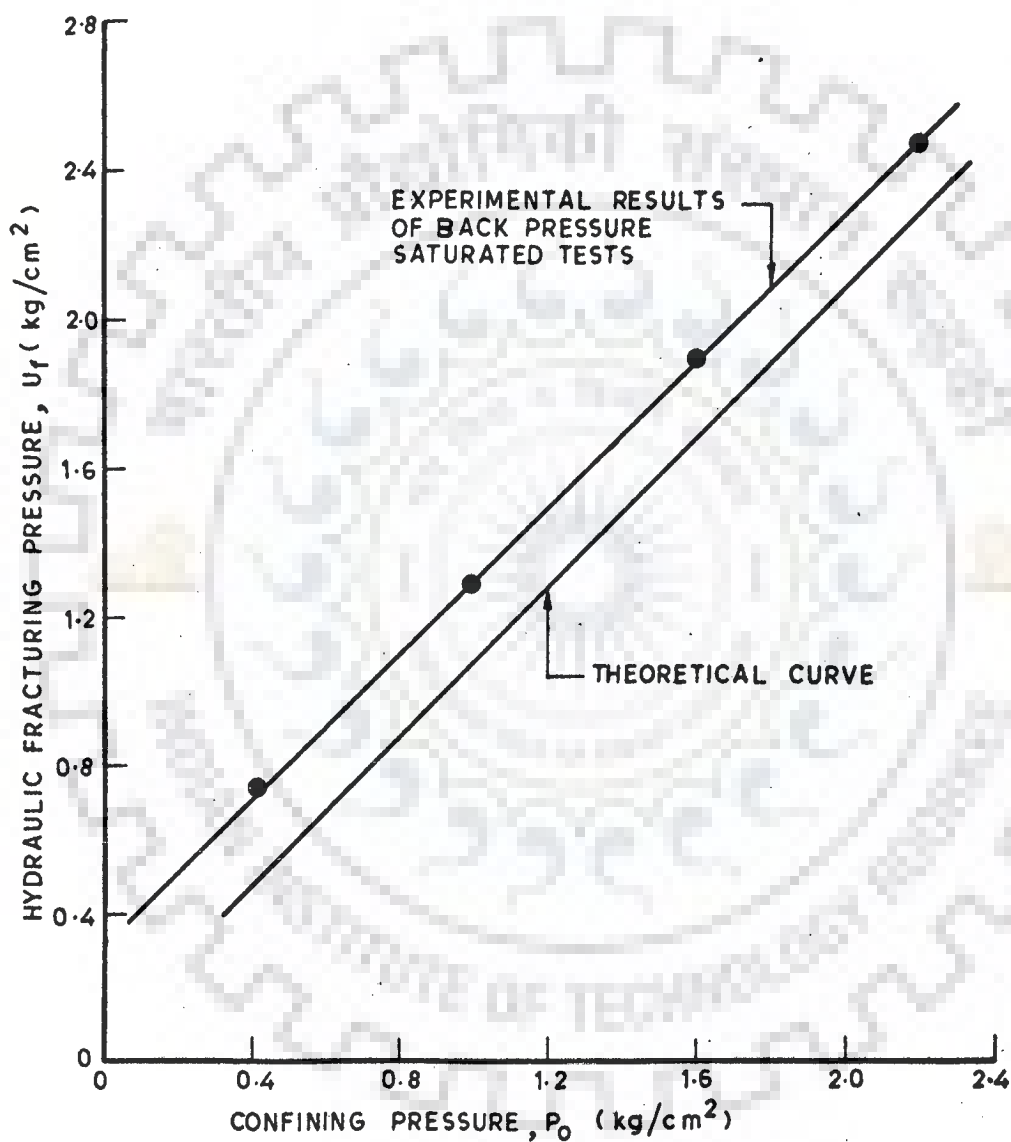VS CONFINING PRESSURE FOR LONG TERM TESTS

FIG. 7.15 _ VARIATION OF HYDRAULIC FRACTURING PRESSURE
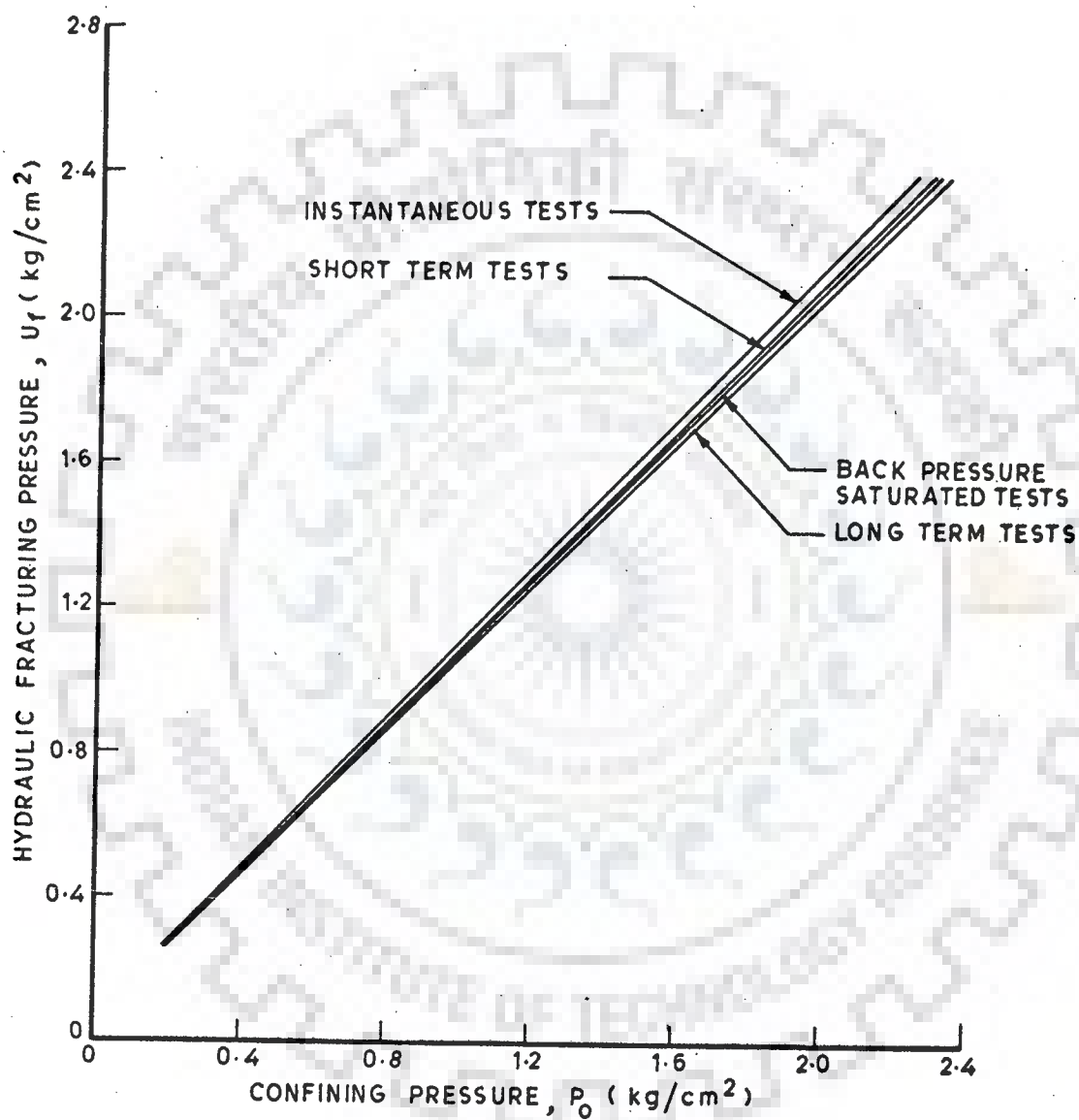VS CONFINING PRESSURE FOR BACK PRESSURE
SATURATED TESTS

FIG. 7.16 _ COMPARISON OF VARIOUS CRITERIA APPLIED TO ACTUAL EXPERIMENTAL CONDITIONS

transition pore pressure values in lesser time. Interestingly, experimental values of u_f were also found to be reducing with increase in duration of test (para 5.2.5).

7.6 COMPARISON OF EXPERIMENTAL AND THEORETICAL RESULTS

With a view to compare the theoretically obtained results of hydraulic fracturing pressure under various test conditions, experimental values of u_f for the corresponding cases of tests, have also been plotted.

The curves presented in Fig. 7.8 show the analytical results computed, using equation (7.11), as well as experimental results obtained for long duration tests. It is seen that analytical results are slightly lower than experimental values. The slope of the line for both the cases, is the same only some minor variation in vertical intercept is there. This may be attributed to the fact that theoretical values are obtained, considering steady state condition whereas experimental values were obtained for a period varying from 3 hours to 24 hours depending upon range of confining pressure.

The effect of anisotropic application of pressure as shown in the Fig. 7.10, indicates that with increase of ratio of vertical axial pressure to lateral pressure, the u_f value decreases. This aspect has been supported by experimental observations as shown in Fig. 5.6.

The theoretical analysis of hydraulic fracturing carried out under transient pore pressure development at various test duration and the experimental values of u_f for corresponding cases of test have been plotted in Figs. 7.12 to 7.15. A study of these figures indicates the following;

1. The experimental values of hydraulic fracturing pressure are always higher than theoretical values, for all the four cases studied, though the quantum of variation differs from one case to another.

2. The difference between observed and theoretical values of hydraulic fracturing pressure decreases with increasing confining pressures.

3. The difference in experimental and theoretical values of hydraulic fracturing pressure is more for instantaneous test condition. For long duration test the difference is very little and for short duration, this difference is in between the two cases. This shows that the gap between experimental and theoretical values is a function of test duration, shorter is the test duration, greater is the gap.

4. Under back pressure saturation the gap between experimental value and the theoretical value of u_f again widens and experimental values are higher than the theoretical values.

The reason for the smaller gap between the observed and theoretical values of u_f, can be attributed to the difference in degree of saturation. In theoretical analysis, complete saturation has been assumed, whereas for experimental test specimens, complete saturation might have not been attained. In the case of longer duration test, it is possible that the saturation of the specimen might be taking place simultaneously with incremental application of internal pressure, whereas in case of instantaneous loading, sufficient time is not available for saturation of the specimen under applied internal pressure. Thus the wider gap in case of instantaneous test and lesser gap for longer duration test stands explained. As regards case of back pressure saturated, it has been shown already in para 5.2.4 that for 98 % degree of saturation, 3.65 Kg/cm^2 pressure would be needed, whereas the test results presented herein are

limited upto 2.2 Kg/cm^2. At 2.2 Kg/cm^2, degree of saturation obtained was 96.3 %. Since the hydraulic fracturing tests for back pressure saturated specimens were carried out only in a period of upto 3 minutes, it can be presumed that the results of this test should be nearer to those of instantaneous tests. It is because of lesser degree of saturation and lesser time duration due to which the gap between the observed and theoretical values of u_f for back pressure saturated case, is on higher side. The point brought out here is corroborated by the fact that the difference between the observed and theoretical value of u_f narrows down as the confining pressure P_o increases (Fig. 7.17). It is interesting to note that at P_o = 6.9 Kg/cm^2, the difference is nominal.

7.7 CONCLUSION

A realistic stress analysis of the experimental model soil cylinder has been carried out and a reasonable comparison of hydraulic fracturing pressure is obtained with the experimental results. The procedure could also be applied to the particular case of earthen structures to evaluate the potential occurrence of hydraulic fracturing, by carrying out a detailed stress analysis.
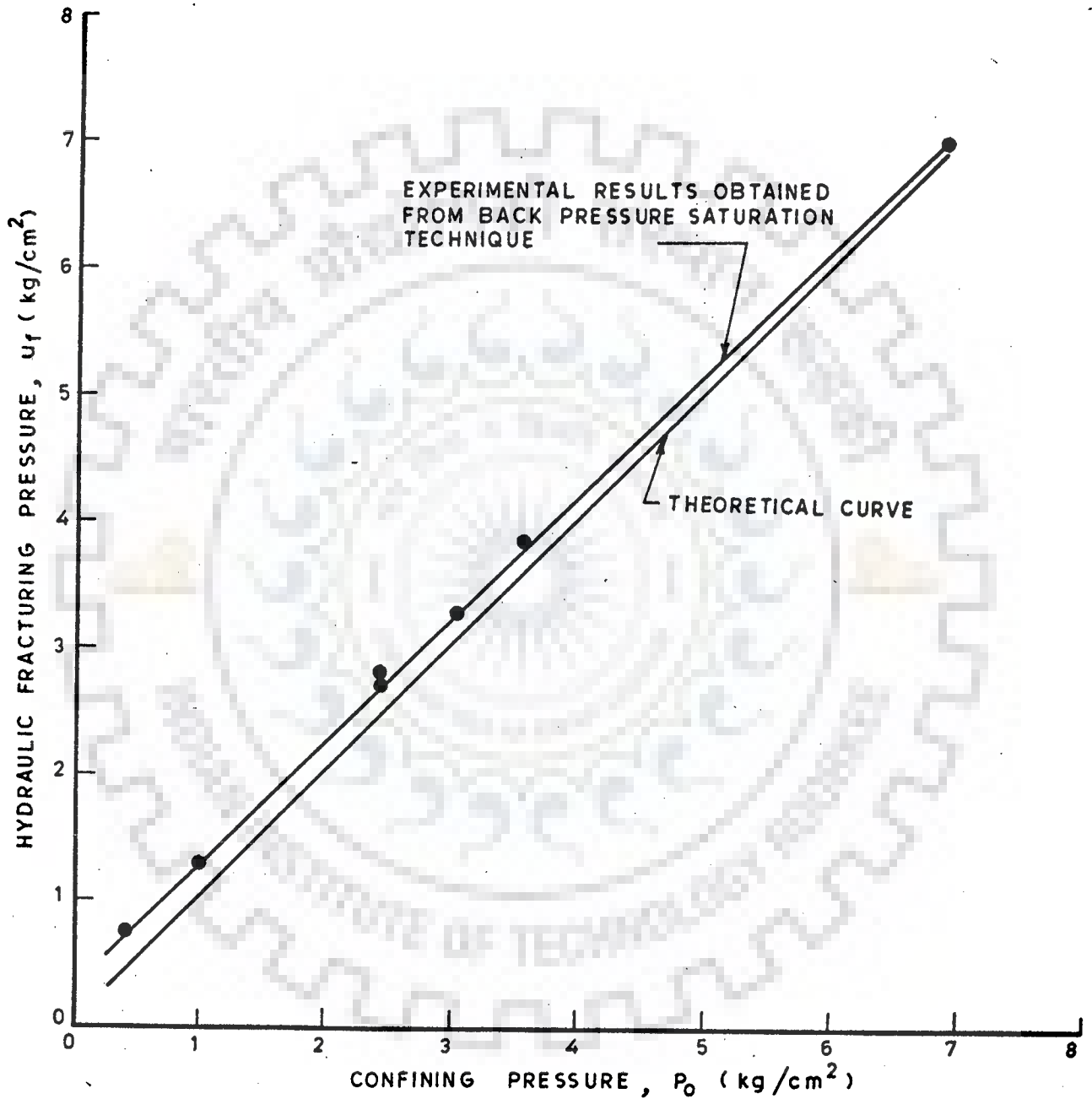
FIG. 7.17 _ VARIATION OF HYDRAULIC FRACTURING PRESSURE
VS CONFINING PRESSURES FOR BACK PRESSURE
SATURATED TESTS

CHAPTER - 8

CONCLUSIONS

To investigate the phenomenon of hydraulic fracturing, an experimental technique has been developed for testing hollow cylindrical soil specimens simulating confined borehole conditions. Theoretical analysis has also been carried out and a reasonable comparison of hydraulic fracturing pressure is obtained with the experimental results. Based on this study, the following conclusions can be drawn;

(1) The experimental results for solid as well as hollow cylindrical specimens have shown that a straight line relationship exists between hydraulic fracturing pressure u_f, and confining pressure P_o. Hydraulic fracturing pressure is always greater than confining pressure for all the cases studied. The slope of line of u_f Vs P_o is nearer to unity irrespective of degree of saturation at time of testing, initial compaction moisture content, time duration of application of hydraulic fracturing pressure and anisotropic loading condition. The vertical intercept at zero confining pressure decreases with increasing initial moisture content. Hydraulic fracturing pressure increases with increase of tensile strength of the soil.

(2) The hydraulic fracturing pressure for partially saturated soil is greater than that for saturated soil.

(3) The hydraulic fracturing pressure required for cracking the soil decreases with increasing initial degree of saturation, for partially saturated as well as fully saturated soils.

(4)   With increase in duration of conducting hydraulic fracturing tests, the hydraulic pressure required for cracking of the soil specimen decreases, provided other conditions remain unchanged.

(5)   Generally vertical cracks were observed for all the hollow cylindrical specimens tested. This indicates that at borehole tests with high fluid pressure, vertical cracks will develop all-round the boreholes.

(6)   The results of tests performed on solid cylindrical soil specimens indicate higher values of u_f compared with the results of tests performed on hollow cylindrical specimens, for the same value of confining pressure.

(7)   The results of vertical intercept, obtained for hollow cylindrical as well as solid cylindrical specimens tested under saturated as well as partially saturated condition as compared to σ_t of the soil indicate that the results of hollow cylindrical specimens are more dependable than the results of solid cylindrical specimens.

(8)   Theoretical analysis shows a good, and reasonable comparison with experimental results.

(9)   Both experimental and theoretical investigations show that u_f decreases with increase in the ratio of vertical pressure to lateral pressure.

(10)   Refracturing occurs at lower pressure than the initial one, provided other conditions remain unchanged. Pre-existing

cracks will heal after some time under high confining stresses, even for low plasticity soil.

(11)   The pressure at which an existing crack fully closes over a period of time, is equal to confining pressure.

(12)   Design curves for prediction of pore pressure under steady state as well as transient conditions around confined boreholes simulated in this study have been prepared. Similar curves can be prepared to cover different rates of pressure application, and various types of soil for actual field conditions.

(13)   Knowing the pore pressure development and existing state of stresses around boreholes, the technique developed for prediction of hydraulic fracturing pressure under steady state as well as transient pressures can be used for actual field conditions.

(14)   The potential of occurrence of hydraulic fracturing in an earthen structure can be investigated by carrying out a realistic stress analysis of the structure under the applied loads.

SCOPE FOR FURTHER RESEARCH
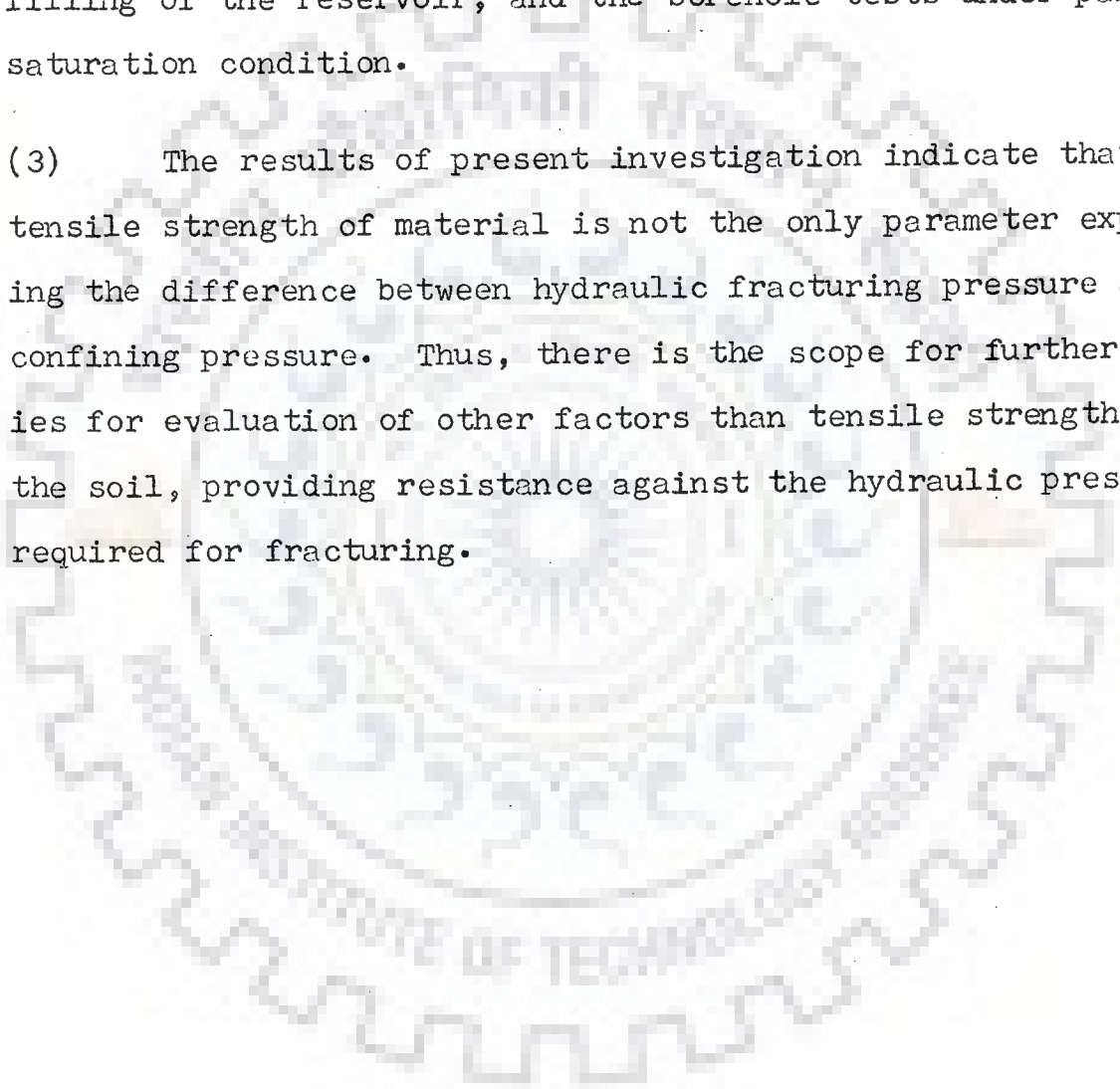
Based on the experience of this study the following suggestions have been listed out, for further work in this area of investigation.

(1)   In order to have better representative prototypes of actual field conditions, it is necessary to investigate larger

size specimens of various dimensions.

(2)   Theoretical modelling of pore pressure development under steady state as well as transient conditions, for partially saturated soil will no doubt enlighten us about the safety of structures against hydraulic fracturing, specially at initial filling of the reservoir, and the borehole tests under partial saturation condition.

(3)   The results of present investigation indicate that tensile strength of material is not the only parameter explaining the difference between hydraulic fracturing pressure and confining pressure. Thus, there is the scope for further studies for evaluation of other factors than tensile strength of the soil, providing resistance against the hydraulic pressure required for fracturing.

REFERENCES

1. Akazawa, T., 'Tension Test Methods of Concrete', Rilem Bulletin, No. 16, Nov. 1953, pp. 11-23.

2. Barden, L. and Sides,G.R., 'The Diffusion of Air Through the Pore Water in Soils', Proc. of 3rd, Asian Conf. on SMFE, Haifa, Israel, 1967, pp. 135-138.

3. Barden, L. and Sides, G.R., 'The Effect of Time on the Undrained Pore Pressure in Compacted Clay', Proc. of 3rd, Asian Conf. on SMFE, Hifa, Israel, 1967, pp. 308-311.

4. Bhandari, R.K., 'Lateral Ground Stress with Focus on Hydraulic Fracturing', Proceedings of the 10th International Conference on Soil Mechanics and Foundation Engineering, Stockholum, 1981, Vol. 4, pp. 778-779.

5. Bharat Singh and Prakash, S., 'Soil Mechanics and Foundation Engineering', Nem Chand and Bros. Roorkee (U.P.), India, 4th Edn. 1976.

6. Bharat Singh and Sharma, H.D., 'Earth and Rockfill Dams', Sarita Prakashan, Meerut, India, 1st Edn. 1976.

7. Bishop, A.W. and Henkel, D.J., 'The Measurement of Soil Properties in the Triaxial Test', Edward Arnold Pub. Ltd., London, 2nd Edn. 1962.

8. Bjerrum, L. and Andersen, K.H., 'In-Situ Measurement of Lateral Pressures in Clay', European Conf. on Soil Mechanics and Foundation Engineering, Madried, 1972, Vol. I, pp. 11-19.

9. Bjerrum, L. et al., 'Hydraulic Fracturing in Field Permeability Testing', Geotechnique, 1972, Vol. 22, No. 2, pp. 319-332.

10. Black, D.K. and Lee, K.L., 'Saturating Laboratory Samples by Back Pressure', Proc., ASCE, SM 1, 1973, pp. 75-93.

11. Connor, J.J. and Brebbia, C.A., 'Finite Element Techniques for Fluid Flow', Newness - Butterworth and Company Ltd., London, 1976.

12. Decker, R.A. and Clemence, S.P., 'Laboratory Study of Hydraulic Fracturing in Clay', 10th Int.Conf. on SMFE, Stockholm, 1981, Vol. I, pp. 573-575.

13. Desai, C.S., 'Finite Element Procedure for Seepage Analysis Using an Isoparametric Elements', Proc. Symp. on Application of Finite Element Method in Geotechnical Engineering, Vicksburg, Miss. 1972, pp. 799-822.

14. Desai, C.S., 'Flow Through Porous Media', Numerical Methods in Geotechnical Engineering, Edited by C.S. Desai and J.T. Christian, McGraw-Hill Book Company, N.Y., 1977, pp. 458-505.

15. Desai, C.S. and Abel, J.F., 'Introduction to the Finite Element Method', An East-West, Edition, Litton Educational Pub., Inc., N.Y., 1972.

16. Finlayson, B.A., 'The Method of Weighted Residual and Variational Principles', Academic Press, N.Y., 1972.

17. France, P.W., 'Finite Element Analysis of Two and Three Dimensional Unconfined Seepage Problem', Proc. of 1st Conf. on Finite Element in Water Resources, Princeton, USA, 1976, pp. 271-285.

18. Frocht, M.M., 'Photo Elasticity', Vols. I and II, John Wiley and Sons, Inc., New York, 1964.

19. Frosythe, G.E. and Wasow, W.R., 'Finite Difference Methods for Partial Differential Equations', Section 20, Wiley, N.Y. 1960.

20. Gambolati, G., 'Equation for One Dimensional Vertical Flow of Ground Water; The Rigorous Theory', Water Resources Research, 1973.

21. Gibson, R.E. and Anderson, W.F., 'In-situ Measurement of Soil Properties with the Pressuremeter', Civil Engineering and Public Work Review, 1961, Vol. 56, No. 658, p. 615.

22. Goel, M.C., 'Drawdown Pore Pressure in Earth Dam', Ph.D. Thesis, University of Roorkee, 1980, Roorkee, India.

23. Haimson, B., 'Hydraulic Fracturing in Porous and Non-Porous Rock and its Potential for Determining In-situ Stresses at Great Depth', U.S. Army Crops of Engineers, Technical Report No. 4-68, 1968, Missouri River Div. Omaha, Nebraska 68101.

24. Hassani, A.W., Bharat Singh and Saini, S.S., 'Experimental Investigation of Hydraulic Fracturing', Indian Jl. of Power and River Valley Development, Vol. 33, No.5-6, 1983, pp. 181-187.

25. Hassani, A.W., Bharat Singh and Saini, S.S., 'A Study of the Mechanism of Hydraulic Fracturing', Jl. of the Institution of Engineers (India), Vol. 64, CI 1, July,1983, pp. 15-22.

26. Hassani, A.W., Bharat Singh and Saini, S.S., 'Finite Element Analysis of Transient Seepage Through Axisymmetric Flow Media', Jl. of the Institution of Engineers (India), Vol. 65, CI 2, Sept. 1984.

27. Hassani, A.W., Bharat Singh and Saini, S.S., 'An Investigation of Hydraulic Fracturing', Submitted for Publication, ASCE, Geotechnical Engineering Division, May, 1984.

28. Hassani, A.W., Bharat Singh, Saini, S.S. and Goel, M.C., 'Laboratory Simulation of Hydraulic Fracturing', Accepted for Publication in 11th Int. Symp. on SMFE to be held in August 1985 in Sanfrancissco.

29. Javandel, I., and Witherspoon, P.A., 'Application of the Finite Element Method to Transient Flow in Porous Media', Society of Petrolium Engineers, Jl. 8 (3), 1968, pp. 241-252.

30. Jaworski, G.W., Duncan, J.M. and Seed, H.B., 'An Experimental Study of Hydraulic Fracturing', Report No. UCG/GT/79-02, University of California, Berkeley, 1979.

31. Jaworski, G.W., Duncan, J.M. and Seed, H.B., 'Laboratory Study of Hydraulic Fracturing, Proc., ASCE, GT6, June,1981, pp. 713-732.

32. Kjarnsli, B., and Torblaa, I., 'Leakage through Horizontal Cracks in the Core of Hyttejuvet Dam', Norwegian Geotechnical Institute, Pub., No. 80, Oslo, 1968, pp. 39-47.

33. Kennard, R.M., 'The Measurement of Soil Permeability In-situ by the Constant Head Test', Ph.D. Thesis, 1970, University of London.

34. Kirsch, G., Verein Deustscher Ingenieur (VDI), Zeitschrift, Vol. 42, 1898.

35. Kochina, P. Ya. P., 'Theory of the Motion of Ground Water', In Russian, Gostekhizdat, Moscow, 1952, Translated by J.M. De Weist, Princeton University Press, Princeton, New Jersey, 1962.

36. Kulhawy, F.H. and Duncan, J.M., 'Stresses and Movements in Oroville Dam', Proc. ASCE, Jl. of SMFE, No. SM 7, 1972, pp. 653-665.

37. Kulhawy, F.H., Duncan, J.M. and Seed, H.B., 'Finite Element Analysis of Stresses and Movements in Embankments during Construction', Contract Report No. TE-69-4, Usaewes, Nov. 1969.

38. Kulhawy, F.H. and Gurtowski, T.M., 'Load Transfer and Hydraulic Fracturing in Zoned Dams', Proc. ASCE, Vol. 102, No. GT9, 1976, pp. 963-974.

39. Ladanyi, B., 'Expansion of a Cavity in Saturated Clay Medium', Proc. ASCE, Vol. 89, No. SM4, 1963, pp. 127-161.

40. Lee, K.L. and Black, D.K., 'Time to Dissolve an Air Bubble in a Drain Line', Proc. ASCE, Vol. 98, No. SM 2, 1972, pp. 181-194.

41. Lefebvre, G., et al., 'Fissuring from Hydraulic Fracture of Clay Soil', 10th ICSMFE, Stockholm, 1981, Vol. 2, pp. 513-518.

42. Leonards, G.A. and Narain, J., 'Flexibility of Clay and Cracking of Earth Dams', Proc., ASCE, Vol. 89, No. SM2, 1963, pp. 47-98.

43. Lewitt, E.W., 'Hydraulic and Fluid Mechanics', Sir Isaac Pitman and Sons Ltd., London, 10th Ed., 1958.

44. Lofquist, B., Discussion on, Cracking in Earth Dams, Proc. of the 4th Int. Conf. on Soil Mechanics and Foundation Engineering, London, Vol. 3, 1957, pp. 261-262.

45. Lowe, J. and Johnson, T.C., 'Use of Back Pressure to Increase Degree of Saturation of Triaxial Specimens', ASCE, Research Conference on Shear Strength of Cohesive Soils, Boulder, Colo. 1960, pp. 819-836.

46. Massarsch, K.R., 'New Aspects of Soil Fracturing in Clay', Proc. ASCE, No. GT8, 1978, pp. 1109-1123.

47. Marino, M.A. and Luthin, J.N., 'Seepage and Ground Water', Development in Water Science, 13, Elsevier Scientific Publishing Company, Amsterdam, 1982, pp. 142-148.

48. Marsal, R.J. and Edmundo, M.G., 'Investigations on the Design and Performance During Construction of Chicoasen Dam in Mexico', Contribution to the 13th ICOLD, New Delhi, 1979.

49. Morgenstern, N.R. and Vaughan, P.R., 'Some Observations on Allowable Grouting Pressures', Proc. of the Conf. on Grouts and Drilling Muds in Engineering Practice, I.E. Butterworths, London, 1963.

50. Nobari, E.S., Lee, K.L. and Duncan, J.M. 'Hydraulic Fracturing in Zoned Earth and Rockfill Dams', Research Report No. TE 73-1, University of California, Berkeley, 1973.

51. Norrie, D.H. and Vries, G. DE., 'Recent Advances in Finite Element Methods Applied to Fluid Dynamics', Int. Conf. on Finite Element Methods in Engineering, University of Adelaide, Australia, 1976.

52. Neuman, S.P., 'Galerkin Approach to Saturated - Unsaturated Flow in Porous Media', Finite Elements in Fluids, Edited by Gallagar, Oden, Tylor and Zienkiewicz, John-Wiley and Sons, London, Vol. I, 1975, pp.201-217.

53. Neuman, S.P., 'Saturated – Unsaturated Seepage by Finite Elements', ASCE, Jl. Hyd. Division, Vol. 99, 1975, pp. 2233-2250.

54. Neuman, S.P. and Witherspoon, P.A., 'Analysis of Nonsteady Flow with a Free Surface Using the Finite Element Method', Jl. Water Resources Research, Vol. 7, No.3, June 1971, pp. 611-623.

55. Penman, A.D.M. and Charless, J.A., 'Assessing the Risk of Hydraulic Fracturing in Dam Cores', 10th Int. Conf. on SMFE, Stockholm, Vol. I, 1981, pp. 457-462.

56. Remson, I. Hornebergar, G.H. and Molz, F.H., 'Numerical Methods in Subsurface Hydrology with an Introduction to the Finite Element Method', Wiley-Interscience, New York, 1971.

57. Schuurman, E., 'The compressibility or an Air/Water Mixture and a Theoretical Relation Between the Air and Water Pressures', Geotechnique, Vol. 16, No. 4, 1966, pp. 269-281.

58. Seed, H.B. and Duncan, J.M., 'The Teton Dam Failure – A Retrospective Review', 10th Int. Conf. on SMFE, Stockholum, 1981, Vol. 4, pp. 219-238.

59. Sharma, H.D., 'Nonlinear Analysis of a High Rockfill Dam with Earth Core', Ph.D. Thesis, University of Roorkee, 1976, Roorkee, India.

60. Sherard, J.L., 'Embankment Dam Cracking', Embankment Dam Engineering, The Casgrande Volume, R.C., Hirschfied and S.J. Poulos End., Wiley-Interscience, New York, 1973, pp. 271-353.

61. Sherard, J.L., Discussion on, Cracking in Earth Dams, Transactions of 10th ICOLD, Vol. 6, 1970, pp. 377-381.

62. Sherard, J.L., Decker, R.S. and Ryker, N.L., 'Hydraulic Fracturing in Low Dams of Dispersive Clay', Proc. of ASCE Specialty Conf. on Performance of Earth and Earth Supported Structures, Purdue University, W. Lafayette, Indiana, Vol. 1, 1972, pp. 653-689.

63. Sherard, J.L., Woodward, R.J., Gizienski, S.F. and Clevenger, W.A., 'Earth and Earth Rock Dams', John Wiley and Sons, 1963.

64. Skempton, A.W., 'The Pore Pressure Coefficients A and B', Jl. of Geotechnique, Vol. 4, No. 4, 1954, pp. 143-147.

65. Sreenivasulu, P. and Das, G.J., 'Finite Element Solution of Transient Ground Water Flow Problems by Galerkin Approach', Jl. of I.E. (India), Vol. 63, CI 2, Sept. 1982, pp. 80-84.

66. Terzaghi, K. and Peck, R.B., 'Soil Mechanics in Engineering Practice', Asia Publishing House, New Delhi, 1972.

67. Timoshenko, S., 'Strength of Material', John Wiley and Sons Ltd., 1965.

68. Timoshenko, S. and Goodier, J.N., 'Theory of Elasticity', McGraw-Hill Book Co., Inc. 2nd. Edn., 1951, New York.

69. Vaughan, P.R., 'The Use of Hydraulic Fracturing Tests to Detect Crack Formation in Embankment Dam Cores', Interim Report, Department of Civil Engineering, Imperial College, London, 1971.

70. Vaughan, P.R., Kluth, D.J., Leonard, M.W. and Pradowa, H.H.M., 'Cracking and Erosion of the Rolled Clay Core of Balderhead Dam and the Remedial Works Adopted for its Repair', Proc. 10th ICOLD, Montreal Canada, Vol. 1, 1970, pp. 73-94.

71. Walton, W.C., 'Ground Water Resources Evaluation', Int. Student Edition, McGraw-Hill, Inc. New York, 1970.

72. Zienkiewicz, O.C., 'The Finite Element Method in Engineering Science', McGraw-Hill Pub. Comp. Ltd. London, 1971.

73. Zienkiewicz, O.C. and Cheung, Y.K., 'Finite Element in the Solution of Field Problems', The Engineer, Sept. 1965, pp. 507-510.

74. Zienkiewicz, O.C. Mayer, P. and Cheung, Y.K., 'Solution of Anistropic Seepage Problems by Finite Elements', Proc. ASCE, Vol. 92, EM1, 1966, pp. 111-120.

75. ———, 'Independent Panel to Reivew Causes of Teton Dam
     Failure', Report to U.S. Department of the Interior
     and State of Idaho on Failure of Teton Dam, 1976.

76. ———, 'Failure of Teton Dam', U.S. Department of the
     Interior Teton Dam Failure Review Group, A Report of
     Findings, 1977.

77. ———, 'Failure of Teton Dam', U.S. Department of the
     Interior Teton Dam Failure Review Group, Final
     Report, 1980.

APPENDIX - A

CASE STUDY OF AN ACTUAL EARTH AND ROCKFILL DAM

INTRODUCTION

Cracks have occurred even in well designed dams. Here, the case study of a 260 m high Tehri dam under construction, is presented with a view to investigate the possibility of hydraulic fracturing. Fig. A-1 shows the cross-section of the dam. Two positions of the core viz. a central vertical core and an inclined core have been considered. The upstream and downstream shells of dam section consist of river terrace material comprising pervious mixture of silt, sand, gravel and boulders. The transition filters consist of silt to gravel size particles. The core of the dam will be a well graded impervious mixture of clayey silt blended with gravelly material upto 15 cm size.

Stress deformation analysis for end of construction and full reservoir conditions was carried out for two dimensional plane strain condition using finite element method, considering isotropic conditions, rigid foundation and nonslipping embankment foundation contact with sequential construction. The stress analysis of the dam has been presented by Sharma[59].

Based on the available laboratory tests data and the studies of Kulhawy et al[37], the material properties was presented in Table A-1 have been used in the analysis. The material properties at the shell-transition and transition-core interfaces, as determined by direct shear tests, are reproduced in Table A-2.

TABLE A-1 MATERIAL PROPERTIES

Parameters	Shell	Transition	Core
Unit weight (tones/m^3)	1.80	1.99	1.96
Cohesion, c (tones/m^2)	–	–	1.00
Friction angle (degree)	38	32	27
Modulus number (k)	2500	3000	500
Modulus exponent, n	0.25	0.30	0.60
Failure ratio, R_f	0.76	0.76	0.90
Poisson's ratio parameters			
Shear modulus G	0.43	0.43	0.48
F	0.19	0.19	0.0
d	14.80	14.80	0.0

A check was kept on the value of the mobilization factor, $m = (\sigma_1 - \sigma_3)/(\sigma_1 - \sigma_3)_f$, and its value was not allowed to exceed unity, which is indicative of material failure. The stresses obtained for end of construction condition were assumed as initial stresses and the stresses obtained during water loading were additive. The upstream shell and transition were taken as submerged.

TABLE A-2 MATERIAL PROPERTIES AT INTERFACES

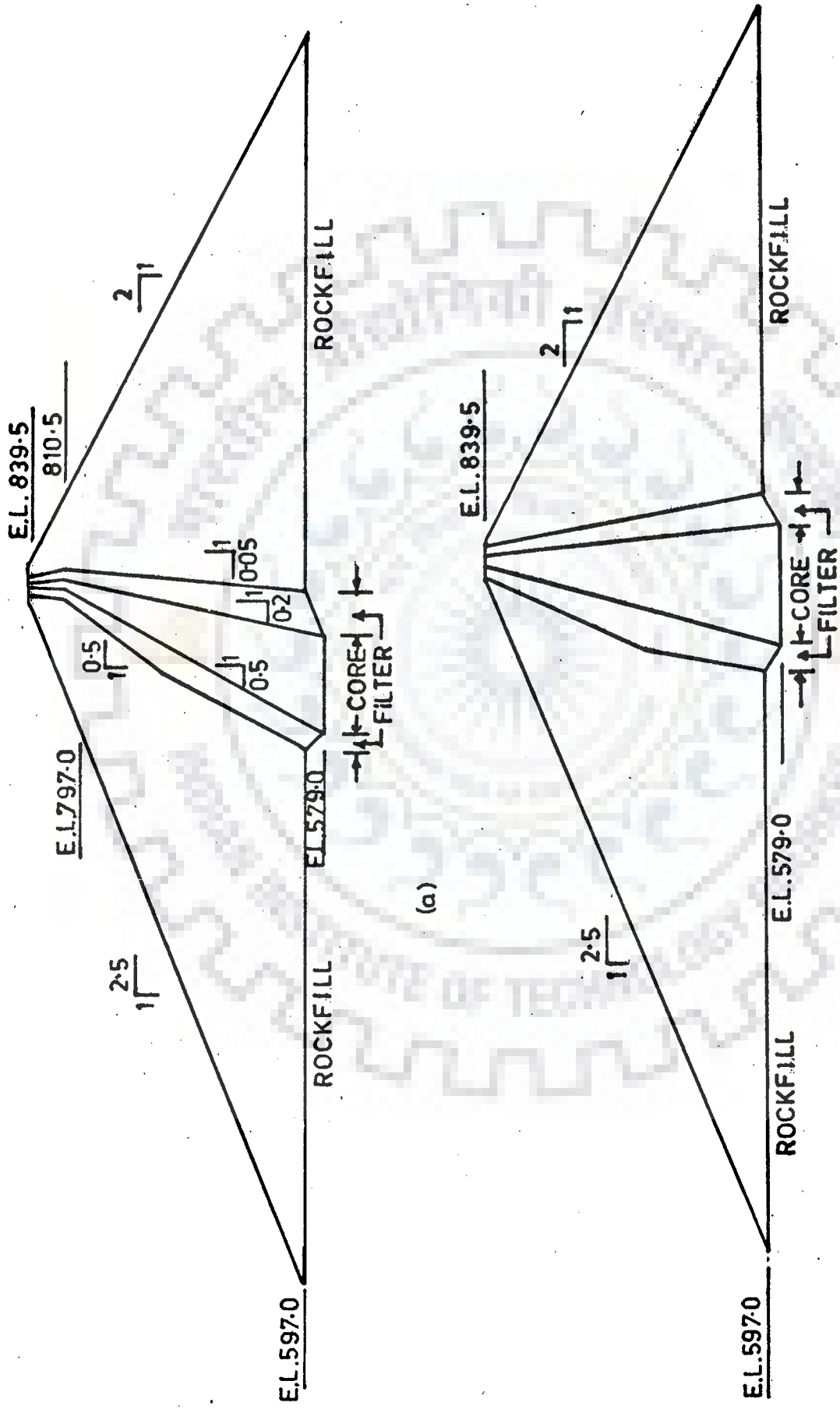| Parameters	Interfaces	
	Shell-Filter	Filter-Core
Adhesion(tones/m^2)	0.0	1.3
Stiffness constant, k_j	4500	6500
Exponent, n'	0.72	0.30
Failure ratio, R_f	0.85	0.90
Angle of adhesion(degree)	39	29

FIG. A-1 TEHRI DAM CROSS SECTION WITH (a) INCLINED
CORE (b) VERTICAL CORE.

(AFTER SHARMA, 1976)

STRESS DISTRIBUTION

The distribution of σ_1 and σ_3 at upstream core-filter interfaces as well as at downstream core-filter interfaces along the height of the dam, is shown in Figs. A-2 and A-3 for inclined and vertical cores, respectively. For reservoir full condition these plots indicate that stresses are lower at the upstream of the core and are higher at downstream of the core. These stress changes may be due to bouyancy effects at upstream shell and transition and application of the water load on the core face, which presses it towards the downstream, and relieves the upstream shell portion.

ANALYSIS FOR HYDRAULIC FRACTURING

To investigate the possibility of hydraulic fracturing, the minimum principal stress σ_3 at upstream and downstream of the impervious core, are plotted in Fig. A-4 for vertical core and, in Fig. A-5 for inclined core. It is generally assumed that the shells as well as transition materials behave as free draining material, thus the pore pressure at upstream of the core should be equal to hydrostatic pressure. For comparison, hydrostatic pressure under full reservoir condition along the height of the dam is also plotted in these figures. Fig. A-4 indicates that at most of the points along the height of the dam, the hydrostatic pressure exerted due to impounding of reservoir is greater than the minor principal stresses along upstream interface, indicating thereby the possibility of hydraulic fracturing to occur at these points. Minor principal stress is higher at downstream interface as compared to upstream
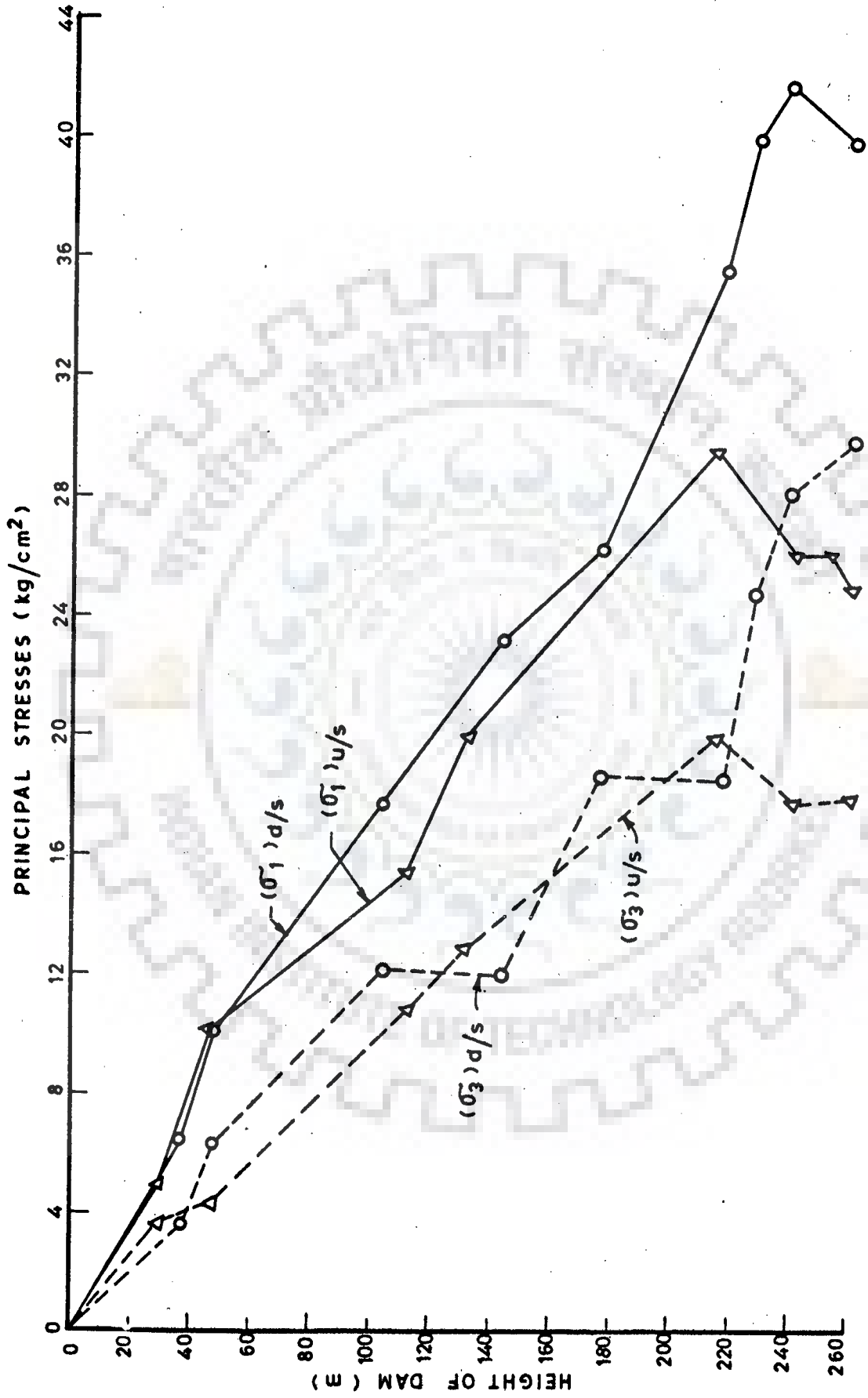
FIG. A-2 – DISTRIBUTION OF PRINCIPAL STRESSES ALONG THE CORE-FILTER INTERFACES OF INCLINED CORE OF TEHRI DAM
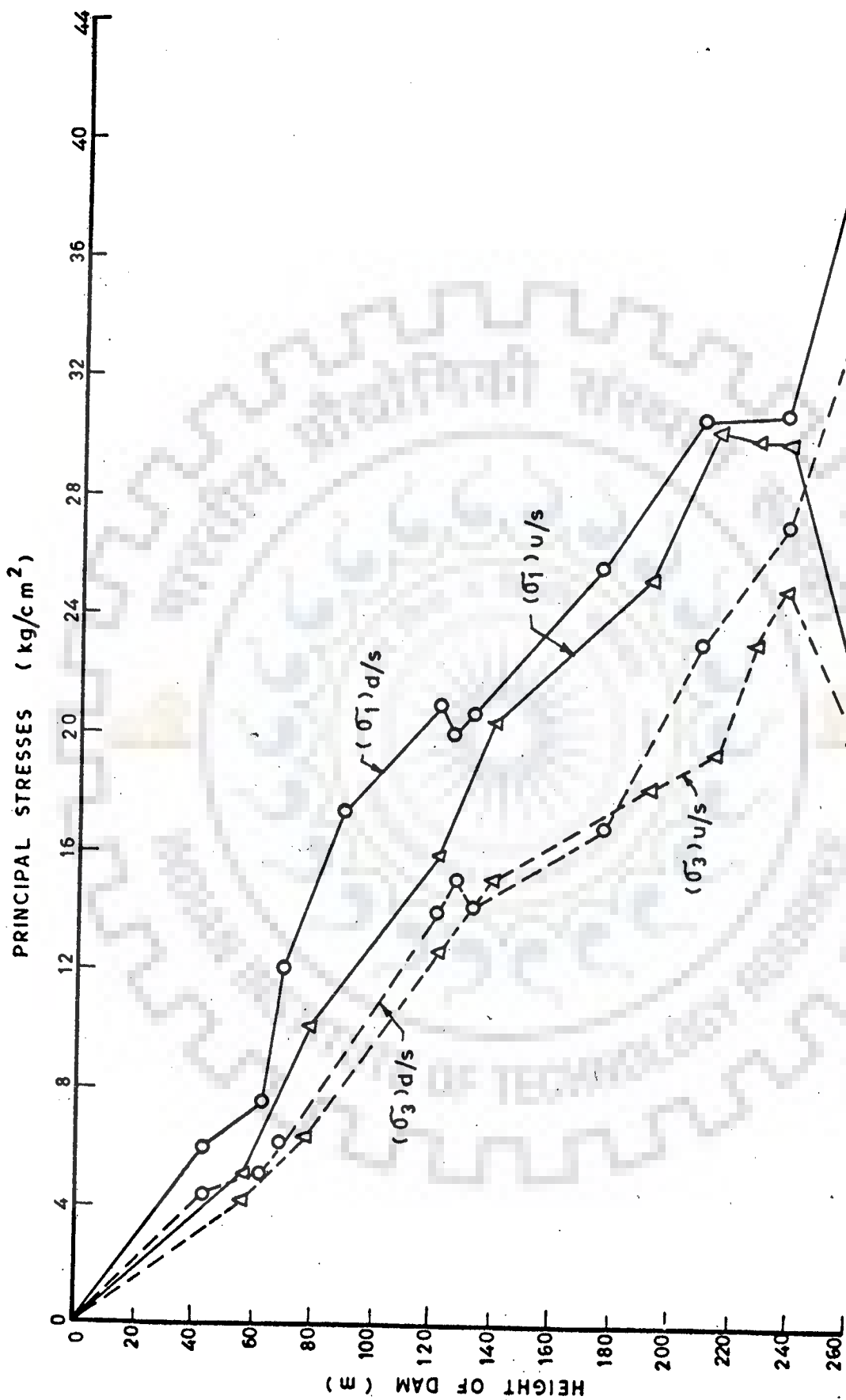
FIG. A-3 – DISTRIBUTION OF PRINCIPAL STRESSES ALONG THE CORE-FILTER INTERFACES OF VERTICAL CORE OF TEHRI DAM
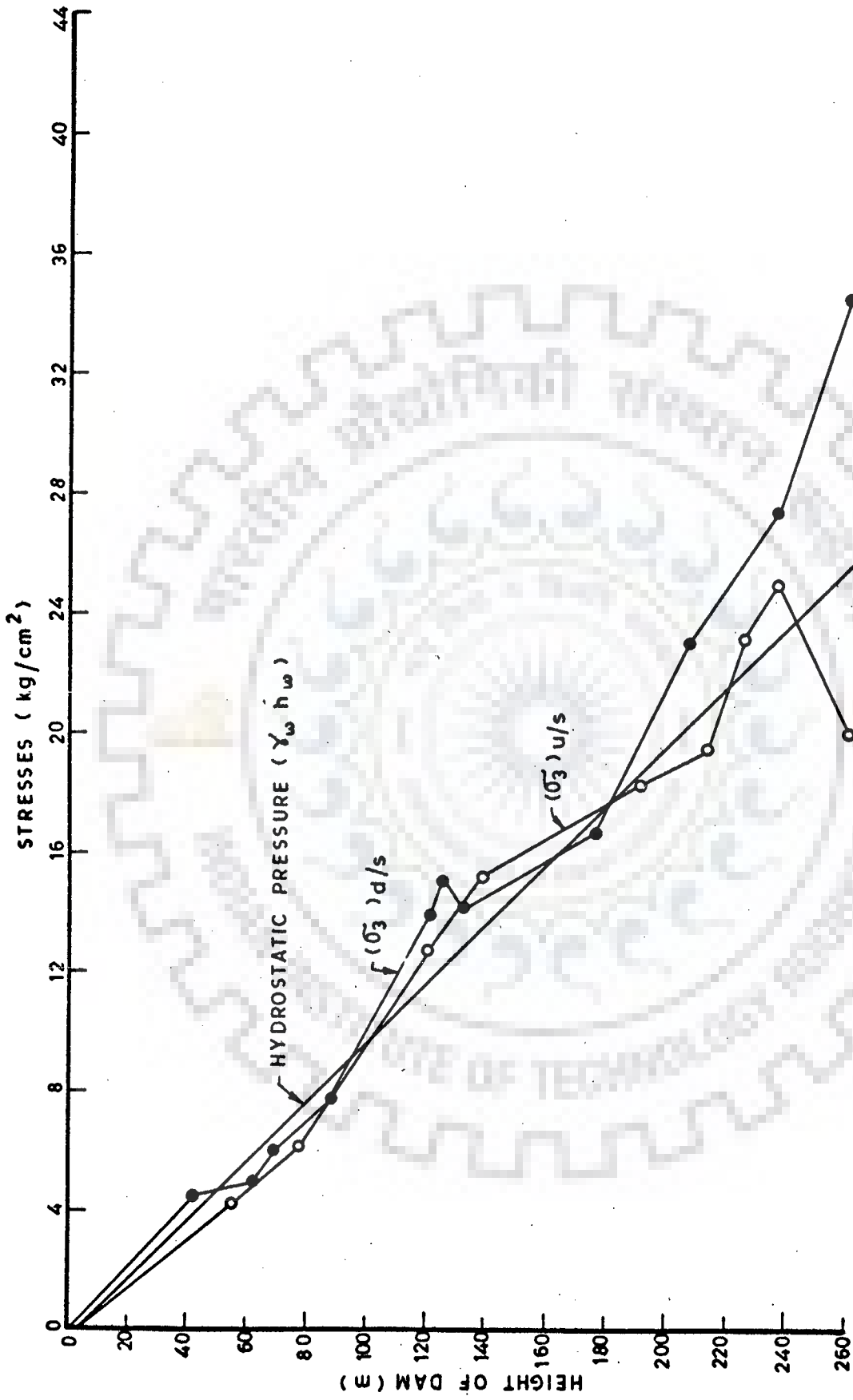
FIG. A-4 — DISTRIBUTION OF STRESSES UNDER RESERVOIR FULL CONDITION ALONG INTERFACES OF VERTICAL CORE
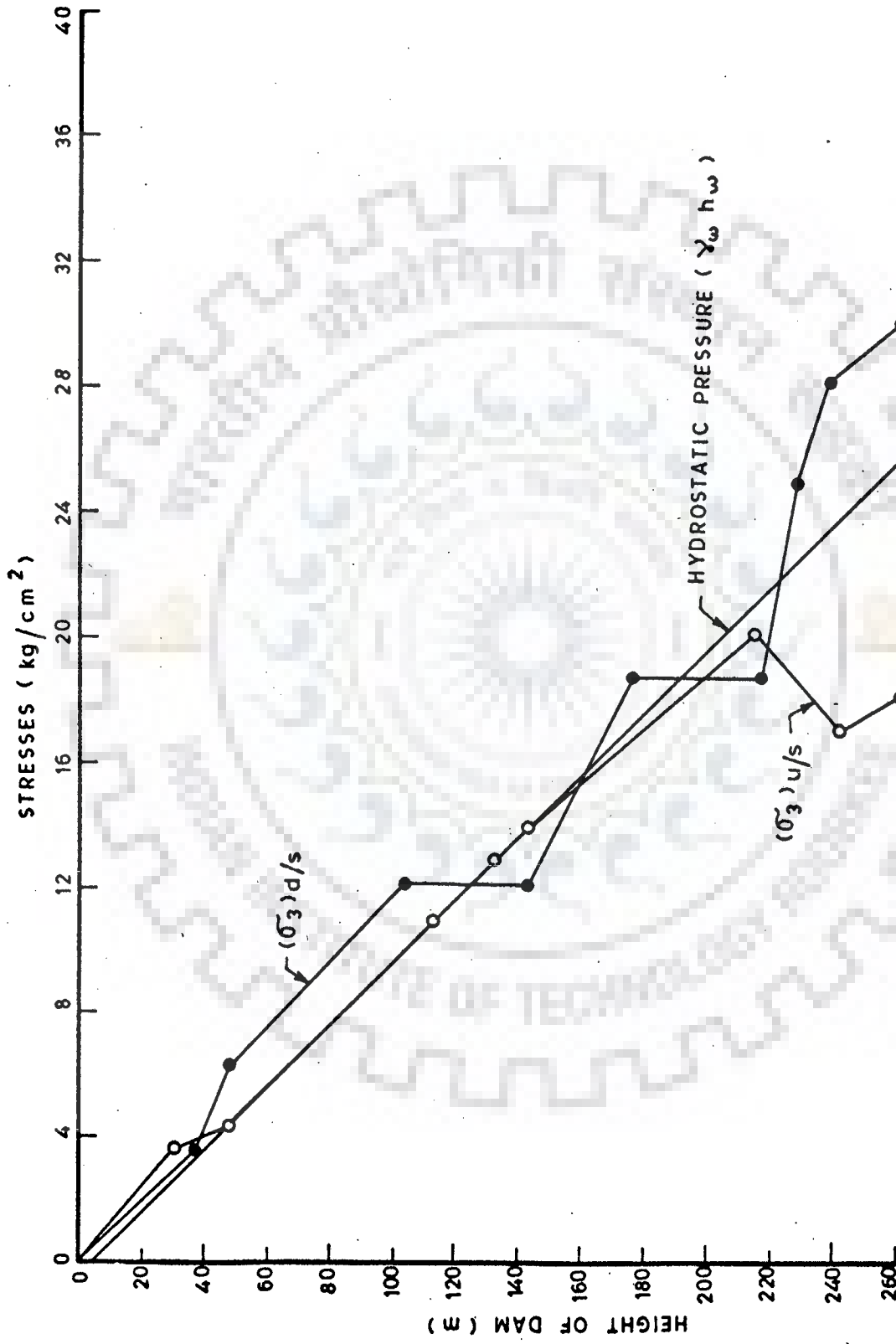
FIG. A-5 _ DISTRIBUTION OF STRESSES UNDER RESERVOIR FULL CONDITION
.ALONG INTERFACES OF INCLINED CORE

interface and hence lesser possibility of its susceptibility to hydraulic fracturing. This is due to the fact that, the pore pressure at downstream of the core will be far lower than hydrostatic pressure. It is seen from Fig. A-5, that in case of inclined core, the minor principal stresses are just equal to pore pressures at upstream of the core in the upper regions of the dam, but towards the base of the dam, minor principal stresses are substantially lower than the pore pressures indicating the possibility of hydraulic fracturing.

A comparison of Figs. A-4 and A-5 indicates that the minor principal stresses for the case of vertical core dam are lower than hydrostatic pressures at upstream of the core, in a significant region along the height of the dam, in comparison to the case of inclined core dam. Thus the, possibility of hydraulic fracturing is more in the case of vertical core dam as compared to inclined core dam.

RECOMMENDATION FOR REMEDIAL MEASURES

On the basis of earlier experience, the following remedial measures could be examined for Tehri dam in order to ensure its safety against hydraulic fracturing,

1. Comparison of stresses reported by Sharma[59] indicate transfer of stresses to the transition and shells. Therefore, a zone of more compressible material within the rockfill mass, both upstream and downstream of the impervious core[45] could help to reduce the arching of the core on shells.

2. Wider filters and transitions of well graded materials with controlled compaction will no doubt contribute to reduce the cracking and concentrated leakage due to high pore pressures in the impervious core.

3. Wider core would reduce the possibility of transverse or horizontal cracks extending through it. This is because of increased seepage path length and the arching action may not extend to its full width[6,63].

4. Slightly upstream curvature in the crest alignment increases compressive stresses to some extent and reduce the tendency for formation of transverse cracks.